Zeb2: A novel regulator of cardiac fibroblast to myofibroblast transition

by

Fahmida Jahan

A Thesis submitted to the Faculty of Graduate Studies of

The University of Manitoba

in partial fulfillment of the requirements of the degree of

MASTER OF SCIENCE

Department of Biochemistry and Medical Genetics

University of Manitoba

Winnipeg

ABSTRACT

Cardiac fibroblast to myofibroblast phenoconversion is a critical step during the development of cardiac fibrosis. Myofibroblasts chronically remodel extracellular matrix that results in myocardial stiffening, cardiac dysfunction and eventually heart failure. Previously we showed that Meox2, a homeobox transcription factor, can inhibit myofibroblast phenoconversion. Here we show that Zeb2, a repressor of Meox2, plays a crucial role during this phenoconversion process. Zeb2 overexpression significantly upregulates the expression of three key myofibroblast markers: α-SMA, SMemb and ED-A fibronectin in primary rat cardiac myofibroblast. We show that Zeb2 is highly expressed in myofibroblast nuclei whereas it is minimally expressed in fibroblast nuclei. Zeb2 overexpression in myofibroblasts results in a less migratory and more contractile mature myofibroblast phenotype. Moreover, Zeb2 overexpression represses Meox2 expression in endothelial cells. Thus, the current study enhances our understanding of the mechanism behind myofibroblast phenoconversion and provides a basis for developing Zeb2-based novel anti-fibrotic drug in the future.

ACKNOWLEDGEMENTS

Firstly, I would like to express my sincere gratitude to my advisor Dr. Jeffrey Wigle for the continuous support of my Master's study and research, for his patience, motivation, and immense knowledge. His guidance helped me in all the time of research and writing of this thesis. I would like to thank the rest of my thesis committee: Dr. Ian Dixon and Dr. Mark Nachtigal, for their insightful comments and encouragement, but also for the questions which incented me to widen my research focus from various perspectives.

I would also like to thank the current and former Wigle lab members for their assistance, expertise, and support, especially David Cheung, Dr. Josette Northcott, Anna Liu, Garret DeGagne, Faisal Haji and Megha Murali.

I extend my gratitude to Sunil Rattan, Dr. Rushita Adhikari Bagchi, Patricia Roche and Morvarid Kavosh, for their expertise and assistance.

Last but not the least, I would like to thank my family: my parents, my sister and my brothers for supporting me throughout my study and my life in general.

DEDICATION

I dedicate this thesis

to

My Parents:

Sabera Khatun and Md. Shah Jahan

CONTENTS

List of Abbreviations

APC	adenomatous polyposis coli
α-SMA	Alpha-smooth muscle actin
ACE	Angiotensin-converting enzyme
AV cushion	Atrio-ventricular cushion
bHLH	basic helix-loop-helix
bFGF	Basic fibroblast growth factor
BMD	bone marrow-derived
BGH	Bovine growth hormone
CID	CtBP interaction domain
BMP	Bone morphogenic protein
ChIP	Chromatin immunoprecipitation
CTGF/CCN	Connective tissue growth factor, Cysteine-rich protein, and Nephroblastoma overexpressed gene
Co-Smad	Common Smad
cVSMC	coronary vascular smooth muscle cells
C-terminal	Carboxyl terminal
CER	Cytoplasmic extraction reagent
DMEM	Dulbecco's modified eagle medium
ECM	Extracellular matrix
ED-A FN	Extracellular domain-A splice variant of fibronectin
EDPC	epicardium-derived cells
EDGF	Epithelial derived growth factor
EGFP	Enhanced green fluorescent protein
EMT	Epithelial to mesenchymal transition
F-Actin	Filamentous actin
FBS	Fetal bovine serum
FSP1	Fibroblast specific protein 1
GA	gentamicin/amphotericin-B
GAPDH	Glyceraldehyde 3-phosphate dehydrogenase

GS	Goat serum
HD	homeodomain
HQ	histidine/glutamine rich domain
HEK	Human embryonic kidney cells
HUVEC	Human umbilical vein endothelial cells
IGF1	Insulin-like growth factor-1
IL	Interleukin
ITR	inverted terminal repeats
I/RC	ischemia/reperfusion cardiomyopathy
MMP	Matrix metalloproteinase
MEOX1	Human Mesenchyme homeobox-1
Meox1	Mouse Mesenchyme homeobox-1
MEOX2	Human Mesenchyme homeobox-2
Meox2	Mouse Mesenchyme homeobox-2
MID	Middle domain
MI	Myocardial infarction
MOI	Multiplicity of infection
NER	Nuclear extraction reagent
NFATc1	Nuclear factor of activated T-cells, cytoplasmic 1
NF1	neurofibromatosis 1
N-Terminal	Amine terminal
ANOVA	One-way analysis of variance
P0/1/2	Passage 0/1/2
PBS	Phosphate buffered saline
PAI-1	plasminogen activator inhibitor-1
PDGF	Platelet-derived growth factor
ROCK	Rho-associated kinase
R-smad	Receptor Smad
SBD	Smad binding domain
SDS-PAGE	Sodium dodecyl sulfate polyacrylamide gel electrophoresis
SMemb	Embryonic non-muscle myosin heavy chain

S-MEM	Spinner Minimum Essential Media
SEM	Standard error of the mean
TBS	Tris buffered saline
TGF-β	Transforming growth factor-β
VIC	Valvular interstitial cells
VEGF	Vascular endothelial growth factor
TIMP	Tissue inhibitor of matrix metalloproteinase
ZEB1	Human Zinc Finger E-Box Binding Homeobox 1
Zeb1	Mouse Zinc Finger E-Box Binding Homeobox 1
ZEB2	Human Zinc Finger E-Box Binding Homeobox 2
Zeb2	Mouse Zinc Finger E-Box Binding Homeobox 2

List of Tables

List of Figures

List of Copyrighted Material for which Permission was obtained

Content	**Source**
Abstract: Zeb2: A novel regulator of cardiac fibroblast to myofibroblast transition	The FASEB Journal vol. 29 no. 1 Supplement 556.1
Book chapter: Diverse cellular origins of cardiac fibroblasts. Contents adapted: Text and figure. Figure title: Diverse sources of cardiac fibroblasts during disease progression.	Springer International Publisher
Article: The Ski-Zeb2-Meox2 pathway provides a novel mechanism for regulation of the cardiac myofibroblast phenotype. Contents adapted: figures. Figure title: I. Zeb2 expression is increased in rat cardiac myofibroblasts than fibroblasts. II. Meox2 levels decrease during the fibroblast-to-myofibroblast phenoconversion process.	Journal of cell science, Company of Biologists Ltd.
Article: Novel therapeutic approaches to post-infarction remodeling. Contents adapted: figure. Figure title: Stages of cardiac fibrosis.	Cardiovascular Research, Oxford University Press

1. CHAPTER I: INTRODUCTION

Fibroblasts are metabolically active cells that are found in most tissues of the body. They are critical for regulating both the composition and the turnover of the extracellular matrix (ECM) components, fluid volume and pressure, and tissue repair [1]. During wound healing, fibroblasts are vital to the precise control of the inflammatory response. Various inflammatory cytokines and growth factors promote the recruitment of fibroblasts to the wounded area. Activated fibroblasts (myofibroblasts) contribute to the wound healing process by producing ECM proteins, responding to, and synthesizing cytokines, chemokines, and other inflammatory mediators [1, 2]. These cells express non-smooth muscle myosin (SMemb) and α-smooth muscle actin (α-SMA), thus they provide a contractile force, which decreases the lesion size. Consequently dysregulation of the wound healing process leads to aberrant fibroblast recruitment and function. Abnormal remodeling of ECM due to excessive or inadequate secretion of matrix components alters organ architecture, impairs function and ultimately leads to organ failure [3-6].

1.1: Phenotypes of fibroblasts

Fibroblasts typically exhibit three phenotypes: a non-contractile fibroblast, intermediate phenotypes sometimes referred to as a protomyofibroblast [7], and a contractile myofibroblast (Figure 1) [6]. Characteristics of these different cellular phenotypes are described below.

1.1.1: Fibroblasts

Fibroblasts are generally flat, spindle-shaped cells, which may also have multiple projections. They populate all of the connective tissues in the body [8, 9]. Although they

were considered to be a homogeneous cell population; it is now apparent that these fibroblasts can arise from multiple origins and fibroblasts from different tissues exhibit differential properties and functions [8]. Although the heart is comprised of various cell types including cardiomyocytes, cardiac fibroblasts, endothelial cells, smooth muscle cells and pericytes; cardiac fibroblasts represent the largest population in the heart by cell number. They account for approximately two-thirds of the total cellular population, whereas cardiomyocytes comprise about two-thirds of the total volume [9]. However, this ratio may vary from species to species [10].

1.1.2: Intermediate Phenotypes

Under stress conditions fibroblasts can differentiate into intermediate phenotypes, also referred to as protomyofibroblasts, which are not equivalent to fully matured myofibroblasts. These intermediate phenotypes are characterized by the synthesis of stress fibres connected to cytoplasmic actins that form fibronexus adhesion complexes under mechanical stress. They also express the ED-A splice variant of fibronectin to form a special organization of cellular fibronectin at the cell surface. These cells are capable of generating contractile force [7]. Mechanical tension is crucial for the induction of contractile force by these cells. However, the exact mechanism behind the formation of these intermediate phenotypes *in vivo* is not well understood. *In vitro* studies have shown that fibroblasts extracted from a range of organs and tissues and plated on plastic tissue-culture dishes spontaneously undergo phenoconversion. These cells gain the ability to rapidly synthesize stress fibres, focal adhesion molecules and fibronectins- characteristic of an intermediate phenotype [7]. It is thought that during the tissue repair process, fibroblasts rapidly move to the site of injury and produce a collagen and fibronectin rich

ECM [7]. These cells acquire the ability to form stress fibres and focal adhesions. When the wound closure is completed, these cells occupying the granulation tissue of the scar become mechanically stressed due to the tractional force generated by various collagen fibres and stress fibres. Moreover, these cells also alter the processing of fibronectin splice variants and re-express those of developmental stages. In addition to mechanical tension, growth factors can also play a significant role in this phenoconversion in early developmental stages and during wound healing in the adult. For example, activated alveolar fibroblasts were absent in platelet-derived growth factor (PDGF)-null mice suggesting that PDGF plays a key role in the generation of protomyofibroblasts [11]. These intermediate phenotypes cover a continuum between a fibroblast and a mature myofibroblast and are not a single intermediate cell type.

1.1.3: Myofibroblasts

Intermediate phenotypes can further be induced to phenoconvert into myofibroblasts in the presence of persistent mechanical stress [7]. It is thought that the intermediate phenotypes represent a continuum when a fibroblast is transitioning into myofibroblast. During this transition, a fibroblast switches its phenotype from being proliferative and migratory to a hypoproliferative, less migratory and synthetic phase of mature myofibroblast phenotype [12, 13]. Expression of α-SMA, formation of more complex and organized stress fibres and fibronexus adhesion complexes or super mature focal adhesion molecules are all characteristic features of myofibroblasts [7, 12, 13]. Soluble factors including hormones, such as angiotensin II, endothelin I and pro-fibrotic cytokines such as transforming growth factor-β (TGF-β), connective tissue growth factor (CCN2/CTGF) and PDGF can induce the generation of myofibroblasts [7, 14]. Among these factors, TGF-β is considered to be

the critical driver of myofibroblast phenoconversion. Although TGF-β acts as an anti-proliferative factor in most cells, TGF-β can induce fibroblasts to proliferate and produce ECM during normal tissue repair [15]. TGF-β is also known to elevate ED-A fibronectin expression levels [15]. Both of these effects under stress condition are critical for inducing the phenoconversion from an intermediate phenotype into a mature myofibroblast. TGF-β potently induces collagen synthesis by fibroblastic cells and increases the levels of plasminogen activator inhibitor-1 (PAI-1) and α-SMA expression. It also reduces matrix metalloproteinase (MMP) activity by activating the production of their inhibitors and ultimately stimulates myofibroblasts to induce rapid ECM turnover and restoration of injured tissue during the healing process [7, 16]. TGF-β is secreted during tissue injury from a variety of cell sources such as white blood cells, particularly macrophages; platelets and parenchymal cells. TGF-β can also be produced and secreted by fibroblasts to function in an autocrine manner; making it another important mode for activation and maintenance of myofibroblast when the external inflammatory signal is lost. Damaged epithelial cells are also known to produce and secrete TGF-β, and thereby contribute to myofibroblast generation in a paracrine fashion [12]. Blocking the interaction of ED-A fibronectin with the cell surface leads to the attenuation of TGF-β mediated myofibroblast phenoconversion. Moreover it has been shown that when mechanical tension is lost, the myofibroblast phenotype fails to persist even in the presence of TGF-β and ED-A fibronectin. Inhibiting TGF-β signaling under mechanical stress condition prevents myofibroblast formation [17]. Therefore, all of these factors are crucial for the generation of myfibroblast from fibroblast but further investigations are required to discern their possible interplay and underlying mechanisms [6].

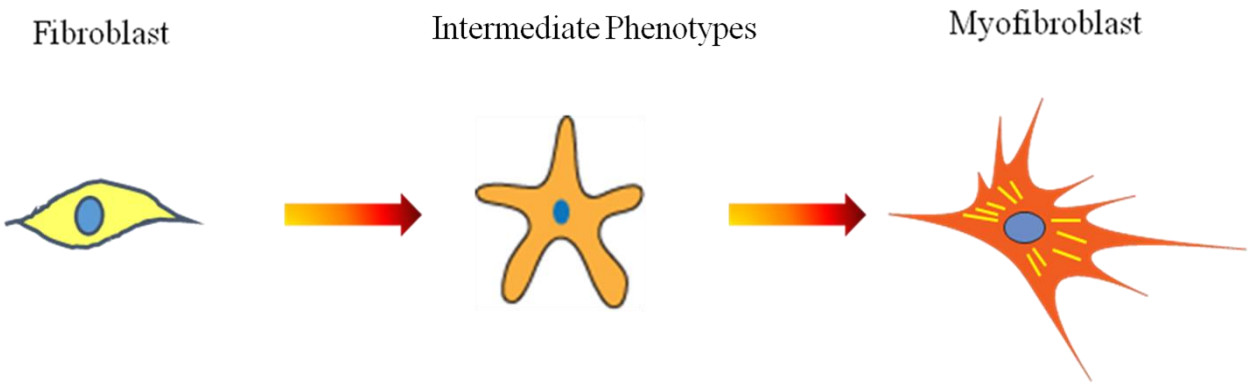

Figure 1: Phenotypes of fibroblasts. Fibroblasts mainly exhibit three phenotypes: a non-contractile fibroblast, intermediate phenotypes, and a contractile myofibroblast. Mechanical stress or signaling molecules for example PDGF, TGF-β, CCN2/CTGF can induce fibroblast to intermediate phenotypes. Intermediate phenotypes are characterized by the synthesis of stress fibres connected to cytoplasmic actins. They also express ED-A fibronectin to form special organization of cellular fibronectin at the cell surface. Intermediate phenotypes can be further phenoconverted into myofibroblasts in the presence of persistent mechanical stress and/or signaling molecules. Expression of α-SMA and formation of more organized stress fibres and fibronexus adhesion complexes or super mature focal adhesion molecules are characteristic features of myofibroblasts.

1.2: Origin of cardiac fibroblasts during development

Fibroblasts play a crucial role during heart development. Depending on the stage of development, their point of origin can vary greatly. During embryogenesis, fibroblasts are considered to be of mesenchymal origin and participate in the formation of the heart. The proepicardial organ and the epithelial–mesenchymal transition (EMT) during cardiac valve formation are considered to be the two principal sources of the cardiac fibroblast population [9]. However, developing bone marrow and their circulating progenitors, neural crest cells and differentiation from vascular walls can also give rise to fibroblasts during embryonic development [10]. Moreover, it has also been reported that fibroblasts can arise from mesoangioblasts. These are multipotent progenitor cells that can differentiate into either vascular endothelial cells or mesodermal fibroblasts. These progenitors originate from the bone marrow hematopoietic stem cells [9].

Cardiac interstitial and annulus fibroblasts are thought to be derived from the embryonic proepicardial mesenchymal cells [18]. The proepicardial cells cover the surface of the embryonic heart and forms the epicardium [19]. In the developing heart, the epicardium is the principal source of cardiac progenitor cells. These progenitor cells give rise to two cell types: (1) coronary vascular smooth muscle cells (cVSMCs) and (2) cardiac fibroblasts. These cells contribute to coronary vasculature, cardiac wall, subendocardium, the atrioventricular (AV) valves, and the fibrous skeleton of the heart [10, 19, 20]. The presence of growth factors, including PDGF, fibroblast growth factor (FGF), and TGF-β, stimulates the epicardium to undergo EMT and form epicardium-derived cells (EPDC). These cells subsequently differentiate into a fibroblast phenotype to form the fibrous heart skeleton. Using chicken-quail chimera, quail derived EPDCs were found in the

subendocardium, myocardium, and AV cushions. These EPDCs at the fibrous annulus region were found to be positive for procollagen-I indicating a cardiac fibroblast lineage and thus revealed their role in the formation of the fibrous heart skeleton. Adventitial fibroblasts were also found to be derived from the epicardium [21]. The Tallquist group has shown the role of an E-box binding basic helix-loop-helix (bHLH) transcription factor, *Tcf21*, in epicardial cell fate determination and cardiac fibroblast development. Using a tamoxifen-inducible Cre expressed from the *Tcf21* locus, they showed that Tcf21-expressing epicardial cells are largely fated to become the cardiac fibroblast lineage specific via EMT. Moreover, *Tcf21* knockout mice lacked cardiac fibroblasts, and fate mapping study showed attenuation of epicardial EMT [22]. It is known that the cardiac endothelium may also give rise to valvular fibroblasts, which are also known as valvular interstitial cells (VICs) [23]. Endothelial cells detach to form the cardiac cushion and undergo endothelial to mesenchymal transition (EndMT) that is stimulated by various cytokines including TGF-β, PDGF and Wnt. These mesenchymal cells enter the cardiac jelly and acquire a fibroblast phenotype. Various signaling pathways and genes such as vascular endothelial growth factor (VEGF), nuclear factor of activated T-cells, cytoplasmic 1 (NFATc1), Notch, Wnt/ β-catenin, bone morphogenetic protein (BMP), TGF-β, ErbB, and neurofibromatosis 1 (NF1)/Ras play important and selective roles in regulating endothelial cell proliferation and differentiation during valve development and maturation. VEGF levels need to be strictly controlled during normal heart development as increased VEGF expression can inhibit endothelial cells from undergoing EndMT [24]. Tissue explants studies have revealed that hypoxia prevents cardiac cushion EndMT by inducing a 10-fold increase in VEGF expression levels. This finding indicates the

possibility that fetal hypoxia may lead to congenital heart defects in the cardiac valves and the interatrial septum [25]. Cushion endothelial cells exposed to hyperglycemic conditions during developmental stages had persistent CD31 expression and were unable to correctly initiate the EndMT program [26, 27]. On the other hand cardiac cushions derived from mice lacking CD31 were able to undergo EndMT, even in hyperglycemic conditions [26, 27]. Studies have also indicated that NFATc1 is downregulated during endocardial EndMT and that NFATc1-expressing cells do not undergo EndMT [28]. Notch signaling is essential for the regulation of endocardial cushion EndMT. In *Notch1*$^{-/-}$ mice, cardiac cushions were found to be hypoplastic suggesting that the endocardium failed to undergo EndMT [29]. Moreover, disruption of Notch signaling particularly diminished TGF-β_2 expression in the heart. In agreement with this result, the expression levels of Snail, a critical the mesenchymal transcription factor, was found to be significantly decreased in the absence of Notch signaling. This finding suggests that Notch signaling may increase the expression of TGF-β_2 in the heart; and TGF-β_2 eventually promotes EndMT in endocardium [29]. Using a homozygous adenomatous polyposis coli (APC) truncation mutant, nuclear β-catenin was detected throughout the heart indicating that a large population of endocardial cells are able to undergo EndMT [26, 30]. Studies have also indicated that Wnt/β-catenin signaling may play a crucial role in valve development by regulating EndMT. β-catenin can activate the expression of genes required for the mesenchymal transition program. It is speculated that upon CD31 repression, β-catenin levels in the cytosol increase and trigger proliferation of cells undergoing EndMT; thus suggesting that β-catenin may activate the EndMT program, which generates the fibroblast population in the cardiac jelly [26]. Using a BMP-2 deficient chick model, mesenchymal

cells were shown to fail to invade through a collagen lattice. Similarly by using mouse AV explants, BMP-2 treatment was found to be sufficient to induce EndMT in the myocardium. Additionally, AV endothelial explants were found to synthesize and secrete TGF-β_2 in an autocrine mechanism upon BMP-2 treatment [26]. Thus during embryonic developmental stages, cardiac fibroblasts can be derived from a number of sources, especially from the proepicardium and cardiac endothelium. However fate mapping studies largely depend on the susceptibility of Cre dependent reporter and on the efficiency of the Cre recombinase, which may represent a limitation of the current findings. Moreover, the lack of specific fibroblast markers makes it challenging to trace their origin. Refining existing fate mapping strategies and identifying appropriate marker genes will enhance our current knowledge of cardiac fibroblast heterogeneity during development [6].

1.3: Sources of fibroblast generation in cardiopathology

In disease, fibroblasts are recruited to the injured area from different sources. Fibroblast generation from nearby sources such as epithelial and endothelial cells via mesenchymal transition (EMT and EndMT), or from fibrocytes, pericytes or from circulating bone marrow progenitor cells is thought to be a very effective means to enable the rapid recruitment of fibroblasts to the injured area since recruitment from more distant sites would require migration, activation, and proliferation of these cells (Figure 2). For instance, during wound healing in epithelial rich areas such as the skin, EMT is a vital process for fibroblast recruitment [31]. Recently there has been increasing evidence suggesting the heterogeneity of cell sources for the fibroblast population found in the damaged heart [6].

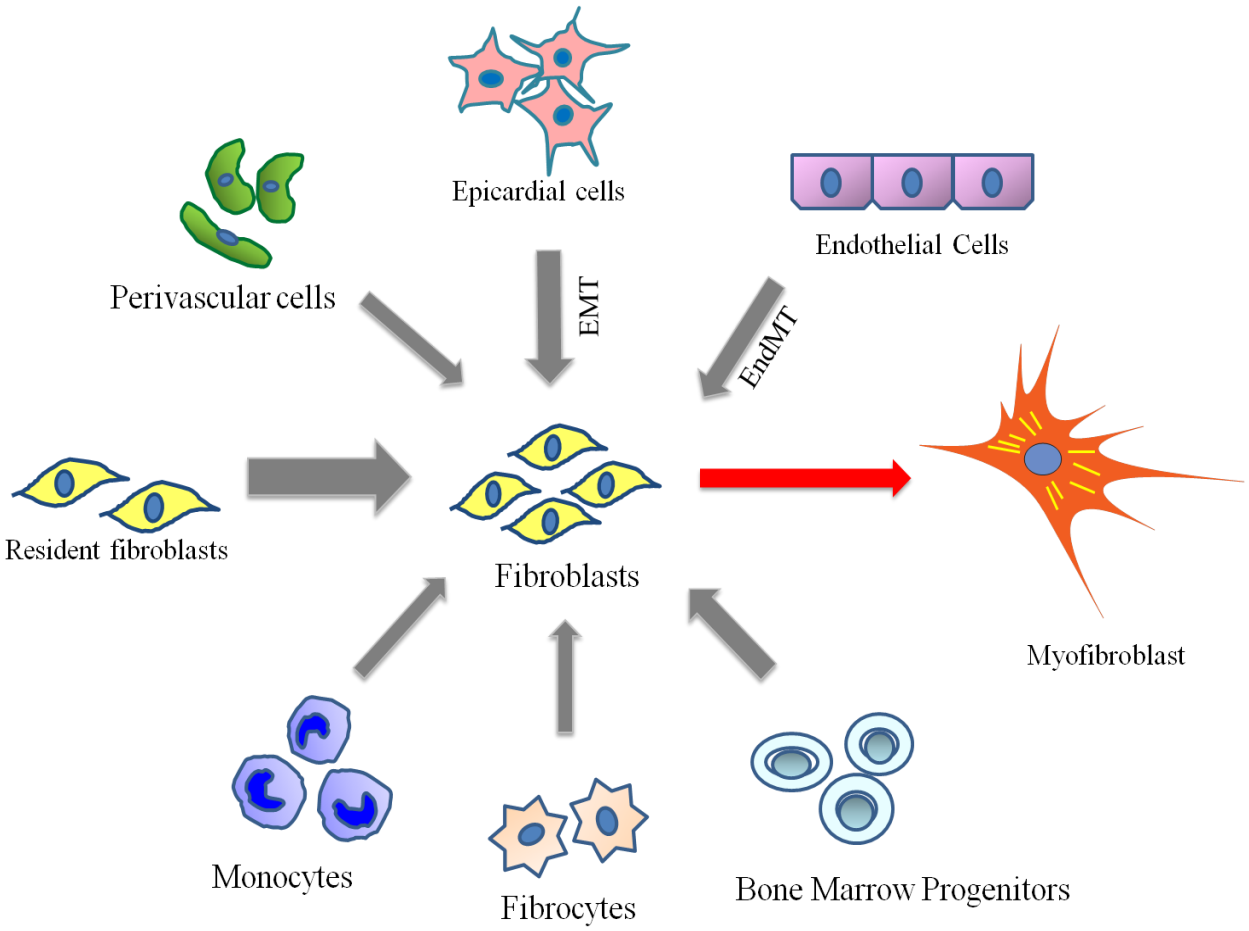

Figure 2: Diverse sources of cardiac fibroblasts during disease progression. During pathological conditions, a dramatic increase in fibroblast number can be derived from various sources such as the proliferation of resident fibroblasts, mesenchymal transition of epithelial (EMT)/endothelial (EndMT) cells; and recruitment and differentiation of circulating bone marrow progenitor cells, monocytes, fibrocytes and perivascular cells. These fibroblasts can further phenoconvert into a mature activated myofibroblast that actively synthesizes extracellular matrix proteins and forms stress fibers. EMT: epithelial to mesenchymal transition, EndMT: endothelial to mesenchymal transition. Figure adapted by author from Jahan and Wigle (2015), a book chapter in Cardiac fibrosis and heart failure. Cause or Effect?

1.3.1: Resident fibroblasts

Previously, it was generally thought that activated fibroblasts or myofibroblasts in fibrotic hearts are derived mainly from the proliferation of existing fibroblasts in the heart called resident fibroblasts [31]. This hypothesis is supported by the fact that cardiac fibroblasts are highly responsive to circulating cues in the surrounding microenvironment that can influence their proliferation and recruitment to the site of pathological inflammation [8]. Initial studies in a pressure-overload mouse model showed that inhibition of TGF-β receptor caused decreased collagen synthesis and deposition; and inhibited the proliferation and activation of myofibroblasts that resulted in dilated cardiomyopathy and dysfunction [32]. During replacement fibrosis in the heart, such stimuli trigger resident fibroblasts to synthesize extracellular matrix components at the site of injury to heal the damaged area [8, 32, 33]. However, increasing evidence suggests that during reactive interstitial fibrosis proliferating pro-fibrotic cells not only come from the resident fibroblast population, but also are rapidly recruited from multiple nearby sources to enhance cardiac healing [8, 34, 35]

1.3.2: EMT derived fibroblasts in cardiac diseases

Although in normal adult heart epicardial cells do not actively undergo EMT, *in vivo* studies of myocardial injuries have shown that epicardium-specific genes expressed during development are re-activated in response to injury [36]. Initially this reactivation is global, but eventually it is confined to the injury area, indicating a role of epicardium in healing cardiac insults. Subsequently, these epicardial cells undergoing EMT proliferate and migrate into the sub-epicardium and form a thick epicardial cap consisting of EPDCs. For

instance, using a *Wt1*^{CreERT2} mouse model, it was previously shown that epicardial cells did not undergo EMT in the normal adult heart. However during cardiac injury, adult mouse epicardium was found to secrete paracrine factors [37, 38]. After myocardial infarction (MI), fetal epicardial genes were shown to be reactivated and led epicardial cells to proliferate and initiated EMT to form a thick layer of mesenchymal cells to protect from myocardial injury [37, 39]. Using a tamoxifen inducible *Wt1*^{CreERT2}*;Rosa*^{26mTmG} mouse model, epicardial cells were selectively labelled with membrane green fluorescence protein (mGFP) to visualize cell fate after cardiac injury. Experimental MI was performed by left arterial ligation. mGFP labelled EPDCs in the infarct region were found to be spindle shaped and expressed myofibroblast and fibroblast markers [37]. In contrast to the human heart, zebrafish hearts regenerate and repair by epicardial activation, proliferation and by undergoing EMT after cardiac injury. In zebrafish, blocking FGF and PDGF signaling prevented epicardial marker expression and inhibited epicardial EMT during cardiac injury repair [20]. *In vitro* studies have shown that PDGF activates stress fiber production and triggers EMT in epicardial cells. Using an explant model, recombinant PDGF-BB treatment induced cell migration and a fibroblast-like phenotype in an epicardial monolayer from sham operated zebrafish [40]. Using RT-PCR, the expression of EMT markers *Snail* and *Twist* genes was found to be upregulated as well which indicates that fibroblasts can arise from epicardial cells during heart regeneration. The expression patterns of *Snail2* and *Twist1b* were found to be increased at the site of injury by *in situ* hybridization [40]. The role of *Wt1*-lineage specific cells in healing of the infarct area were analyzed in a mouse model of MI. The epicardial layer over the ischemic area was found to be disrupted immediately after the injury but began to regenerate within 3

days of MI. In the regenerated epicardium, the fetal epicardial genes (*Wt1, Tbx18, Raldh*) were transiently re-activated and induced epicardial proliferation. Within 2 weeks post-MI, *Wt1*-lineage positive subepicardial mesenchymal cells were observed. These cells replaced the lost cardiomyocytes and contributed to the fibroblasts, myofibroblast and the coronary endothelium, and later also contributed to the cardiomyocyte population. In epicardium adjacent to the site of injury, EMT marker Snai1 and myofibroblast marker α-SMA were expressed and mesenchyme populated the subepicardial space [36]. Using tamoxifen inducible $Wt1^{CreERT2}$ mice, another study showed that cells derived from adult epicardium after MI differentiated into myofibroblast/fibroblast and smooth muscle lineages and mainly populated a perivascular niche in the thickened epicardium [20]. Moreover, Wnt1 and Notch signaling pathways have been found to regulate the activation of epicardial EMT and contribute to fibrosis repair in a mouse model of MI and ventricular pressure overload [41].

Therefore, reactivated epicardium and EMT plays a pivotal role in the repair process of injured heart by contributing to the fibroblast pool. However, constitutive reactivation of EMT leads to chronic remodeling of the heart. Thus, blocking the reactivation of this evolutionarily conserved pathway may represent a novel approach to combat fibrosis.

1.3.3: Endothelial to mesenchymal transition (EndMT)

Studies have shown that vascular endothelial cells can also phenoconvert and acquire a fibroblast-like phenotype upon stimulation with pro-fibrotic signals such as TGF-β_1 or hypoxia, a process called endothelial to mesenchymal transition (EndMT) [42, 43]. These mesenchymal cells leave the microvascular bed and mature to become interstitial

fibroblasts. EndMT may have two possible roles in cardiac fibrosis by both giving rise to the fibroblast population and also by decreasing microvasculature density [44]. However, under normal physiological condition the contribution of this process to form the resident fibroblast population was not found to be significant [44]. This indicates that only after pathological damage or injury cardiac fibroblasts are generated from endothelial cells. Recently, Zeisberg *et al.* showed for the first time that adult cardiac endothelial cells can undergo EndMT. A fate mapping study using endothelial-specific reporter gene *Tie1* has shown that between 27–30% of all fibroblasts were derived from endothelial origin via EndMT in a pressure overload–induced cardiac fibrosis model [44]. Similarly, another group observed that in the hearts of diabetic wild-type mice, 15–20% of fibroblasts co-expressed both the endothelial marker CD31 and the fibroblast specific marker S100A4/FSP1, whereas CD31/S100A4 double positive cells were only rarely detected in the diabetic *ET-1f/f;Tie2-Cre* mice hearts. This result indicates that endothelial cell derived ET-1 plays a crucial role in regulating EndMT. However, CD31/S100A4 double labeling, as well as the presence of CD31/α-SMA and CD31/vimentin cells, only allows for the characterization of the intermediate stage of EndMT [45]. Thus, these observations may under-represent the actual number of fibroblasts that are of endothelial origin since in the later stages of diabetes mellitus, EndMT-derived fibroblasts may migrate to the surrounding area and lose expression of endothelial markers [45]. Likewise in EMT, TGF-β is considered to be a major signaling pathway that stimulates EndMT in cardiac injury. Recombinant BMP7 has been shown to inhibit TGF-β function in endothelial cells and thus inhibit EndMT and reduce cardiac fibrosis in aortic banding models [44]. Although TGF-β has been previously shown to induce PAI-1 expression, another study

demonstrated that PAI-1 can block TGF-β signaling in the normal heart and PAI-1 mutants showed activated TGF-β signaling with a corresponding increase in fibroblast population and developed cardiac fibrosis [46, 47]. Further investigation showed increased TGF-β mediated mesenchymal marker expression in PAI-1 null endothelial cells suggesting that these cells are more likely to undergo EndMT. However, this study did not show any direct evidence of EndMT through lineage tracing experiments [46]. Canonical Wnt signaling was also implicated in the EndMT-mediated cardiac fibrosis following MI. Using a TOPGAL Wnt reporter mouse, canonical Wnt signaling was shown to be increased in the evolving infarct scar and this activity was mainly confined to endothelial and α-SMA-expressing cells. Cre-loxP genetic lineage tracing experiments showed that approximately 40% of these cells arose from endothelial precursors. Moreover, activation of canonical Wnt signaling triggered morphological and molecular changes to induce a mesenchymal phenotype. Other studies have also reported activation of Wnt expression in the epicardium and in fibroblasts after ischemic myocardial injury [20, 48]. Although recent studies have achieved remarkable success in giving insights into cardiac fibroblast generation from endothelial origin, understanding how these cells are differentiated exclusively during pathological conditions needs to be further investigated.

1.3.4: Bone marrow-derived (BMD) progenitor cells

Bone marrow-derived progenitor cells are another important source of fibroblasts in the diseased heart (Figure 2). It was initially speculated by the Yano group that cardiac myofibroblasts can arise from bone marrow (BM) during pathological condition, since bone marrow-derived (BMD) cells have been found to contribute to both fibroblast and myofibroblast populations in other organs such as the kidney, lung, liver, stomach, small

and large intestines and cancerous tumours [49]. Later on GFP labelled bone marrow transplant studies showed the presence of GFP positive fibroblasts and especially myofibroblasts in the scar and the nearby remnant area after myocardial injury [50]. A similar study showed that 57% of the myofibroblasts were of bone marrow origin at day 7 post-MI, which decreased to 32% on day 21 post-MI [51]. This finding raised the debate that these cells may be simply contributing to the inflammatory response following injury. A significant population of these cells are actually playing role as a specific type of inflammatory cell during acute healing phase and are largely not contributing in the formation of chronic lesion. Similar results were obtained using two different mice models- BM transgenic EGFP reporter, or BM cells expressing two reporter genes: luciferase and β-galactosidase under the control of collagen I (α2 chain) gene promoter. After inducing MI by permanent coronary artery ligation technique, the number of α-SMA and collagen I positive myofibroblasts was found to be increased significantly at the site of injury until day 14 and persisted afterwards. A significant number of EGFP-positive BMD cells were observed during the first week post-MI, however the number gradually declined after day 28. Around 21% of the BMD cells in the infarct area were found to be myofibroblasts. The highest number of BMD myofibroblasts (EGFP and α-SMA double positive) was found on day 7 post-MI. These cells constituted 24% of all myofibroblasts present in the scar. These BMD myofibroblasts actively synthesized collagen I and were confined to the site of injury [52]. Using a transgenic *Mst1* mouse model, bone marrow-derived cells were shown to contribute to about 17% of all fibroblasts present in the failing heart [53]. In an aortic banded mouse model, bone marrow transplantation experiments showed that 13.4% FSP positive fibroblasts and 21.1% α-SMA positive myofibroblasts in

the heart were bone marrow derived [44]. These findings suggest that BMD cells may play an important role in myofibroblast generation and can accelerate healing after MI.

1.3.5: Monocytes

Monocytes are also considered to be a novel source of pathology-associated fibroblasts (Figure. 2). Using a mouse model of fibrotic ischemia/reperfusion cardiomyopathy(I/RC), it has been demonstrated that 3% of all non-myocytes in the I/RC heart expressed monocytic markers- CD45, CD11b, CD35 and myofibroblast markers S100A4, α-SMA [54]. Moreover the inhibition of monocyte recruitment by injecting CL2MDP liposomes after cryoinjury, dramatically decreased fibroblast number in the infarct area and attenuated myocardial remodeling [55]. CL2MDP liposomes are termed as 'suicide' liposomes that encapsulate clodronate molecules. These liposomes are engulfed by macrophages via endocytosis and then fuse with lysosomes. Phospholipase in the lysosome disrupt the liposomes and causes release of clodronate into the cytoplasm which eventually leads to apoptosis [56]. The above mentioned findings indirectly suggest that monocytes could be a pivotal source for fibroblast and myofibroblast generation and recruitment during injury.

1.3.6: Fibrocytes

Fibrocytes are blood-borne mesenchymal progenitor cells that have unique characteristics of expressing cell surface markers of leukocytes, hematopoietic progenitor cells as well as of fibroblasts such as CD11b, CD13, CD34, CD45RO, MHC class II, CD86, collagen I and vimentin. During wound healing, circulating fibrocytes rapidly enter the injury site which indicates their potential critical role in the repair process [57]. Data suggests that

they are an important source of fibroblasts during pathological conditions (Figure 2) [58, 59]. They are of hematopoietic origin and exhibit leukocyte-like characteristics [60]. One study showed that 10% of all cells within the scar area of nephrotic wound were spindle-shaped and positive for procollagen and CD34 markers. In the presence of profibrotic cytokines such as TGF-β or endothelin-1 *in vitro*, fibrocytes can produce fibroblast and myofibroblast markers (fibronectin, collagen and α-SMA) and differentiate into myofibroblasts [58]. In a wound healing model, profibrotic cytokines- IL-4 and IL-13 have also been found to promote fibrocyte differentiation into myofibroblast. On the other hand, the anti-fibrotic cytokine, IFN-γ, inhibits fibrocyte differentiation [59]. In a rabbit atherosclerotic model, CD34-positive cells were also found to be positive for α-SMA [61].

1.3.7: Perivascular cells

Perivascular cells of the cardiac vessels may present another source of fibroblasts following injury (Figure 2). In a dermal scarring model, pericytes were shown to phenoconvert into fibroblast-like cells and contributed in collagen production [62]. *In vitro* studies have also shown that retinal pericytes acquire a functionally active fibroblast-like phenotype [63]. Fate mapping studies have demonstrated that CD73+ pericytes can serve as a potential source of fibroblasts during kidney fibrosis [64]. Moreover during lung fibrosis, activated fibroblasts or myofibroblasts have been found to arise from perivascular and peribronchial areas [65]. However, due to lack of pericyte and fibroblast specific markers and difficulty in designing specific fate mapping techniques, it is currently difficult to conclude on the significance of the pericyte's contribution to cardiac fibrosis [6].

1.4: Function of cardiac fibroblasts

Cardiac fibroblasts perform various functions that are responsible for proper cardiac development and function. They maintain the structural, biochemical, mechanical and electrical properties of the heart [8].

1.4.1: Homeostasis of the ECM

ECM is composed of both structural and non-structural proteins. Structural proteins include collagens, proteoglycans and glycoproteins; and non-structural proteins include cytokines, growth factors, and proteases [66, 67]. The ECM forms a scaffold that holds and interconnects the cardiac cells; and transmits mechanical forces throughout the myocardium to send mechanical signal to the surrounding cells. Moreover, the ECM keeps the atria and the ventricles electrophysiologically separated in order to make proper cardiac contraction and relaxation possible [8]. Cardiac fibroblasts maintain ECM homeostasis by secreting and breaking down ECM proteins. They produce the fibrillar collagens, type I and type III, which comprises 90% of all collagen in the myocardium. They also produce other ECM proteins such as collagen type IV, V, VI, elastin, and laminin [68]. On the other hand, cardiac fibroblasts also regulate ECM degradation by controlling the expression of the matrix metalloproteinases (MMP) and tissue inhibitors of MMP (TIMP) [69].

1.4.2: Production of signaling molecules

One of the major functions of cardiac fibroblasts is to synthesize and secrete signaling molecules including growth factors and cytokines, which have autocrine and paracrine effects on cardiac cells. Thus, they modulate proliferation, contractions and apoptosis of

other cardiac cell types. The secretion of these signaling factors by the cardiac fibroblasts is mainly dependent on the presence of external stimuli. Chemical stimuli include cytokines and growth factors; electrical signals, hypoxia, or mechanical signals can also trigger fibroblasts to release signaling molecules. The presence of higher levels of pro-inflammatory factors such as IL-1, IL-6, and TNF; and pro-fibrotic TGF-β is commonly observed in heart failure patients. Depending on their levels of expression and the composition of factors present, the exact effects of these factors may vary in diseased heart [9].

1.4.3: Cardiac electrophysiology

The notion that cardiac fibroblasts can actively contribute to cardiac electrophysiology has emerged in recent times. They produce ECM layers that act as an insulator to physically separate groups of myocytes in order to reduce local electrical coupling and slow down conduction. For example, the annulus fibrosis separates the atria and ventricles and thus facilitates proper contraction and relaxation for proper heart function [18]. During myocardial ischemia and hypertrophy, development of interstitial fibrosis and excess collagen deposition by fibroblasts accelerate local anisotropy leading to cardiac arrhythmogenesis. *In vitro* studies have reported that myocyte and fibroblast interaction provides a means for electrical signal transduction [70, 71], suggesting its role in connecting myocytes that are insulated by the ECM. Another active potential role would be their mechanosensitivity. Fibroblasts take action in response to mechanical stresses such as contractile force of the surrounding myocardium, or by external stresses, such as variation in membrane potential. They actively express multiple stress-induced ion channels for Na^+, K^+, and Ca^{2+} [19, 72]. Mechanical stress activates these ion channels and

thus reduces fibroblast membrane potential to facilitate mechano-electrical transduction [73, 74]. Such aberrant electrical properties of fibroblasts coupled with myocyte alter pacemaker activity and ultimately can cause depression of heart rate.

1.4.4: Angiogenesis and vessel homeostasis

Cardiac fibroblasts play a vital role in maintaining the homeostasis of cardiac vessels. Angiogenesis is termed as the generation of new capillaries from pre-existing ones. It depends on external stimuli that trigger endothelial cells to proliferate and migrate [75]. Cardiac fibroblasts produce and secrete the two key inducers of angiogenesis- FGF and VEGF. These factors stimulate vascular endothelial cells and promote angiogenesis. Thus, they aid in restoring the blood supply to the injured myocardium. On the other hand, it has also been reported that they can express pigment epithelium-derived factor (PEDF) known to block VEGF-induced proliferation of endothelial cells. Thus, cardiac fibroblasts can regulate angiogenesis by expressing both pro- and anti-angiogenic factors which is crucial for vascular development and maintenance. Other factors that play roles in angiogenesis, such as MMPs and TIMPs are also produced by fibroblasts. MMPs degrade the ECM and thus provide space for endothelial cell migration and sprouting. On the contrary, TIMPs can both inhibit angiogenesis as well as promote vessel formation [8].

1.4.5: Role in cardiomyocyte growth

Cardiac fibroblasts produce mitogens that are essential for myocyte development and maintenance. Although cardiomyocytes are considered to be non-proliferating cells, recent findings indicate that adult cardiomyocytes are actually slowly proliferating cells [76].

Both *in vitro* and *in vivo* studies have reported that fibroblasts produce FGF and periostin and stimulate adult myocyte proliferation [77, 78].

1.5: Fibroblasts and disease

Fibroblasts are intimately involved in cardiac development, maintenance, and disease. They are often implicated as being the major contributors to cardiac fibrosis. Their unique features make them attractive cellular targets for reducing pathological remodeling. Although cardiac fibrosis and fibroblast-associated pathologies are among the largest groups of diseases, at present there are no effective therapies available for them. Activated cardiac fibroblasts (myofibroblasts) contribute to fibrosis by chronic ECM remodeling and the development of scar tissue which subsequently results in myocardial stiffening, cardiac dysfunction and eventually to heart failure [79, 80]. Thus, an improved therapeutic option would be to restrict their generation or recruitment. Recent studies also implicated importance of fibroblasts in the formation and maintenance of blood vessels, which opens up a new avenue for cardiac therapies. Fibroblasts are prominent modifiers of cancer progression and invasion. Like organ fibrosis, these fibroblasts within the tumour stroma stay persistently active. They acquire an activated phenotype as seen during wound healing [81]. These phenoconverted fibroblasts at the site of the tumour are referred to as peritumoral or reactive stromal fibroblasts, or tumour-associated fibroblasts that contribute to cancer progression [81]. Moreover, dysregulation of fibroblast and myofibroblast function and differentiation leads to diseases such as emphysema, asthma, interstitial and chronic obstructive pulmonary diseases in lung; rheumatoid arthritis and osteoarthritis in bones and joints; scleroderma, hypertrophic scars, lipodermatosclerosis in skin; and diseases in other organs including fibrosis related to kidney, liver, eye, nervous system and

brain etc [82]. Most importantly, fibrosis in the heart due to uncontrolled fibroblast proliferation and their phenoconversion to myofibroblast is closely associated with clinically important conditions such as hypertension, atherosclerosis, ischemia, dilated cardiomyopathies, valvular diseases, arrhythmias and heart failure; thus making it one of the major health problem worldwide [83]. Hence, a better understanding of their origin and underlying mechanisms will aid in developing successful therapies for improving patient outcome in all aspects of diseases linked to fibroblast dysregulation [6].

1.6: Fibroblast and wound healing process

After injury, the damaged tissue undergoes a series of events to repair the injury and return to the normal state. Presently the dermal wound healing process is the most well-defined of all wound healing mechanisms and it involves the following steps:

1.6.1: Inflammation and homeostasis

Would healing begins with the inflammation step which is triggered by various events for example physical injury, infection by pathogens and contact with toxins. Platelets aggregate to form a hemostatic plug and prevent blood loss by forming a fibrin clot, which occurs within few minutes after the injury [84, 85]. Platelets secrete cytokines and growth factors that attract inflammatory cells, for example, neutrophils, monocytes/ macrophages, and lymphocytes to migrate and proliferate at the site of injury. At first neutrophils appear to provide defense against bacteria that may have come in contact to the injury. Subsequently neutrophils undergo apoptosis and monocytes and macrophages arrive. These cells remove cell debris and phagocytose bacteria, and secrete growth factors such as TGF-β, FGFs, and PDGF that induce fibroblast infiltration and proliferation to the site

of injury [85]. In case of chronic inflammation, there is a persistent presence of macrophages by their continued infiltration and proliferation [85].

1.6.2: Proliferation phase

As fibroblasts infiltrate the injured area, they undergo rapid proliferation and myofibroblast phenoconversion which is the key step of fibrogenesis. Myofibroblasts are the hypersynthetic phenoconverted fibroblasts that serve as the main player in ECM remodeling by synthesizing high amounts of ECM proteins [85, 86]. They also express contractile proteins such α-SMA and SMemb that provide force for wound contraction which facilitate wound closure [87]. Pro-angiogenic growth factors TGF-β_1, FGF-2, angiopoietin, PDGF and VEGF released at the injury site stimulate endothelial cell proliferation and induces vascularization and thus restore tissue perfusion. Epidermal epithelial cells migrate to the site of injury for re-epithelialization [88].

1.6.3: Remodeling/scar formation

During this phase the ECM undergoes remodeling by continued matrix synthesis by fibroblasts and myofibroblasts and simultaneous degradation of matrix by metalloproteinases and plasmin/plasminogen family. The ratio of ECM synthesis and breakdown determines the net ECM build up [88, 89] that ultimately contributes to tissue remodeling and scar maturation. Initially type III collagen is produced in large amounts during matrix synthesis, however, it is eventually degraded and is replaced by the synthesis of type I collagen which increases matrix strength and enhances the repair process. At the same time, MMP activity is controlled by TIMPs. Fibroblast/myofibroblasts exerts tensile force and their contraction helps in reducing

wound area and thus facilitates rapid healing [85]. It is thought that myofibroblasts show higher expression levels of the contractile proteins, α-SMA and SMemb compared to fibroblasts and therefore play the most crucial role in tension generation by their contractile force. Gradually the injured tissue regains its normal strength (approximately 80% of the original) and the healing process is terminated. The remaining myofibroblasts and newly formed blood vessels are removed by apoptosis [90]. With age the ability of normal wound healing goes awry and defective wound healing leads to chronic scar formation for example in case of cardiac fibrosis (Figure 3) [85].

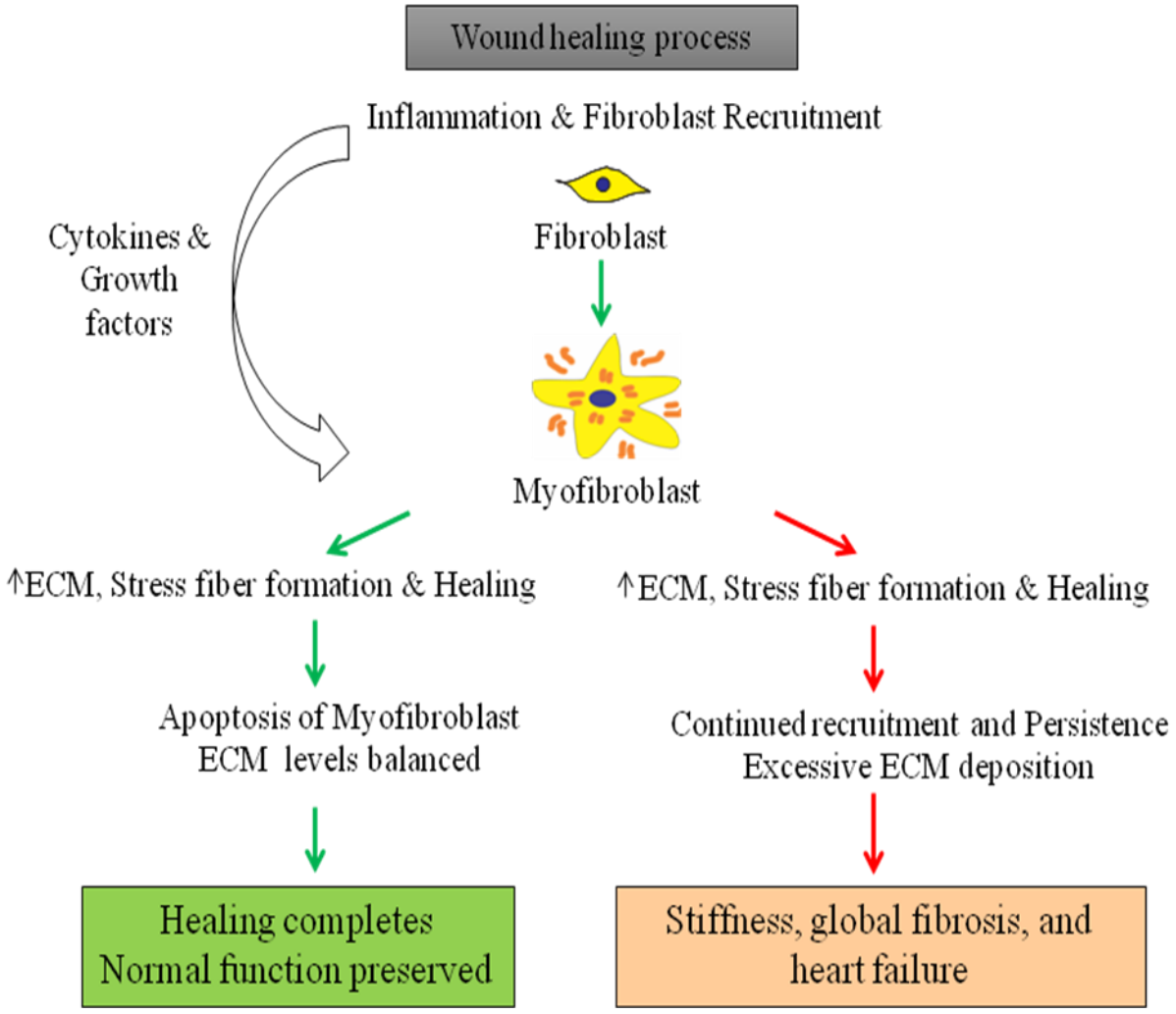

Figure 3: Normal wound healing process versus defective wound healing. Although both events involve similar steps of tissue repair, however, in case of defective wound healing there is continued phenoconversion of myofibroblasts and these myofibroblasts tends to persist in the scar area for a long time instead of undergoing apoptosis.

1.6.4: Defective wound healing, myocardial infarction and fibrosis

In case of a chronic non-healing wound, all of the areas may not be at the same stage of healing and thus progression to next step is not synchronous. Consequently the healing process fails to terminate and accumulation of excess matrix results in scar formation. There are two types of defective healing- 1) chronic wounds: healing process is blocked, interrupted or delayed, for example ulcerous lesions. 2) Excessive wound healing: healing process fails to terminate or hyperactivated, for example hypertrophic scars, keloids etc [85].

Cardiac muscles need a continuous supply of nutrients and oxygen to maintain a functioning heart. Rupture of atherosclerotic plaques can block the coronary arteries and prevent nutrients and oxygen to reach cardiac muscles. Persistent blockage leads to cell death and eventually to infarction. Similar to dermal wound healing, platelets and inflammatory cells migrate to the injured area [85]. Cell debris is removed and secreted growth factors and cytokines induce fibroblasts to enter to the site of injury and phenoconvert to myofibroblasts. These myofibroblasts can originate from many sources, for example, resident fibroblasts, circulating fibrocytes, epithelial/endothelial mesenchymal transition of epicardial and endothelial cells, pericytes etc (Figure 2) [8]. This ensures fast recruitment and proliferation of fibroblasts and myofibroblasts at the site of injury leading to rapid remodeling of ECM due to the activity of hypersynthetic myofibroblasts. This is called the beneficial ‘reparative fibrosis’ [85]. In case of dermal wound healing, the scar is mostly reduced by means of recellularization and removal of myofibroblasts. However, in cardiac fibrosis after myocardial infarction the process of scar remodeling is not well understood [80]. In the case of myocardial infarction,

continued inflammation causes myofibroblasts to persist for many years and as cardiomyocytes are terminally differentiated cells they fail to proliferate and replace the myocyte loss. As a result, this scar persists for the life time of the person. This leads to undesirable effects that cause cardiac dysfunction, for example, impaired contraction and relaxation. The unusual electrical properties produced by the persisting myofibroblasts and the fibrotic ECM ultimately leads to arrhythmia. Moreover, the distal/uninfarcted regions gradually undergo a process called 'reactive' fibrosis and ECM synthesis continues which makes the myocardium increasingly stiffer leading to impairment of contraction and relaxation [80, 85]. This results in lower cardiac output and eventually causes heart failure (Figure 4). Cardiac fibrosis is a common consequence of other cardiovascular disorders as well, for example congenital defects, hypertension, dilated cardiomyopathy, ischemia etc. Various factors can lead to cardiac fibroblast to myofibroblast phenoconversion including mechanical stress, hypoxia, signaling pathways such as TGF-β, CCN2/CTGF, PDGF, angiotensin II, endothelin I contribute to myofibroblast phenoconversion [85]. Among various markers of heart failure, Periostin and Galectin-3 are considered to be important. Periostin is a matricellular protein. It is a TGF-β responsive gene and important for collagen fibrillogenesis. Increased Periostin expression is found upon mechanical stretch and during activated TGF-β signaling. Periostin expression is upregulated in the heart after myocardial infarction. *Postn* knockout mice showed reduced fibrosis but exhibited ruptured ventricular wall upon hemodynamic pressure [91]. On the other hand, *Postn* overexpression showed improved protection against ventricular wall rupture. Galectin-3 is a β-galactoside-binding lectin. It can interact with laminin, collagen, synexin, and integrins; and regulates cell migration, cell-cell interaction, cell cycle and apoptosis.

Galectin-3 has been found to contribute to excess collagen deposition and the induction of heart failure [92].

A

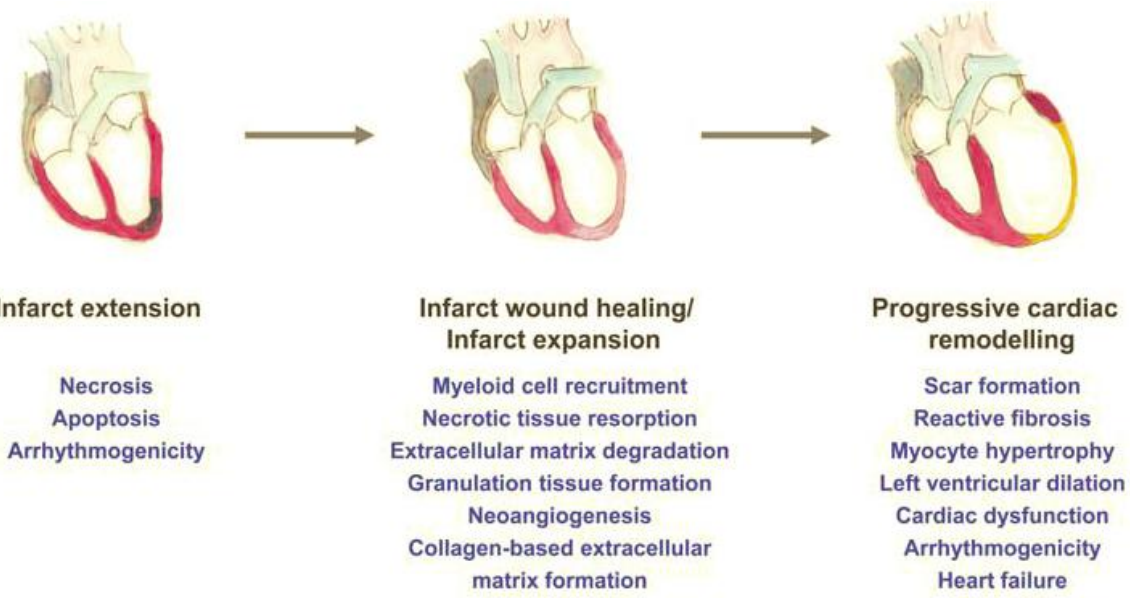
Infarct extension
Necrosis
Apoptosis
Arrhythmogenicity
Infarct wound healing/
Infarct expansion
Myeloid cell recruitment
Necrotic tissue resorption
Extracellular matrix degradation
Granulation tissue formation
Neoangiogenesis
Collagen-based extracellular
matrix formation
Progressive cardiac
remodelling
Scar formation
Reactive fibrosis
Myocyte hypertrophy
Left ventricular dilation
Cardiac dysfunction
Arrhythmogenicity
Heart failure

B

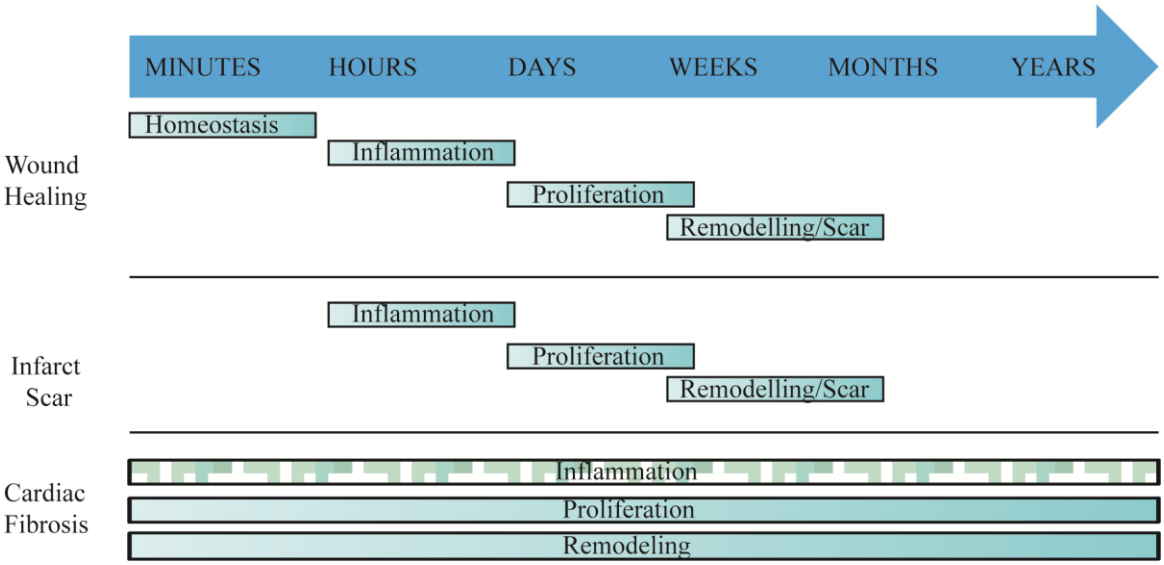
MINUTES
HOURS
DAYS
WEEKS
MONTHS
YEARS
Wound Healing
Homeostasis
Inflammation
Proliferation
Remodelling/Scar
Infarct Scar
Inflammation
Proliferation
Remodelling/Scar
Cardiac Fibrosis
Inflammation
Proliferation
Remodeling

Figure 4: A) Stages of cardiac fibrosis. Healing of a post-MI heart starts with the similar steps of tissue repair in which necrosis and cell death leads to the inflammation step of repair mechanism. In this step inflammatory cells are recruited, cell debris are removed, fibroblasts/myofibroblasts are recruited, ECM is synthesized and new blood vessels are formed to repair the injury. Persistence and continued recruitment of myofibroblasts in the scar leads to chronic remodeling and the heart gradually undergoes a process called reactive fibrosis in which distal regions also become fibrosed due to progressive ECM synthesis (figure adapted from Daniela et al., Cardiovascular research, 2012). **B) Timeline of normal wound healing Vs infarct scar and progressive cardiac fibrosis.** The timing of these events may vary according to the intensity of the wound and existing inflammatory factors. In case of normal healing the wound is almost fully healed. But, in case of cardiac fibrosis the inflammation, proliferation and remodeling stages persists for a long time (figure information adapted from Michael P Czubryt, Fibrogenesis & Tissue Repair 2012).

1.7: Zeb2

Zeb2 is a member of the zinc finger transcription factor family that plays crucial role in embryonic development and EMT. In vertebrates there are two Zeb proteins. The first member Zeb1 is also named as dEF1, Nil-2-a, Tcf8, Bzp, Areb6, Meb1, Zfhx1a and Zfhep, is a transcription factor that was found to repress the lens-specific Δ1- crystallin enhancer in chicken [93]. The second member Zeb2 is also known as Smad-Interacting Protein 1 (SIP1) or Zfhx1b, was isolated from mouse cDNA that encodes a protein which can bind the MH2 domain of *Xenopus* Smad1 (XSmad1) [94].

1.7.1: Structure of Zeb2 protein

Zeb2 protein has several functional domains. It belongs to the delta-EF1/ZFH-1 C2H2-type zinc-finger family. It contains 1 homeobox DNA-binding domain and 7 C2H2-type zinc fingers. C2H2-type Zn-finger domains are arranged into two separate clusters at two ends and a homeodomain in the centre (Figure 5). The N-terminal cluster (NZF) consists of a total of four Zn-fingers: three of which are CCHH fingers and one of them is CCHC finger. The C-terminal cluster (CZF) has three CCHH type zinc fingers. These clusters are capable of binding to the 5-CACCT(G) promoter region of the target genes. There is a high degree of identity between mouse Zeb1 and Zeb2 proteins at the nucleotide level. The sequence identity at the amino acid level for NZF is 88% and for CZF is 93% and regions outside these clusters are comparatively less conserved (Homeodomain 42%) [94].

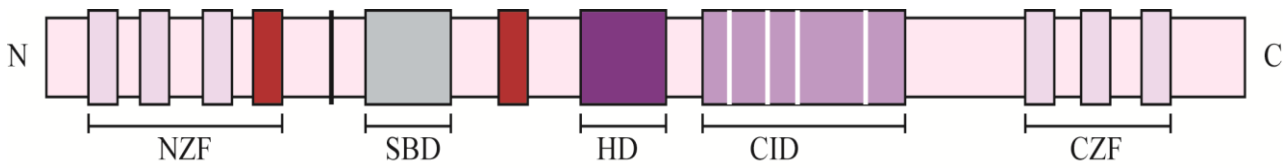

Figure 5: Schematic diagram of Zeb2 protein. It has two characteristic zinc finger (ZF) clusters, N terminal ZF and C terminal ZF and a central homeodomain (HD). There are two other domains: Smad binding domain (SBD) and the CtBP interaction domain (CID). Both N terminal and C terminal zinc finger clusters contain three CCHH fingers. N terminal zinc finger cluster contains an additional CCHC finger indicated by red colour.

1.7.2: Zeb2 in development

Studies have shown that Zeb2 is critical for enteric nervous system and skeletal muscle development [94]. *Zeb2* knockout mice were found to lack postotic vagal neural crest cells which are the precursors of the enteric nervous system. This feature is similar to patients with Hirschsprung disease [94, 95]. Moreover, these mice showed a block in the delamination of cranial neural crest cells, which leads to craniofacial defects. These data indicate that Zeb2 is required for vagal neural crest formation and for the migration of cranial neural crest cells. These embryos did not develop any specific border between the neural plate and the ectoderm and the first bronchial arch was absent. *Zeb2* null mice are embryonic lethal, suggesting that *Zeb2* is essential for neuroepithelium specification. Neural crest precursor cell specific deletion of *Zeb2* was also found to be embryonic lethal [95]. Moreover, *Zeb2* was found to be essential for cortical interneuron generation and guidance and mutations in *Zeb2* led to neurological and cardiac defects [94, 96]. These features were found to be similar to Mowat-Wilson syndrome in which *ZEB2* insufficiency causes developmental delay and craniofacial, heart and neuromuscular abnormalities [97].

1.7.3: Zeb2 in the heart

In Mowat–Wilson syndrome 50% of the patients develop heart defects at birth for example, pulmonary artery sling and stenosis, tracheal stenosis, patent ductus arteriosus and atrial septal defect etc [98-100]. Studies show that Zeb2 expressing vagal neural crest cells give rise to the cells which remodel the conotruncus outflow tract and thereby contribute to the development of two distinct circulatory systems: the pulmonic and the systemic. Moreover, they were found to form the neurons and ganglia of sympathetic and

parasympathetic cardiac innervations [101]. At E10.5, Zeb2 positive cells were found to be present in the cardiac outflow tract of mouse embryo. At E11.5, Zeb2 mutant mouse embryos displayed anemic yolk sac in spite of having blood vessels. Due to inadequate blood supply to embryonic and extra embryonic tissues, there was no heart function [101].

1.7.4: Zeb2 in EMT

Zeb2 is essential for EMT, a process which includes a set of events that leads to the loss of epithelial cell-cell contact and cell polarity [102]. EMT regulates cell migration during embryonic development and maintains tissue homeostasis in adults [103]. Epithelial cells exhibit characteristic expression of E-cadherin, a cell-cell adhesion molecule [17]. Zeb2 functions by repressing E-cadherin transcription directly. It binds to the promoter region of the E-cadherin gene and represses its expression [94]. Studies have reported that Zeb2 controls migration of breast cancer cells [104]. Similarly, expression of nuclear Zeb2 enhanced progression of EMT and acquisition of an aggressive property in ovarian cancer [105].

1.8: Meox2

Meox2 is a mesenchymal homeobox gene that belongs to the ANTP class and HOXL subclass [106]. The Meox gene family is comprised of two members- *Meox1* and *Meox2.* During mouse embryonic development, their expression is restricted to the mesodermal somites at the initial stage and in the mesenchymal tissues at the later stages. Both *Meox1* and *Meox2* are essential for the development of muscle and bone formation [107]. They contain a DNA binding specific homeodomain (Figure 6). These domains have also been found to be important for protein-protein interaction. The amino acid sequence identity of

the human MEOX1 and MEOX2 within the homeodomain is 95%, however, regions outside of this domain does not exhibit strong sequence identity (N-terminal 33%, middle domain 30% and C-terminal 0%) [108].

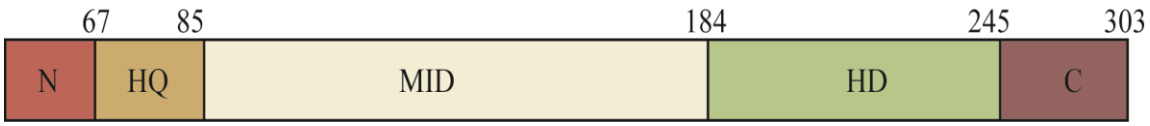

Figure 6: Schematic diagram of MEOX2 protein. It has a total of four domains: a characteristic DNA binding homeodomain (HD), N terminal and C terminal domains, histidine/glutamine rich domain (HQ) and a middle domain (MID).

1.8.1: Meox2 in the heart

Studies have shown that *Meox2* expression is mainly restricted to the cardiovascular system during post-natal development. High levels of *Meox2* transcripts were found in the adult rat heart and aorta [109]. It has been found to be expressed in VSMCs and endothelial cells of human arteries [110]. Moreover, Meox2 has been shown to be a negative regulator of VSMC, endothelial cells and cardiomyocyte proliferation [110, 111]. It has been shown to block endothelial cell migration and tube formation [111]. In adventitial fibroblasts, Meox2 blocked the pro-fibrotic action of TGF-β by binding to R-Smad complexes [111].

1.8.2: Meox2 in EMT

In mouse and humans Meox2 has been shown to be important for mesenchyme and epithelial interaction and for the correct induction of EMT during the development of palate [112, 113], teeth [114], kidney [115], and placenta [116]. Studies have shown that in human keratinocytes MEOX2 overexpression inhibited TGF-β_1 mediated EMT [117]. Moreover, knockdown of Meox2 expression leads to the increased generation of induced pluripotent stem cell (iPSC) from mouse fibroblasts via a process called mesenchymal to epithelial transition (MET) [118].

1.9: Zeb2 and Meox2 interaction

Studies have shown that increased Meox2 expression can block the pro-fibrotic TGF-β pathway and inhibits proper EMT induction. Moreover, Meox2 has been shown to bind to Smad2, Smad3 and Smad4 [117]. Recently we have reported that Meox2 overexpression can partially inhibit cardiac myofibroblast phenoconversion [119]. On the other hand,

Zeb2 is a well known inducer of EMT and miR221/Zeb2 pathway has been found to regulate the expression of Meox2. Zeb2 has been shown to repress Meox2 expression by binding to two Zeb2 consensus binding sites in the *Meox2* promoter [120].

2. CHAPTER II: RATIONALE, HYPOTHESIS & SPECIFIC OBJECTIVES

2.1: Rationale

In this study we investigated the role of the transcription factor Zeb2 in modulating the fibroblast to myofibroblast phenoconversion process, which is the key step during the development of cardiac fibrosis. Although cardiac fibrosis is a major health problem the need for effective anti-fibrotic therapies remains unmet as the underlying mechanisms are still poorly understood [15, 121]. Therefore, it is crucial to better understand the molecular mechanisms leading to chronic fibrosis in order to improve outcomes for patients. Following a myocardial infarction, phenoconverted cardiac myofibroblasts migrate to the injured area, secrete collagens, express focal adhesion molecules and contractile proteins to help repair the infarct zone [85]. Various factors that contribute to this process include hormones, such as angiotensin II, endothelin I and profibrotic cytokines such as TGF-β, CCN2/CTGF, PDGF. These factors induce the phenoconversion of fibroblasts to myofibroblasts which synthesize and contract ECM [121]. However, the broad targeting of these pro-fibrotic pathways has unwanted side effects, which necessitates the discovery of rationally designed anti-fibrotic drugs [121]. Among the various pro-fibrotic factors, TGF-β is considered to be the most potent [15]. It induces mesenchymal cells to proliferate and produce ECM during normal tissue repair process. TGF-β has also been found to induce expression of the ED-A fibronectin splice variant which in turn triggers TGF-β mediated synthesis of fibrillar collagens and α-SMA. Moreover, it regulates MMP activity by enhancing the expression of their inhibitors and ultimately causing rapid ECM remodeling during wound healing process. As a result aberrant TGF-β signaling is directly associated with the pathogenesis of chronic fibrotic diseases [122]. Among the three TGF-β (β_1, β_2

and β_3) isoforms, TGF-β_1 is the most abundant isoform in the heart and has been found to be associated with diabetic nephropathy, ulcerative colitis, hepatic fibrosis and cardiac fibrosis [123-125]. TGF-β_1 can both inhibit and induce cell proliferation which makes it more challenging to block this pathway for therapeutic purpose [126]. TGF-β_1 null mice are embryonic lethal due to aberrant cardiac and pulmonary inflammation [127]. Mice lacking Smad3 exhibits cardiac fibroblast dysfunction and incomplete infarct healing [128]. Blocking TGF-β_1–Smad pathway globally induces uncontrolled endothelial cell proliferation [129]. TGF-β_1 heterozygous null mice showed decreased apoptosis and increased cell proliferation in hepatocyte and mammary epithelial [130].

Previous studies have reported that the homeodomain transcription factor Meox2, a negative growth regulator of cell proliferation, has the potential to block the pro-fibrotic action of TGF-β by binding to R-Smad complexes in fibroblasts [111]. Recently our group has shown that Meox2 partially blocks the myofibroblast phenoconversion process by downregulating two key myofibroblast markers- α-SMA and ED-A fibronectin [119]. Zeb2 is a known repressor of Meox2 and enhances EMT process in concert with TGF-β [85, 120]. However, the role of Zeb2 in fibroblast to myofibroblast phenoconversion remains elusive. Our group has reported that Ski, a protooncogene, can prevent myofibroblast phenoconversion by downregulating Zeb2 which in turn causes up-regulation of Meox2 [119]. Thus, we predict that Zeb2 plays a crucial role in myofibroblast formation either directly and/or indirectly by inhibiting the anti-fibrotic Meox2 pathway.

2.2: Hypothesis

Our hypothesis is that Zeb2 is a critical contributor to the fibroblast to myofibroblast phenoconversion process *in vitro*. Zeb2 can promote the myofibroblast phenotype by enhancing the expression of myofibroblast markers and by inhibiting the anti-fibrotic Meox2 pathway (Figure 7).

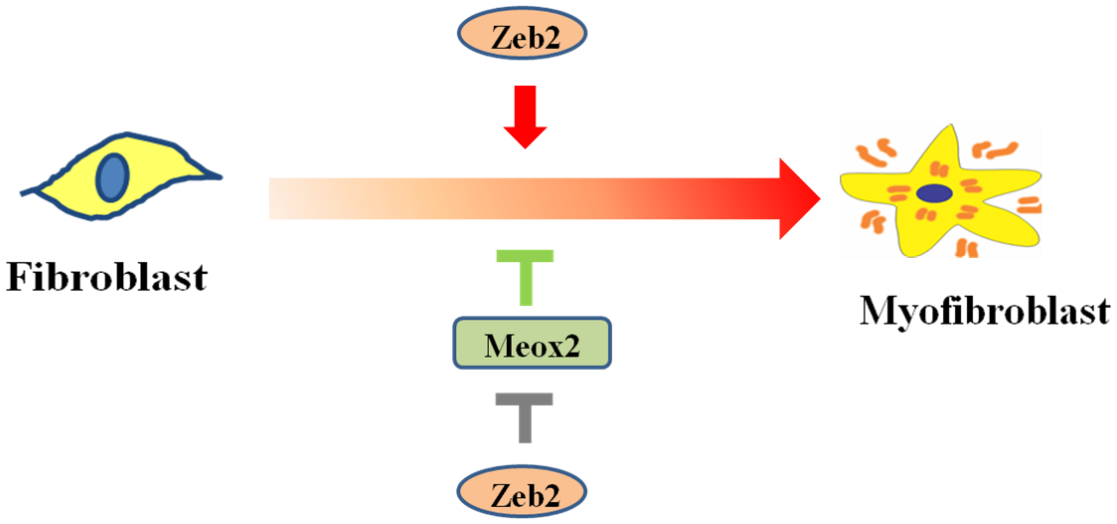

Figure 7: Hypothesis: Zeb2 is a critical contributor to the fibroblast to myofibroblast phenoconversion process *in vitro*. Zeb2 can promote the myofibroblast phenotype by enhancing the expression of myofibroblast markers and by inhibiting the anti-fibrotic Meox2 pathway.

2.3: Specific Objectives

Objective 1: Compare the levels of expression and subcellular localization of Zeb2 and Meox2 during the phenoconversion of fibroblast to myofibroblast *in vitro*.

To achieve this aim, we have used primary rat cardiac fibroblasts as an *in vitro* experimental model. Primary fibroblasts spontaneously phenoconvert to myofibroblasts when cultured on standard tissue culture plastic plates, thus passage 0 (P0) cells were considered to be fibroblasts and P1 and P2 cells were considered as phenoconverted myofibroblasts. Western blotting and immunofluorescence techniques were used to determine the expression pattern of Zeb2 and Meox2.

Objective 2: Study the effect of Zeb2 on the myofibroblast phenotype and function *in vitro*.

To study the effect of increased Zeb2 expression on the phenoconversion process, P1 myofibroblasts were infected with either adenovirus encoding HA epitope tagged Zeb2 (Ad.HA.Zeb2) or adenovirus encoding enhanced green fluorescence protein (Ad.EGFP) or LacZ (Ad.LacZ) viral controls at 200 multiplicity of infection (MOI). Cultures were assessed at different time points of post infection (24h, 48h, 72h and 96h). For assessing the effect of Zeb2 gain of function on myofibroblast phenotype, we have employed Western blotting technique. We determined the expression levels of the well characterized myofibroblast markers such as α-SMA, SMemb and ED-A fibronectin. Functional changes in parameters such as myofibroblast migration and contractility were determined by performing the wound healing migration assay and the collagen gel contraction assay, respectively.

3. CHAPTER III: MATERIALS & METHODS

3.1: Cell isolation and culture

Approval for experimental protocols for animal studies was received from the Animal Care Committee of the University of Manitoba, Canada, and the protocols conform to the guidelines established by the Canadian Institutes of Health Research and the Canadian Council on Animal Care. For the isolation of cardiac fibroblasts, hearts from adult male Sprague-Dawley rats (150–200 g) were obtained. The Langendorff perfusion method was performed with Dulbucco's Modified Eagle's Medium (DMEM)/F12 (Gibco, Carlsbad, CA) followed by Spinner Minimum Essential Medium (SMEM) (Gibco, Carlsbad, CA). After perfusion, hearts were digested with 0.1% w/v collagenase type 2 (Worthington) in SMEM for 20 minutes at room temperature. Hearts were then transferred to 10 cm^2 plate and minced in 10 mL of diluted collagenase solution (0.05% w/v) for 15 minutes. Then growth medium [DMEM-F12 supplemented with 10% fetal bovine serum (FBS), 100 U/ml penicillin (Gibco, Carlsbad, CA), 100 µg/mL streptomycin (Gibco) and 1 µM ascorbic acid (Sigma, St Louis, MO)] was added. Large tissue pieces were allowed to settle to the bottom of a 50 ml conical tube and the supernatant was transferred to another conical tube and subjected to centrifugation at 2000 rpm for 5 minutes. Cell pellets were resuspended in growth medium and plated on to 10 cm^2 plates. Cells were allowed to adhere for 3-4 hours in a 5% CO_2 incubator at 37°C, then washed 2-3 times with phosphate-buffered saline (PBS) and fresh growth medium was added. The following day, cells were washed with PBS twice and fresh medium was added and cells were allowed to grow for 2-3 days before passaging (Figure 8). After that Passage 0 (P0) cells were

passaged to P1 myofibroblasts. After 48 hours, P1 cells were further passaged to P2 myofibroblasts.

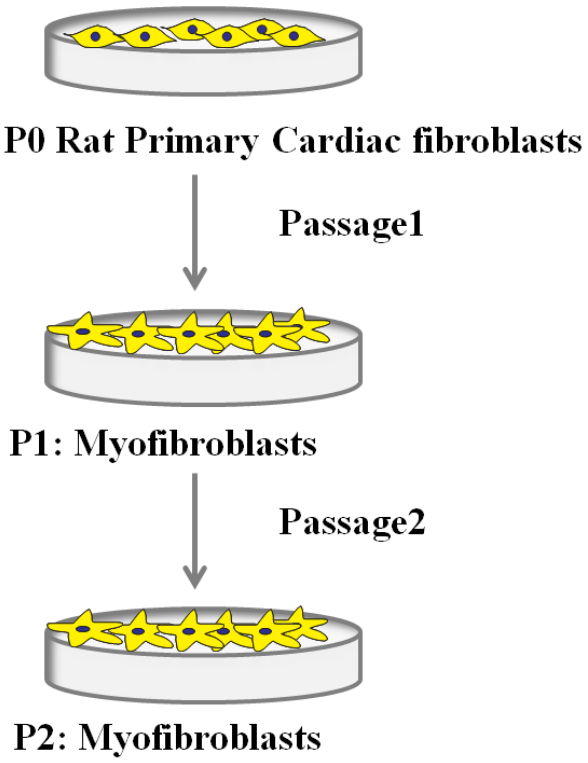

Figure 8: Culture conditions for Passage 0 (P0) rat cardiac fibroblasts and P1 and P2 rat cardiac myofibroblasts. P0 cells were allowed to grow for 2-3 days. P0 cells were then passaged to P1 myofibroblasts. After 48 hours, P1 cells were further passaged to P2 myofibroblasts.

Human embryonic kidney cells (HEK293) from ATCC (Manassas, USA), were cultured using DMEM/High Glucose (Supplemented with 4.0 mM L-glutamine and sodium pyruvate, Hyclone) containing 5% FBS and 100 U/ml penicillin (Gibco, Carlsbad, CA), 100 µg/mL streptomycin (Gibco, Carlsbad, CA). Human umbilical vein endothelial cells (HUVECs) were cultured using endothelial cell growth medium (EGM-2 Bullet kit) (Clonetics) supplemented with 2% FBS, 0.1% human epidermal growth factor (rhEGF), 0.1% vascular endothelial growth factor (VEGF), 0.1% R3-insulin-like growth factor-1 (R3-IGF-1), 0.1% ascorbic acid, 0.04% hydrocortisone, 2% human fibroblast growth factor-beta (rhFGF-β), 0.1% gentamicin/amphotericin-B (GA) and 0.1% heparin. In case of HUVECs, cells of passages 5-7 were used for experiments.

3.2: Total cell lysate

Following incubation, cells were washed twice with 1x PBS and RIPA lysis buffer (50 mM, 150 mM NaCl, 1 mM EDTA, 1 mM EGTA, 1% Triton X-100, 1% NaDeoxycholate, 1% SDS, pH=7.4) containing Complete Mini Protease Inhibitor Cocktail (Roche) was added to lyse cells. Cells were then mechanically scraped and lysates were vortexed once and incubated on ice for 45 minutes. Lysates were vortexed again and centrifuged at 14,000 rpm at 4°C for 10 minutes. Supernatants were transferred to new tubes and protein assay was performed using the DC protein assay [131].

3.3: Nuclear/cytoplasmic fractionation

P0 cardiac fibroblasts were allowed to grow for 72 hours to achieve ~70% confluency before harvesting. To generate P1 myofibroblasts, P0 cells were passaged at 72 hours and

allowed to grow for 48 hours to either harvest or passage to P2 cells. Similarly, P2 myofibroblasts were allowed to grow for 48 hours before harvesting. Fractionation was then carried out using the NE-PER Nuclear and Cytoplasmic Extraction Reagents (Pierce Biotechnology) according to the manufacturer's instructions. Cytoplasmic Extraction Reagent I (CER I), CER II and Nuclear Extraction Reagent (NER) were used at 200:11:100 μL volume ratios, respectively. Briefly, cells were harvested with trypsin-EDTA (3 minutes, at 37°C) and neutralized with 10% FBS containing DMEM F-12 medium. Cell suspension was then centrifuged at 5000 rpm for 5 minutes. Cells were washed by resuspending the cell pellet with 1 mL PBS and the suspension was then transferred to a 1.5 mL microcentrifuge tube and centrifuged at 5000 rpm for 5 minutes at 4°C. Supernatant was discarded and 200 μL of ice cold CER I was added to the cell pellet. To suspend the pellet, the tube was vortexed vigorously for 15 seconds and kept on ice for 10 minutes. 11 μL of ice-cold CER II was added to the tube and vortexed for 5 seconds. After 1 minute of incubation on ice, lysates were vortexed again and centrifuged at 14,000 rpm for 5 minutes at 4°C. The supernatant (cytoplasmic extract) was transferred to a pre-chilled tube. The insoluble fraction (nuclei) was resuspended in 100 μL of NER and vortexed for 15 seconds. Samples were kept on ice and vortexed for 15 seconds every 10 minutes (a total of 40 minutes). Samples were then centrifuged at 14,000 rpm for 10 minutes at 4°C. The supernatant (nuclear extract) was immediately transferred to a pre-chilled tube. Samples were stored at -80°C until use. Protein assay was performed using the DC protein assay [131].

3.4: Testing of Meox2 and Zeb2 antibodies

Mouse HA tagged Zeb2 pcDNA3.1 or FLAG tagged 4AMeox2 plasmids were transfected into HEK293 cells. Briefly, 5 x 10^5 cells were seeded onto 6 cm^2 plates and grown overnight in 2 mL of 5% FBS containing DMEM medium. The following day, feeding medium was replaced with 2 mL of 2% FBS containing reduced serum medium called Opti-MEM (Gibco, Carlsbad, CA). Control plasmids pcDNA3.1 or 4A; or plasmids encoding transcription factors pcDNA3.1-HA.Zeb2 or 4A-Meox2-FLAG were suspended in Opti-MEM (serum free) in separate tubes and were mixed mildly and incubated for 5 minutes at room temperature. In two tubes, 96 µL of basal medium (DMEM without serum) and 4 µL of Lipofectamine-2000 (Invitrogen) were added and mixed gently. Lipofectamine solution was then added to tubes containing DNA and mixed gently. Lipofectamine-DNA mixtures were incubated for 20 minutes at room temperature. Then solutions were added to the cells and incubated for 4 hours in 5% CO_2 incubator at 37°C. After 4 hours, Opti-MEM was replaced with the feeding medium (5% FBS containing DMEM) and incubated for 48 hours for harvesting protein.

3.5: siRNA mediated knockdown of Meox2

5 x 10^5 HUVECs were plated onto 6 cm^2 plates and allowed to grow overnight in 2% FBS containing EGM-2 medium. The next day, the medium was replaced with fresh medium (2% FBS containing EGM-2). 2 µM of either Control siRNA or Meox2 siRNA was suspended in 100 µL of basal medium (EBM-2 without serum) in a microcentrifuge tube and vortexed gently. In another tube, 96 µL of basal media and 4 µL of Dharmafect (Dharmacon) were mixed mildly. After 5 minutes, solutions from two tubes were mixed

together and incubated for 20 minutes at room temperature. Then the siRNA-Dharmafect solution was added to the cells and incubated for 48 hours in 5% CO_2 incubator at 37°C. Subcellular fractions were obtained as described previously.

3.6: Western blot analysis

SDS-PAGE of 10-25 µg of protein was performed on 8 or 10% polyacrylamide gels. Pre-Stained Standard (Bio-Rad, Hercules, CA) molecular mass marker was used as a standard. Proteins were transferred to a 0.45 µM nitrocellulose membrane (Bio-Rad, Hercules, CA) using an electrophoretic transfer tank. Membranes were stained with Ponceau S solution (0.1% w/v Ponceau S- Fisher, 5% v/v acetic acid) to verify protein transfer. Membranes were destained by washing with 1x Tris buffered saline (TBS). Membranes were then blocked in 1x TBS containing 5% skimmed milk for 1 hour at room temperature with constant shaking. Primary antibodies were diluted in 1x TBS with 5% skimmed milk as follows: Zeb2 (1:1000) (Sigma), α-tubulin (1:5000) (Abcam, Cambridge, UK), α-SMA (1:5000) (Sigma), ED-A fibronectin (1:1000) (Millipore), FLAG (1:2000) (Sigma), SMemb (1:1000) (Abcam), HA (1:1000) (Rockland), Meox2 [JJ-7] (1:1000) (Santa Cruz Biotechnology, Santa Cruz, CA), Lamin A+C (Millipore) and Glyceraldehyde 3-phosphate dehydrogenase (GAPDH) (1:2000) (Abcam) [Table 1]. Membranes were incubated for 1 hour at room temperature or overnight at 4°C with shaking. Zeb2, Meox2, Lamin A+C, HA, GAPDH and SMemb antibodies were incubated overnight while α-SMA, ED-A fibronectin, FLAG and Tubulin antibodies were incubated for 1 hour at room temperature. Secondary antibodies were horseradish peroxidase (HRP)-conjugated goat anti-rabbit or goat anti-mouse antibodies, which were diluted at 1:5000 with 1x TBS containing 5% skimmed milk and incubated for 1 hour at room temperature with constant shaking. Equal

protein loading was confirmed using α-tubulin, GAPDH or Lamin A+C. Protein bands were detected using Western Blotting Luminol Reagent (Santa Cruz Biotechnology) and images were developed on CL-Xposure blue X-ray films using Flour S Max Multi Imager (Biorad, Hercules, CA). Protein expression was quantified by taking adjusted volume of bands measured via densitometry (GS-800 Calibrated Densitometer, Bio-Rad, USA) using QuantityOne software (Bio-Rad, USA). Adjusted volumes of bands were normalized by the respective loading controls.

Table 1: List of primary antibodies and the dilution conditions

Antibodies	**Company**	**Clonality**	**Host**	**Dilution**
α-SMA	Sigma	Monoclonal	Mouse	1:5000
GAPDH	Millipore	Monoclonal	Mouse	1:2000
ED-A fibronectin	Millipore	Monoclonal	Mouse	1:1000
FLAG	Sigma	Polyclonal	Rabbit	1:2000
HA	Rockland	Polyclonal	Rabbit	1:1000
Lamin A+C	Millipore	Monoclonal	Mouse	1:1000
Meox2	Santa Cruz	Monoclonal	Mouse	1:1000
SMemb	Abcam	Monoclonal	Mouse	1:1000
α-Tubulin	Abcam	Monoclonal	Mouse	1:2000
Zeb2	Sigma	Polyclonal	Rabbit	1:1000

3.7: Immunofluorescence:

Cells were allowed to grow up to 48 hours for each passage. After incubation of 48 hours, cells were washed with 1x PBS and fixed with 4% paraformaldehyde (PFA) for 10 minutes. Cells were then washed twice for 10 minutes with 1x PBS and permeabilized with 1x PBST (0.2% Triton X-100) for 15 minutes followed by two additional washes in 1x PBS for 5 minutes each. Slides were blocked with 5% goat serum (GS) in 1x PBST for 1 hour, washed with 1x PBST, and incubated overnight in primary antibody (Zeb2- 1:350, Meox2- 1:100) diluted in 1x PBST containing 5% GS at 4°C. Cells were washed three times with 1x PBS and incubated with Alexa Fluor-conjugated secondary antibody (Invitrogen) for 1 hour followed by three times 10 minutes washing with 1x PBS. Using a vacuum, solution was removed and cover slips were mounted on slides using Slowfade gold with DAPI mounting media (Thermofisher) and sealed with nail polish.

3.8: Adenoviral constructs

Ad.EGFP was a gift from Dr. Pierce (University of Manitoba) and Ad.LacZ was a gift from Dr. M. Czubryt (University of Manitoba). Ad.HA.Zeb2 virus was constructed in our laboratory using the pAdEasy™ Adenoviral Vector System protocol (Aligent technologies). Briefly, adenovirus encoding N-terminal HA-tagged Zeb2 (mouse) was created by excising the Zeb2 cDNA from pcDNA 3.1 (Figure 9) by restriction digestion with *Kpn*I and *Xba*I enzymes. Zeb2 cDNA was cloned into the pShuttle-CMV vector. pShuttle-Zeb2 plasmid DNA was linearized using *Pme*I and complete digestion was confirmed by agarose gel electrophoresis. Once complete digestion with *Pme*I was confirmed, DNA was purified by the Stratagene StrataPrep PCR purification kit. The

purified DNA was treated with alkaline phosphatase for 30 minutes at 37°C. Agarose gel electrophoresis was used to visualize and confirm linearized, dephosphorylated pShuttle vector and DNA was gel purified. 1 μg of linearized, dephosphorylated pShuttle-CMV-Zeb2 vector and 100 ng of pAdEasy vector were co-transformed into BJ5183 competent *E. coli* cells by electroporation. Recombinants were selected by kanamycin resistance and confirmed by doing restriction digestion and gel electrophoresis. Recombined plasmids were transferred into DH5α cells for isolation of DNA. Recombinants were digested with *Pac*I to release both inverted terminal repeats (ITRs). Recombinants were then transfected into HEK293 cells that allows adenovirus production from backbone vectors since they express E1 gene essential for adenovirus production. Recombinant adenoviruses were generated in 20 days. Cells were harvested and primary viral stock was prepared. Primary stock was then amplified using HEK293 cells and viruses were purified. Finally, Ad.HA.Zeb2 virus titration was performed using Adeno-X™ Rapid Titer Kit (Clontech Laboratories, Takara Bio Inc.). Briefly, serial dilutions of adenovirus were prepared and HEK293 cells were infected. After 48 hours, the cells were fixed and labelled with hexon specific antibody (Clontech Laboratories, Takara Bio Inc.) and a HRP-conjugate antibody. Bound antibodies were detected with DAB Substrate which labels positive cells as brown. Positive cells were counted under a 20x objective and pfu was calculated by taking the average number of positive cells/unit dilution (Figure 10).

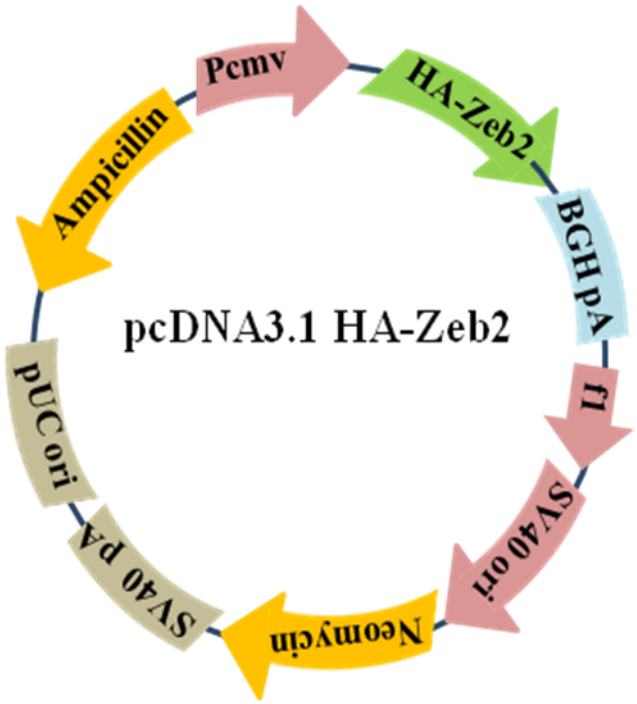

Figure 9: pcDNA3.1 HA-Zeb2 plasmid. pcDNA3.1 mammalian expression vector encodes HA tagged mouse Zeb2. The expression vector contains CMV promoter, neomycin selection marker, Bovine Growth Hormone (BGH) polyadenylation signal and transcription termination sequence to provide mRNA stability, SV40 origin for episomal replication, ampicillin resistance gene and pUC origin for selection and maintenance in *E. coli*.

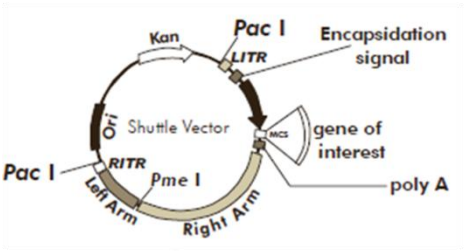

pShuttle-CMV-HA-Zeb2

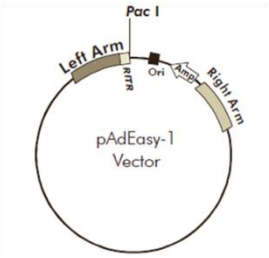

pAdEasy-1 DNA

Linearization with *Pme*I

Cotransformation in BJ5138 and recombination

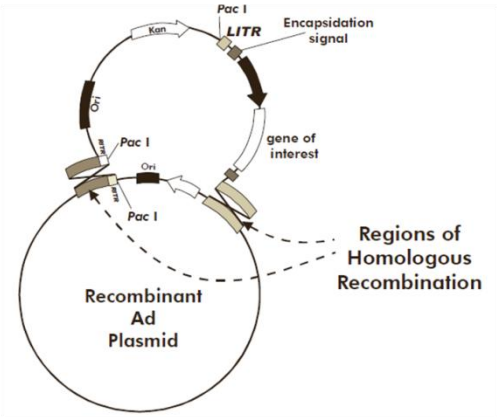

Recombination

Selection of recombinants

Amplification in DH5α

Linearization and transfection into HEK293 cells

Plaque formation and screening of recombinant virus

Amplification and purification

Virus titration

Figure 10: Production of Ad.HA.Zeb2 virus. Steps of virus production: Zeb2 cDNA was cloned into the pShuttle-CMV vector, pShuttle-Zeb2 plasmid DNA was linearized using *Pme*I, pShuttle-Zeb2 and pAdEasy vector were cotransformed in BJ5138, recombinants were selected and amplification in DH5α cells, recombinants were linearized with *Pac*I and transfected into HEK293 cells for plaque formation, viruses were screened, amplified, purified and titred. Images of vectors were adapted from instruction manual of Aligent technologies. [http://www.agilent.com/cs/library/user manuals/public/240009.pdf]

3.9: Zeb2 overexpression in P1 cardiac myofibroblasts

For Western blotting, 1.4 x 10^5 P1 rat cardiac myofibroblasts were plated onto 6 cm^2 plates in 2mL of 10% FBS containing DMEM-F12 medium and infected with either Ad.EGFP or Ad.HA.Zeb2 at a multiplicity of infection (MOI) of 200 and incubated in 5% CO_2 incubator at 37°C. The following day, feeding medium was replaced with 1% FBS containing DMEM-F12 medium and incubated for another 72 hours (Figure 11).

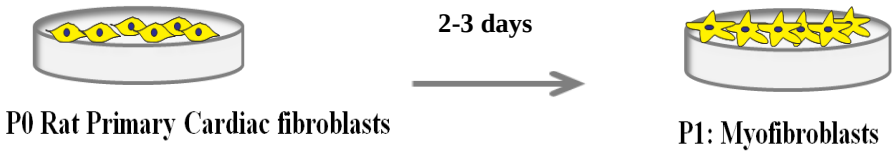

Figure 11: Culture conditions for Zeb2 overexpression in P1 rat cardiac myofibroblasts. P0 cells were allowed to grow for 2-3 days and then passaged into P1 myofibroblasts. Cells were infected at the time of plating and the following day feeding medium was replaced with 1% FBS containing DMEM-F12 medium.

3.10: Wound healing migration assay

P1 cardiac myofibroblasts (2.5 x 10^4 cells in 70 µL of 10% FBS containing DMEM-F12 medium) were plated inside culture inserts (ibidi GmbH, Germany) and grown overnight in 5% CO_2 incubator at 37°C. The following day, cells were transduced with either Ad.EGFP (200 MOI) or Ad.HA.Zeb2 (200 MOI) and incubated for 96 hours in 10% FBS containing DMEM-F12 medium. After 96 hours, culture inserts were carefully removed and cells were washed with 1x PBS and medium was replaced with 1% FBS containing DMEM-F12 medium. Images were taken at 0 hour, 6 hours, 12 hours, 18 hours and 24 hours using a 4x objective (Figure 12).

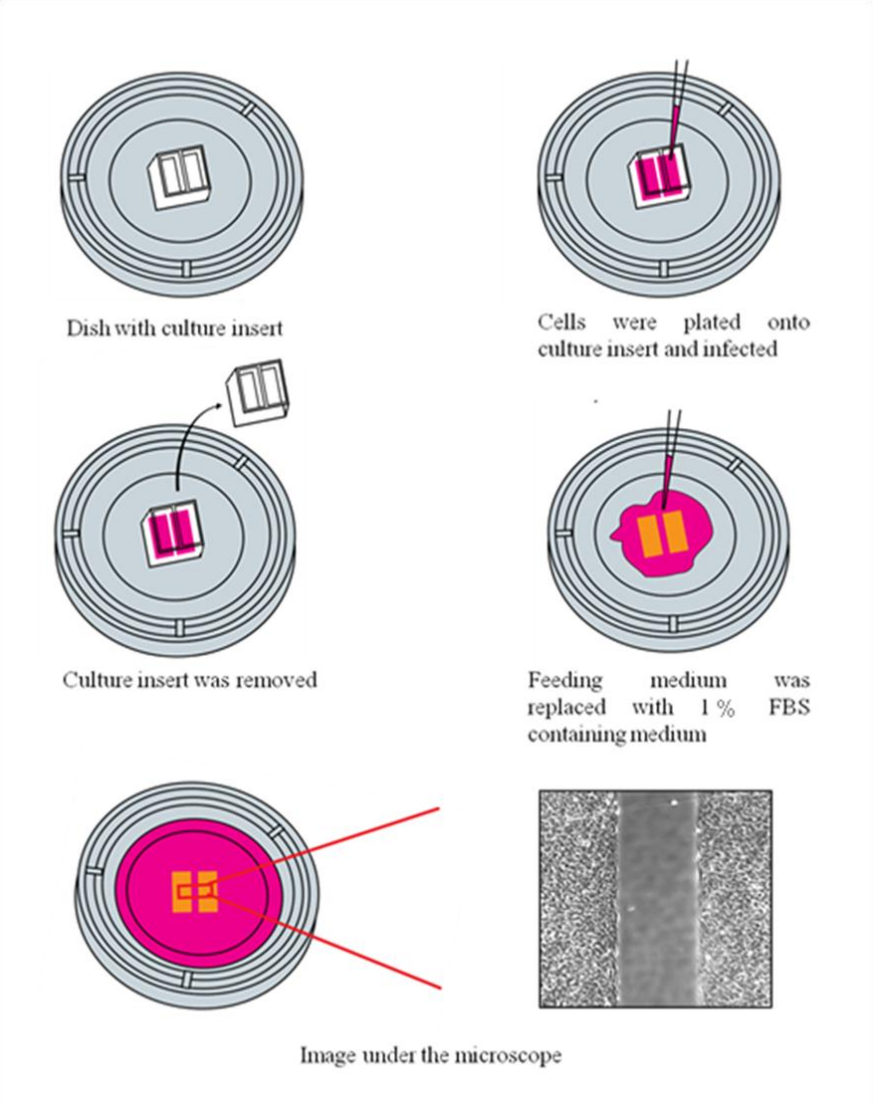

Figure 12: Wound healing migration assay procedure. P1 cells were transduced with either Ad.EGFP or Ad.HA.Zeb2 (200 MOI) and after 96 hours culture inserts were removed and medium was replaced with 1% FBS containing DMEM-F12 medium and images were taken.

3.11: Collagen gel contraction assay

7 ml of cold collagen I solution (Worthington) was mixed with 2 ml of 5x culture medium (DMEM-F12 without serum and antibiotics) in a 50 ml centrifuge tube. pH of solution was checked by removing a small volume with a pipette and blotting on a pH paper. Optimal pH was between 7–7.5. Volume was then adjusted to 10 ml with ddH_2O. Solution was then mixed and kept in the 4°C refrigerator for a few minutes to allow bubbles to dissipate. After that, 500 µL of aliquot was added per well of a 24-well plate. Gels were allowed to solidify by incubating at 37°C for minimum 3 hours or overnight. P1 cells (5×10^4 per well) were then plated on to wells and transduced with either Ad.LacZ (200 MOI) or Ad.HA.Zeb2 (200 MOI) in 10% FBS containing DMEM-F12 medium. The following day, medium was replaced with 1% FBS containing DMEM-F12 medium and incubated for another 48 hours. After 48 hours of incubation, medium was replaced with fresh serum free DMEM-F12 medium. Gels were cut around the edges using pipette tips. Images were taken at 0 hour and 12 hours. Using IDL Measure gel software, gel surface area was determined at each time point (Figure 13).

.

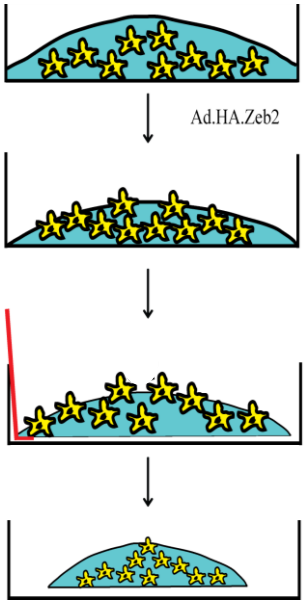

Gels were prepared. Cells were plated on solidified gel and infected.

Following day, medium is replaced with 1% FBS containing DMEM-F12 and incubated for 48 hours.

Gels were then cut and allowed to contract for 12 hours. Images are taken at time 0 hour and 12 hours.

Figure 13: Collagen gel contraction assay procedure. P1 cells were plated on collagen gels and transduced with either Ad.LacZ (200 MOI) or Ad.HA.Zeb2 (200 MOI) and following day growth medium was replaced with 1% FBS containing DMEM-F12 and incubated for 48 hours. After 72 hours, collagen gels were cut and allowed to contract for 12 hours. Images were taken at 0 hour and 12 hours time points.

3.12: F-actin staining for stress fibers

P1 myofibroblasts (1.5 x 10^3) were plated on chamber slides and transduced with either Ad.LacZ (200 MOI) or Ad.HA.Zeb2 (200 MOI) and grown overnight in 1 mL of 10% FBS containing DMEM-F12 medium in a 5% CO_2 incubator at 37°C. The following day, feeding medium was replaced with 1% FBS containing DMEM-F12 medium. Cells were then fixed with 4% PFA at different time points: 16 hours, 24 hours, 48 hours and 72 hours and stained with rhodamine phalloidin stain (Life technologies) and counterstained with DAPI.

3.13: Zeb2 overexpression in endothelial cells

3 x 10^5 HUVECs were plated onto 6 cm^2 plates in 2 ml of 2% FBS containing EGM-2 medium and infected with either Ad.EGFP or Ad.HA.Zeb2 at 200 MOI. Cells were incubated in 5% CO_2 incubator at 37°C for 72 hours and harvested for protein.

3.14: Statistical analysis

All the experiments were repeated with 3 biological replicates (n=3). For primary cells different rats have been used as cell source. Student's t-test was used to compare two samples and one-way analysis of variance (ANOVA) with Brown-Forsythe test for equal variance and Tukey post-hoc analysis was used for experiments with multiple samples and results with $P \leq 0.05$ were considered statistically significant.

4. CHAPTER IV: RESULTS

4.1: Expression of Zeb2 is increased in myofibroblasts

To investigate the role of Zeb2 in myofibroblast phenoconversion, we first determined the expression levels of Zeb2 protein in P0 cardiac fibroblasts and P1 and P2 myofibroblasts. We tested two rabbit anti-Zeb2 polyclonal antibodies from- Sigma and Santa Cruz. A pcDNA3.1 plasmid vector encoding HA tagged mouse Zeb2 was transfected into HEK293 cells. After 48 hours, we performed Western blotting and probed blots with both HA or the two Zeb2 antibodies. We found both of the antibodies detected Zeb2 at the same size as HA antibody (approximately 171 kDa) (Figure 14). However, the Zeb2 antibody from Sigma gave a stronger signal (Figure 14). The antibodies also detected additional lower bands on the blots which might be due to non-specific reactions of the antibodies since the size of the lower band was different in each case. To determine the expression of Zeb2 protein in fibroblasts and myofibroblasts, we have used P0 rat cardiac fibroblasts and P1 and P2 myofibroblasts as our model. P0 fibroblasts were grown for 48 hours and harvested for protein or passaged for P1 myofibroblasts. P1 myofibroblasts were grown for 48 hours and either harvested for protein lysate or passaged to P2 myofibroblasts. P2 myofibroblasts were also allowed to grow for 48 hours before harvesting. By Western blotting, Zeb2 protein was found to be highly expressed in P1 and P2 myofibroblasts but not expressed in the P0 fibroblasts ($n=3$, $p \leq 0.01$) (Figure 15). This data suggested that Zeb2 may be regulating the transition from fibroblast to myofibroblast.

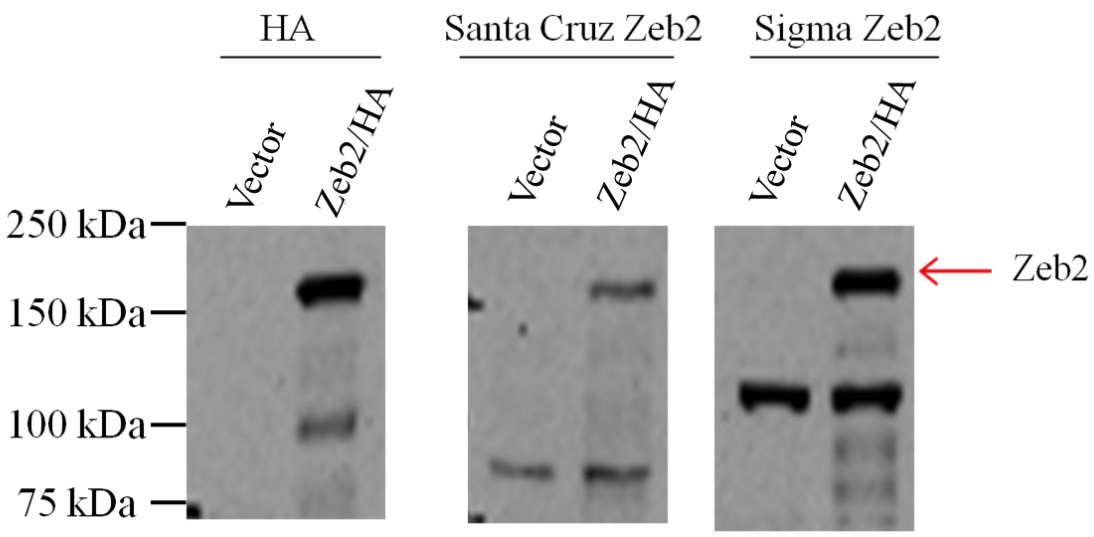

Figure 14: Comparison of Zeb2 antibodies. Rabbit polyclonal Zeb2 antibodies from Sigma and Santa Cruz were tested. HA tagged Zeb2 pcDNA3.1 (Zeb2/HA) or empty pcDNA3.1 (vector) were transfected into HEK293 cells and incubated for 48 hours. Both of the antibodies detected Zeb2 at the same size as HA antibody (approximately 171 kDa). Zeb2 antibody from Sigma gave a stronger signal as compared to Zeb2 antibody from Santa Cruz.

A

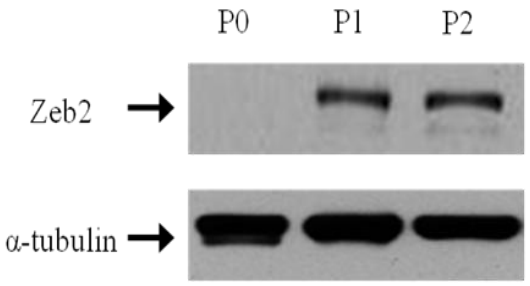

B

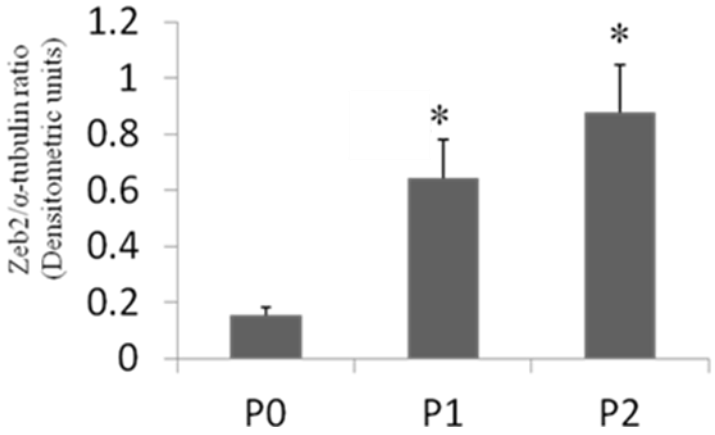

Figure 15: Zeb2 expression is elevated in rat cardiac myofibroblasts as compared to fibroblasts. A) Zeb2 protein expression was examined via Western blot using α-tubulin as a loading control. B) Histographic representation of data in Panel A. The data shown are from n=3 independent experiments; *P < 0.01 vs. P0. Error bars represent standard error of the mean (SEM). Data were analyzed by ANOVA with Brown-Forsythe test for equal variance and Tukey post-hoc analysis.

4.2: Subcellular distribution of Zeb2 in fibroblasts and myofibroblasts

After determining Zeb2 expression at the total protein level, we determined the subcellular localization of Zeb2. For this purpose, P0 fibroblasts were grown for 72 hours to achieve ~70% confluency before harvesting in order to have sufficient starting material. Similarly, for P1 cardiac myofibroblasts, P0 cells were grown for 72 hours and passaged to P1 cells. P1 myofibroblasts were grown for 48 hours and either harvested for protein lysate or passaged to P2 myofibroblasts. P2 myofibroblasts were also allowed to grow for 48 hours before harvesting. By Western blotting, Zeb2 protein was found to be highly expressed in P1 myofibroblast nuclei as compared to P0 fibroblast ($n=4$, $p \leq 0.05$) (Figure 16). However, Zeb2 expression levels decreased in P2 myofibroblast nuclei. In this experiment, lamin A/C was used as a nuclear loading control and GAPDH was used as a cytoplasmic loading control.

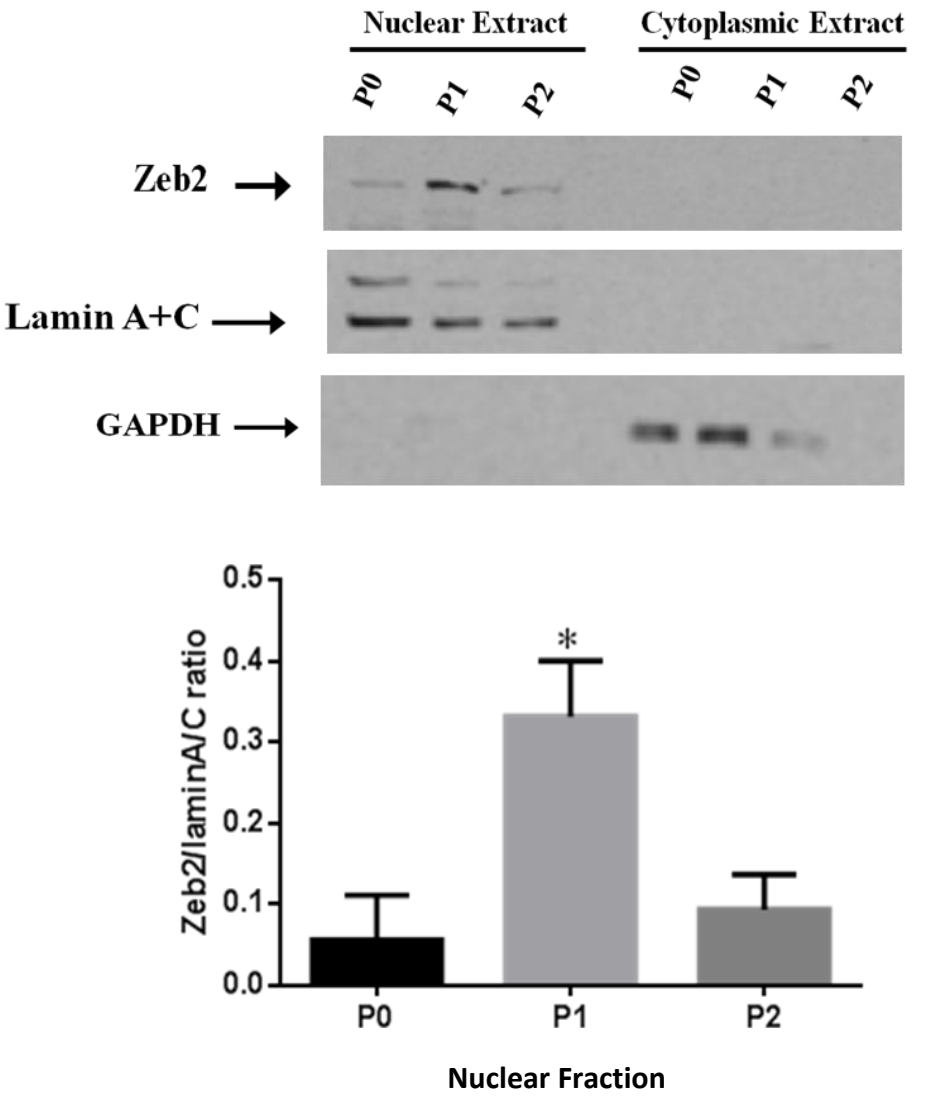

Figure 16: Subcellular distribution of Zeb2 in rat cardiac fibroblasts and myofibroblasts. Zeb2 protein expression was enriched in the nuclear fractions from P1 rat cardiac myofibroblasts as compare to P0 fibroblasts and the expression levels decreased in P2 myofibroblasts. Lamin and GAPDH were used as nuclear and cytoplasmic loading controls, respectively. The data shown are from n=4 independent experiments, *P $\leq$ 0.05 vs. P0. Error bars represent SEM. Data were analyzed by ANOVA with Brown-Forsythe test for equal variance and Tukey post-hoc analysis.

4.3: Subcellular localization of Zeb2 protein

To confirm the subcellular fraction data, we performed immunocytochemical staining. P0 fibroblasts were grown up to 48 hours and either fixed with 4% PFA or passaged for P1 myofibroblasts. Similarly, P1 myofibroblasts were allowed to grow up to 48 hours and either fixed with 4% PFA or passaged to P2 myofibroblasts. P2 myofibroblasts were also allowed to grow for 48 hours before fixing with 4% PFA. Nuclear localization of Zeb2 protein (green) was observed in both P1 and P2 myofibroblasts. Low levels of cytoplasmic distribution were also seen. DAPI (blue) was used as a nuclear stain (Figure 17).

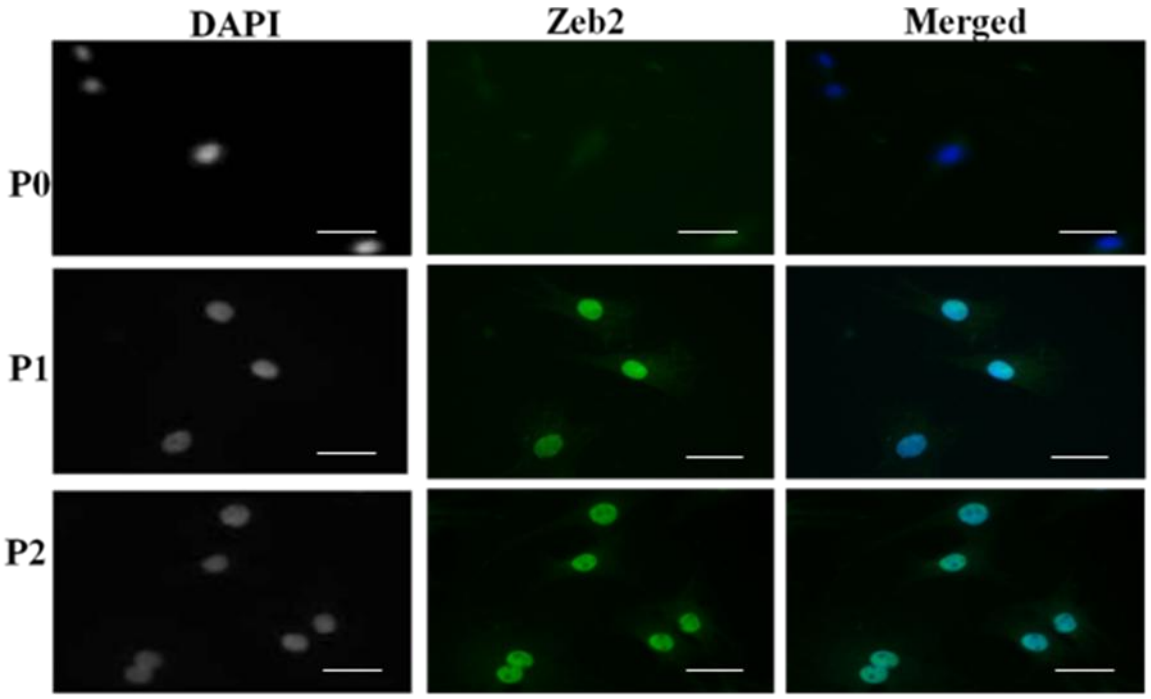

Figure 17: Zeb2 is localized to the nuclei of rat cardiac myofibroblasts. Nuclear localization of Zeb2 was observed in P1 and P2 myofibroblasts. Low level of cytoplasmic localization was also seen. Zeb2 (green) and DAPI nuclear stain (blue). Scale bar represents 50μM. Images are representative for 2 different experiments.

4.4: Expression of Meox2 is decreased in myofibroblasts

As Zeb2 is a transcriptional repressor of Meox2 and Meox2 is anti-fibrotic molecule, we compared Meox2 and Zeb2 expression patterns during fibroblast to myofibroblast phenoconversion [117]. To determine Meox2 expression in fibroblasts and myofibroblasts, we first tested the ability of the mouse monoclonal anti-Meox2 antibody to detect Meox2. FLAG tagged Meox1 and Meox2 4A expression vectors were transfected into HEK293 cells. Forty-eight hours later, we performed Western blotting and probed blots with FLAG or the Meox2 antibody. We found that the anti-Meox2 antibody specifically detects Meox2 (but not Meox1) at the same molecular weight as detected by the anti-FLAG antibody (approximately 37 kDa) (Figure 18).

We have also performed siRNA mediated Meox2 knockdown in HUVECs to confirm the antibody specificity. Cells were either transfected with control siRNA or Meox2 siRNA and incubated for 48 hours. Both total protein and subcellular fractions were obtained and a significant knockdown of Meox2 protein was observed (Figure 19). For total protein, α-tubulin was used as a loading control. For subcellular fraction, lamin A/C was used as a nuclear loading control and GAPDH was used as a cytoplasmic loading control.

To determine the expression of Meox2 protein in fibroblasts and myofibroblasts, we have used P0 rat cardiac fibroblasts and P1 and P2 myofibroblasts as described previously. By Western blotting, Meox2 protein was found to be highly expressed in P0 fibroblasts as compared to P1 and P2 myofibroblasts ($n=4$, $p \leq 0.01$) (Figure 20).

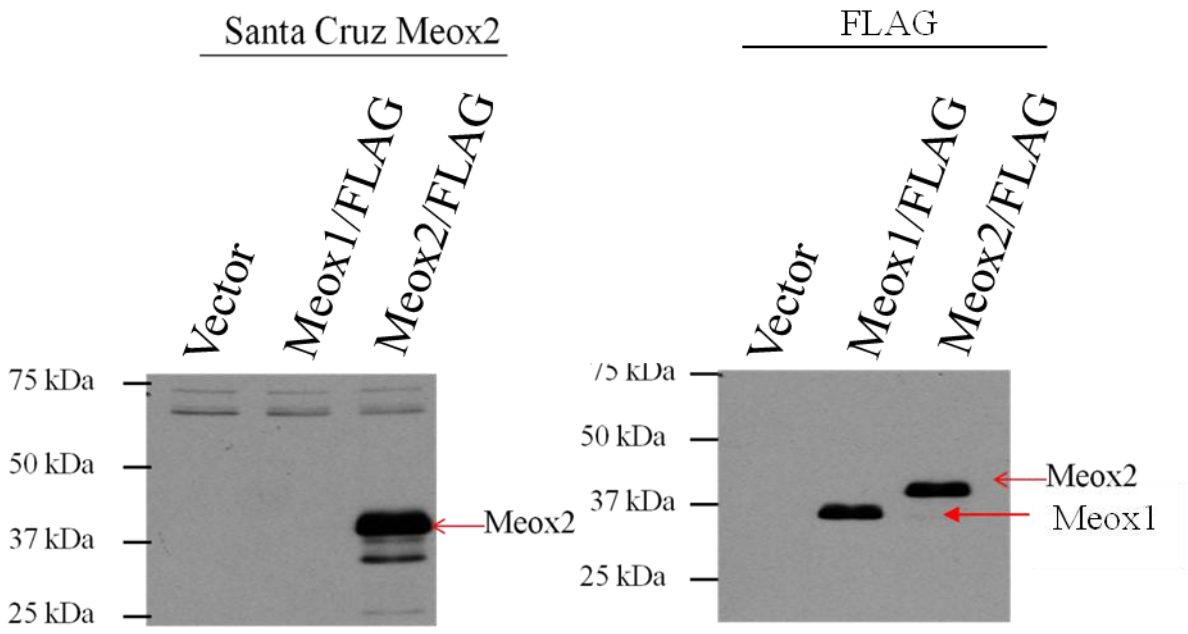

Figure 18: Testing of the anti-Meox2 monoclonal antibody. FLAG tagged Meox1 (Meox1/FLAG) or Meox2 4A (Meox2/FLAG) or the empty 4A (vector) were transfected into HEK293 cells. The anti-Meox2 antibody specifically detects Meox2 protein (but not Meox1) at the same size as anti-FLAG antibody detected Meox2 (approximately 37 kDa). On the other hand, the anti-FLAG antibody detected both Meox1 (approximately 35 kDa) and Meox2 (approximately 37 kDa) as indicated by the molecular weight markers on the side.

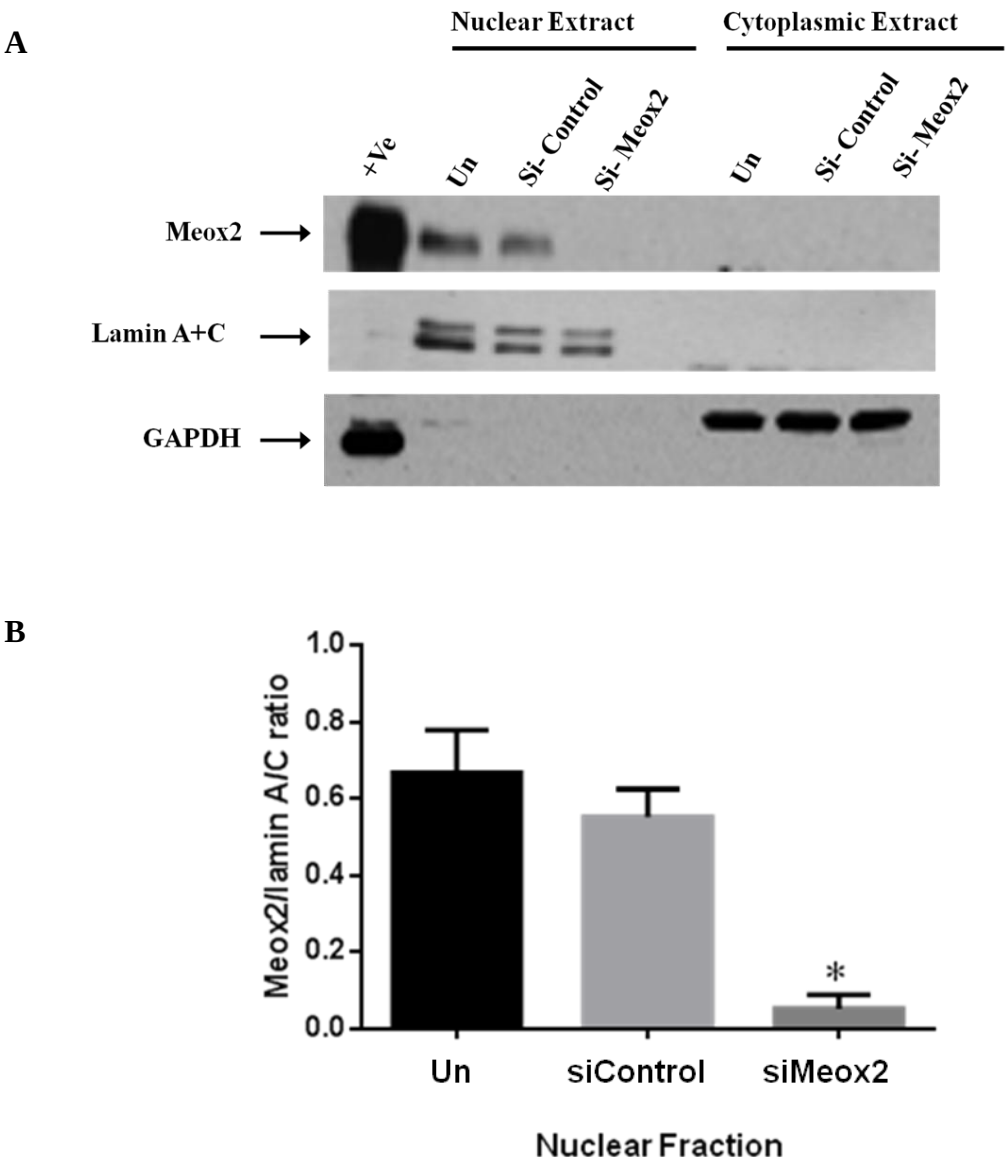

Figure 19. Knockdown of Meox2 in endothelial cells. Cells were either transfected with control non-targeting siRNA or Meox2 specific siRNA and incubated for 48 hours and subcellular fractions were obtained. A) Significant knockdown of Meox2 protein was achieved with siMeox2 as compared to the non-targeting control siRNA transfected samples. B) Histographic representation of data in Panel A. The data shown are from

n=3 independent experiments; *P < 0.05 vs. siControl. Error bars represent SEM. Data were analyzed by ANOVA with Brown-Forsythe test for equal variance and Tukey post-hoc analysis.

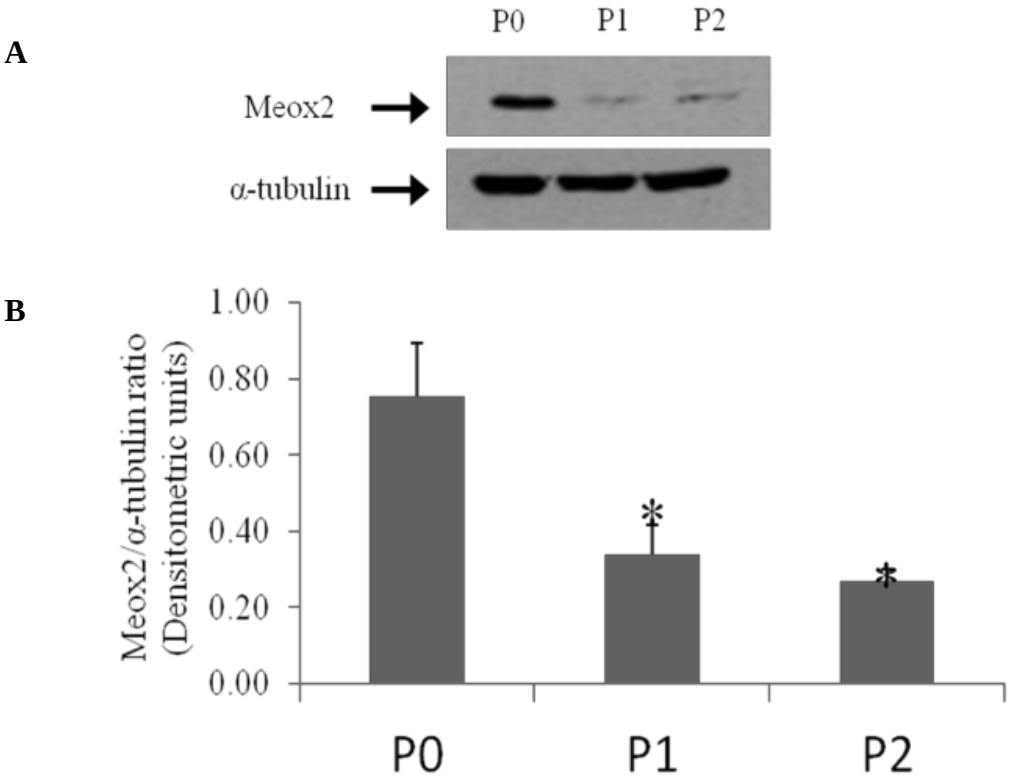

Figure 20: Meox2 levels decrease during the fibroblast to myofibroblast phenoconversion process. P0 rat cardiac fibroblasts and P1 and P2 rat cardiac myofibroblasts were analyzed. A) By Western blotting, Meox2 protein levels were found to be reduced during fibroblast to myofibroblast phenoconversion. Here, α-tubulin was used as a loading control. B) Histographic representation of data in Panel A. The data shown are from n=4 independent experiments; *P < 0.05 vs. P0. Error bars represent SEM. Data were analyzed by ANOVA with Brown-Forsythe test for equal variance and Tukey post-hoc analysis.

4.5: Subcellular fraction of Meox2 in fibroblasts and myofibroblasts

After determining Meox2 expression at the total protein level, we determined its subcellular localization. P0 fibroblasts were grown for 72 hours to achieve ~70% confluency before harvesting. For P1 cardiac myofibroblasts, P0 cells were allowed to grow for 72 hours and passaged to P1 cells. P1 myofibroblasts were allowed to grow up to 48 hours and either harvested for protein lysate or passaged to P2 myofibroblasts. P2 myofibroblasts were also allowed to grow for 48 hours before harvesting. By Western blotting, Meox2 protein was found to be highly expressed in the P0 fibroblast nuclear fraction as compared to P1 and P2 myofibroblast nuclear fractions (Figure 21). A cytoplasmic band was also observed in P0, P1 and P2 cytoplasmic fraction. In this experiment, lamin A/C was used as a nuclear loading control and GAPDH was used as a cytoplasmic loading control.

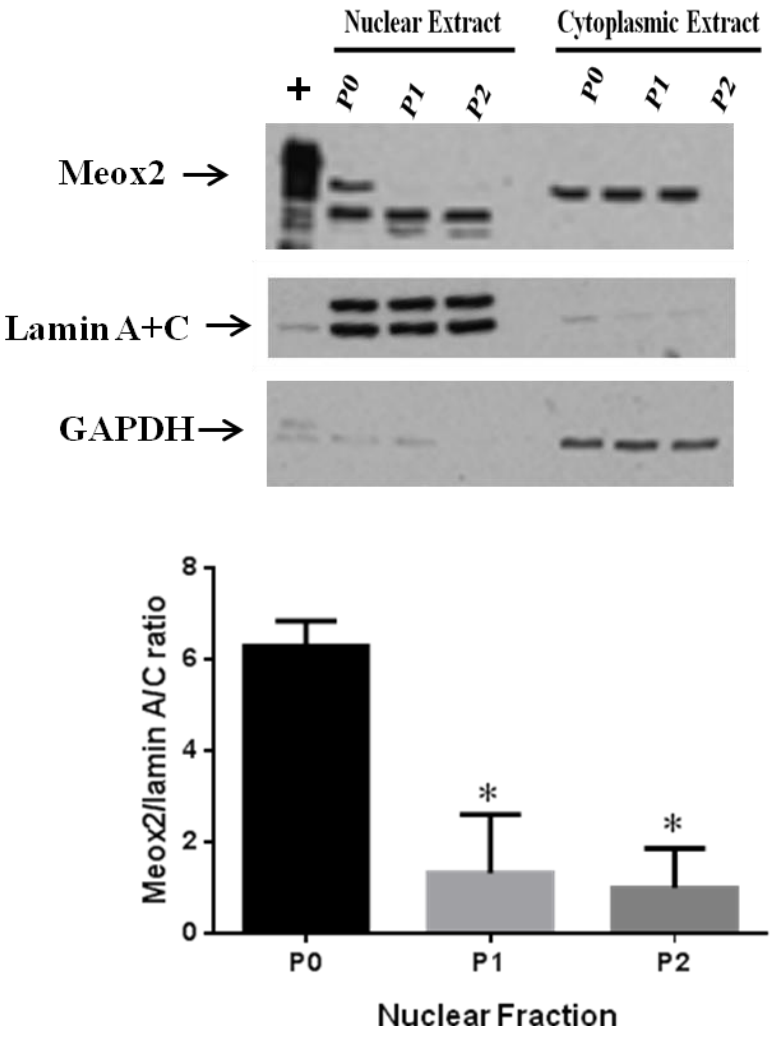

Figure 21: Subcellular localization of Meox2 in rat cardiac fibroblasts and myofibroblasts. Meox2 protein expression was higher in the nuclear fraction from P0 rat cardiac fibroblasts as compared to the nuclear fraction of P1 and P2 myofibroblasts. A cytoplasmic band was also observed in P0, P1 and P2 cytoplasmic fraction that did not change in expression level during myofibroblast phenoconversion. Lamin and GAPDH were used as nuclear and cytoplasmic loading controls, respectively. The data shown are from n=3 independent experiments. *P < 0.05 vs. P0. Error bars represent SEM. Data were analyzed by ANOVA with Brown-Forsythe test for equal variance and Tukey post-hoc analysis.

4.6: Subcellular distribution of Moex2 protein

To confirm the subcellular fraction experiment, we performed immunocytochemistry experiments. Nuclear localization of Meox2 protein (red) was observed in P0 fibroblasts (Figure 22). P1 and P2 myofibroblasts showed dramatically decreased nuclear localization of Meox2. Cytoplasmic localization of Meox2 was not observed.

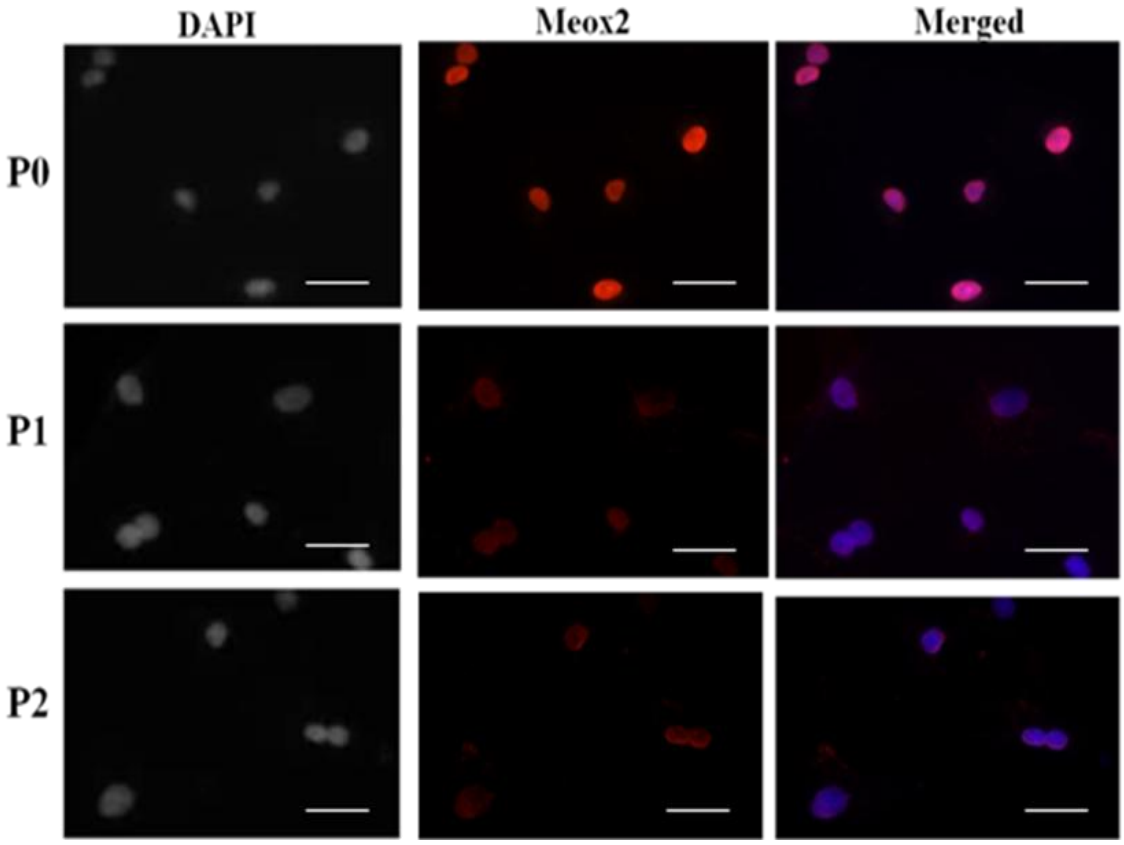

Figure 22: Subcellular distribution of Meox2 protein in P0, P1 and P2 rat cardiac fibroblasts and myofibroblasts. By immunofluorescence, nuclear localization of Meox2 was observed in P0 fibroblasts. P1 and P2 myofibroblasts showed decreased nuclear localization of Meox2. Cells were stained for Meox2 (red) and with DAPI nuclear stain (blue). Scale bar represents 50µM. Images are representative of 4 different experiments.

4.7: Adenoviral mediated overexpression of HA-Zeb2 in P1 cardiac myofibroblasts

Next we performed gain of function studies to determine the effect of increased Zeb2 expression on myofibroblast phenotype and function. To optimize the adenoviral mediated HA-Zeb2 overexpression (Ad.HA.Zeb2), P1 cardiac myofibroblasts were transduced with different MOI of adenoviral vectors (25, 50, 100 and 200 MOI) encoding Zeb2 (Ad.HA.Zeb2) or EGFP (Ad.EGFP) control and incubated for different time periods (24, 48, 72 and 96 hours). By Western blot analysis, we have achieved a physiologically relevant four-fold induction of Zeb2 expression at 200 MOI and 96 hours of incubation (Figure 23). In this experiment, the rabbit polyclonal anti-Zeb2 antibody (Sigma) was used to determine the level of Zeb2 overexpression and α-tubulin was used as a loading control.

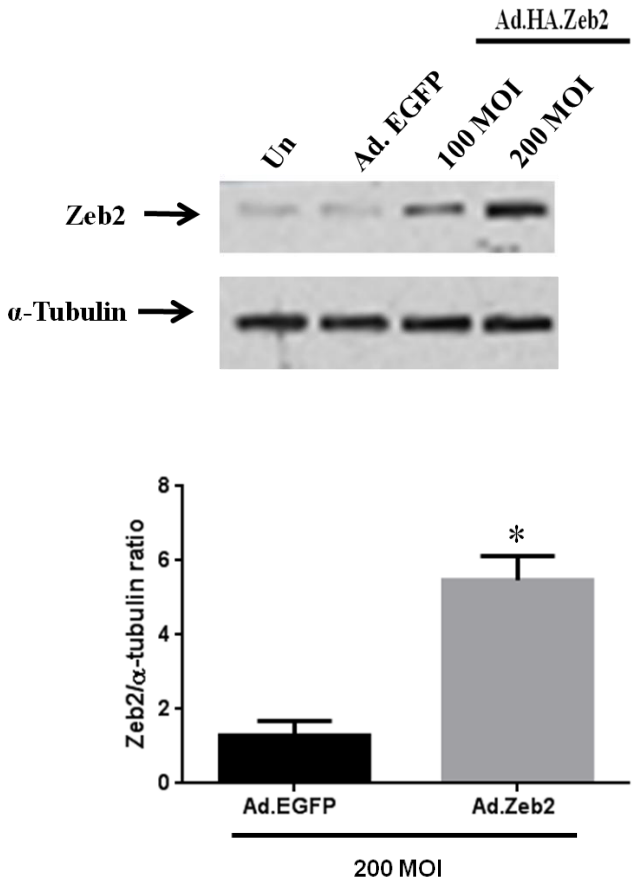

Figure 23: Adenoviral mediated overexpression of Zeb2 in P1 rat cardiac myofibroblasts. P1 cardiac myofibroblasts were transduced with either adenovirus encoding EGFP (Ad-EGFP, 200 MOI) or encoding HA-Zeb2 (Ad-HA-Zeb2, 100 or 200 MOI) and incubated for 96 hours. We have achieved a physiologically relevant four-fold induction of Zeb2 expression at 200 MOI. Rabbit polyclonal anti-Zeb2 antibody was used to determine Zeb2 overexpression and α-tubulin was used as a loading control. The data shown are from n=3 independent experiments. *P < 0.05 vs. Ad.EGFP (200 MOI). Error bars represent SEM. Data were analyzed by performing Student's t-test.

4.8: The effect of Zeb2 on the expression of myofibroblast markers

We have determined the effect of Zeb2 on three key markers of the myofibroblast phenotype: α-SMA, SMemb and ED-A fibronectin. P1 myofibroblasts were transduced with Ad.EGFP (200 MOI) or Ad.HA.Zeb2 (200 MOI) and incubated for 96 hours. Analysis of the Western blot data shows that Zeb2 overexpression significantly increased the expression levels of α-SMA (n=4, $*P \leq 0.05$), SMemb (n=4, $*P \leq 0.05$) and ED-A fibronectin (n=3, $*P \leq 0.05$) as compared to the Ad.EGFP viral controls. Expression levels were compared by using α-tubulin as a loading control (Figure 24-26).

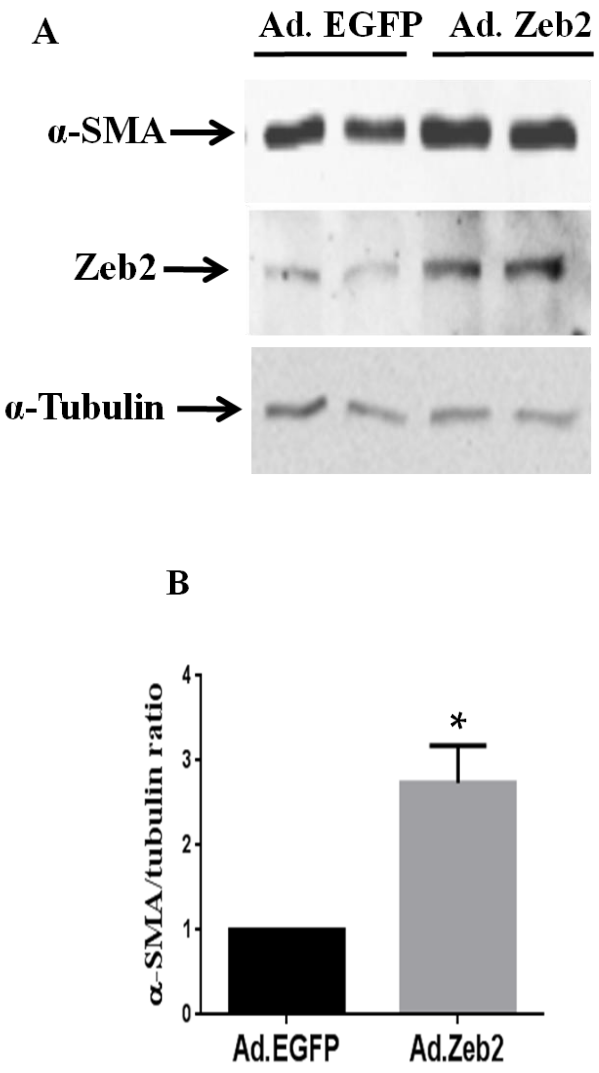

Figure 24: Zeb2 overexpression increases protein levels of α-SMA in P1 rat cardiac myofibroblasts. A) P1 cells were transduced with Ad.EGFP (200 MOI) or Ad.HA.Zeb2 (200 MOI) and incubated for 96 hours for Western blot analysis. α-SMA expression was determined with α-tubulin as a loading control. B) Histographic representation of α-SMA expression in Ad.EGFP (200 MOI) and Ad.HA.Zeb2 (200 MOI) infected cells. The data shown are from n=4 independent

experiments. * $P < 0.05$ vs. Ad.EGFP. Error bars represent SEM. Data were analyzed by performing Student's t-test.

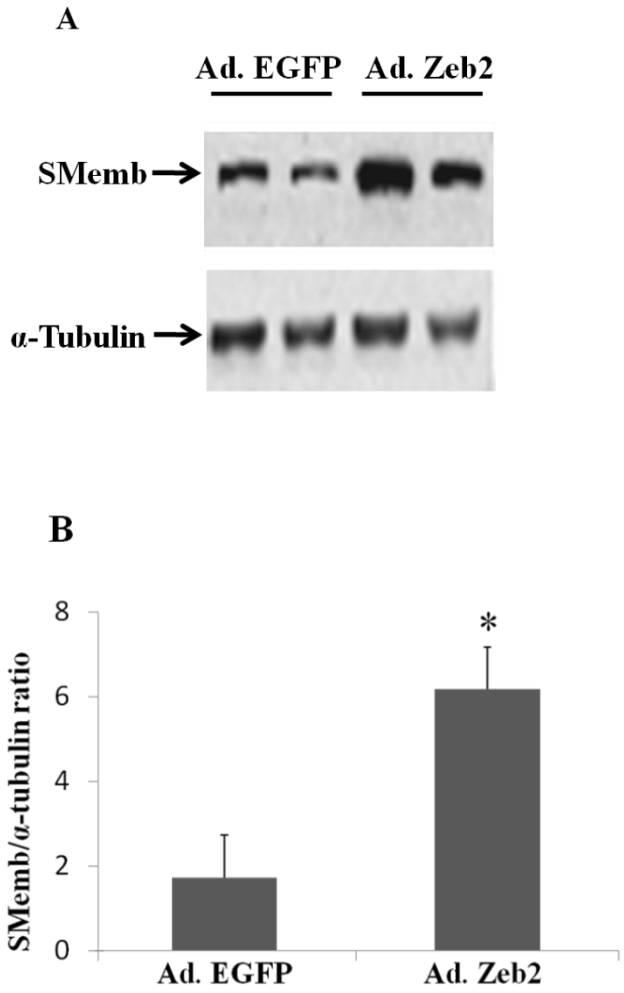

Figure 25: Zeb2 overexpression increases protein levels of SMemb in P1 rat cardiac myofibroblasts. A) P1 cells were transduced with Ad-EGFP (200 MOI) or Ad.HA.Zeb2 (200 MOI) and incubated for 96 hours for Western blot analysis. SMemb expression was determined with α-tubulin as a loading control. B) Histographic representation of SMemb expression in Ad.EGFP (200 MOI) and Ad.HA.Zeb2 (200 MOI) infected cells. The data shown are from n=4 independent experiments. * $P \leq 0.05$ Vs Ad.EGFP. Error bars represent SEM. Data were analyzed by performing Student's t-test.

A

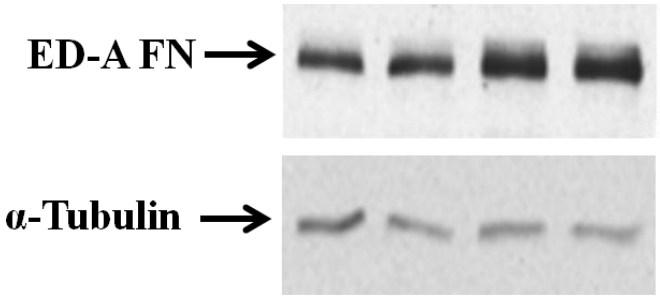

B

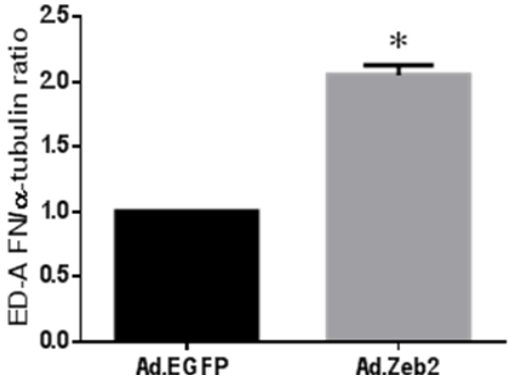

Figure 26: Zeb2 overexpression increases protein levels of ED-A FN in P1 rat cardiac myofibroblasts. A) P1 cells were transduced with Ad.EGFP (200 MOI) or Ad.HA.Zeb2 (200 MOI) and incubated for 96 hours for Western blot analysis. ED-A fibronectin expression was determined with α-tubulin as a loading control. B) Histographic representation of ED-A fibronectin expression in Ad.EGFP (200 MOI) and Ad.HA.Zeb2 (200 MOI) infected cells. The data shown are from n=3 independent experiments. *P < 0.05 vs. Ad.EGFP. Error bars represent SEM. Data were analyzed by performing Student's t-test.

4.9: Effect of Zeb2 on myofibroblast function

Two major functional properties of myofibroblasts are: 1) they tend to be less motile than fibroblasts and 2) they are more contractile than fibroblasts. Thus, we have investigated the effect of Zeb2 on both migration and contractility of myofibroblasts.

4.9.1: Zeb2 overexpression inhibits the migration of P1 myofibroblasts

To determine the effect of Zeb2 on myofibroblast migration property, P1 myofibroblasts were transduced with Ad.EGFP (200 MOI) or Ad.HA.Zeb2 (200 MOI) and incubated for 96 hours. After 96 hours, culture inserts were removed and feeding medium was changed to 1% FBS containing medium. Images were taken every 6 hours. At 18 hours and 24 hours time points there were significantly less migration of cells in Ad.HA.Zeb2 infected plates compared to Ad.EGFP control (Figure 27).

4.9.2: Zeb2 overexpression increases contraction of P1 myofibroblasts

To determine the effect of Zeb2 on myofibroblast contractility, P1 myofibroblasts were plated on collagen gels and transduced with either Ad.LacZ (200 MOI) or Ad.HA.Zeb2 (200 MOI) and incubated for 72 hours. After 72 hours, medium was changed to serum free medium and collagen gels were detached and allowed to contract for 12 hours. Images were taken at 0 hour and 12 hours time points. Zeb2 overexpression increased contractility of P1 myofibroblasts compared to cells infected with Ad.LacZ which is indicated by reduced gel size. The gel size was quantified using Measuregel software and showed that there is a significant increase in the percentage of change of area in case of Zeb2 infected gels compared to Ad.LacZ control (Figure 28).

A

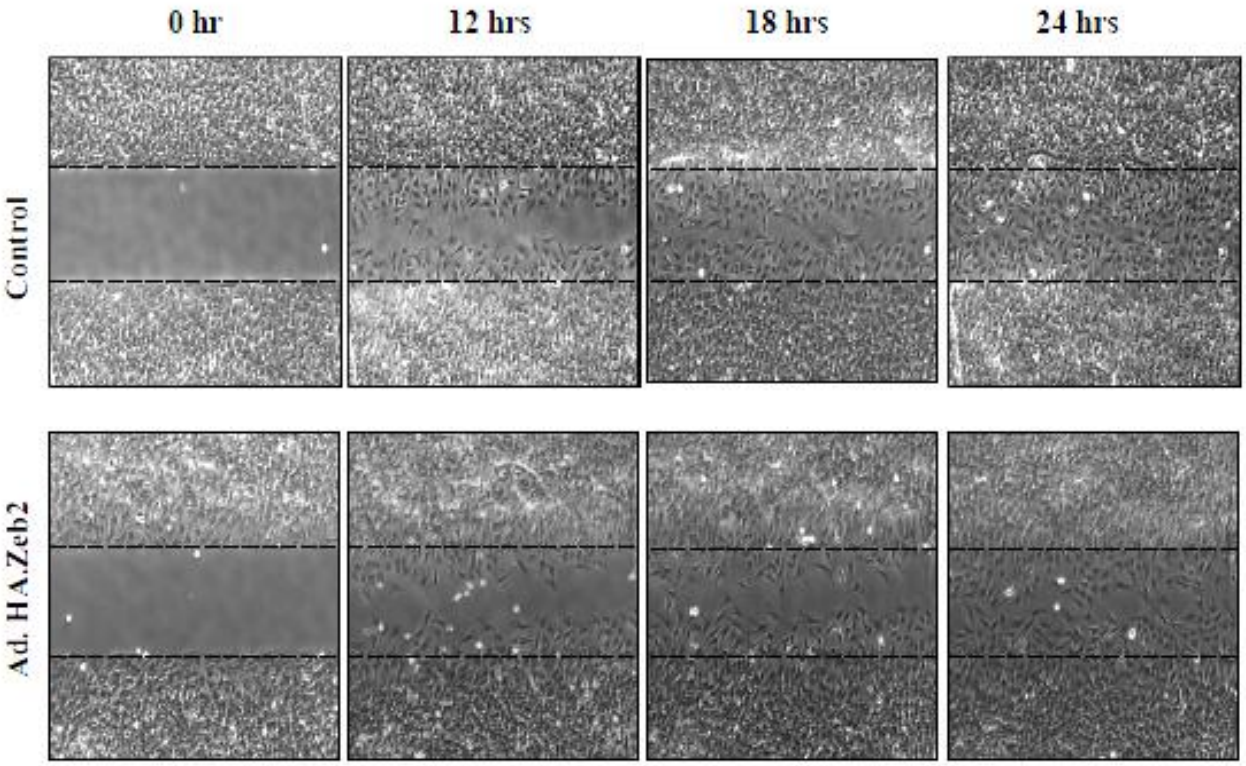
0 hr
12 hrs
18 hrs
24 hrs
Control
Ad. HA.Zeb2

B

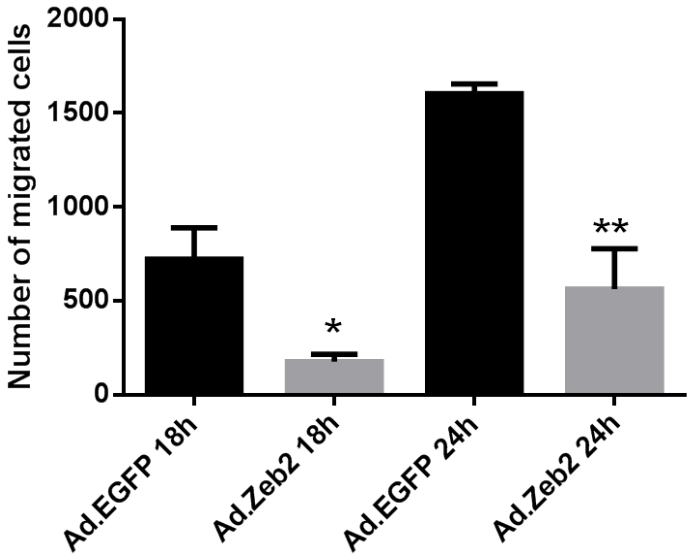
Number of migrated cells
2000
1500
1000
500
0
*
**
Ad.EGFP 18h
Ad.Zeb2 18h
Ad.EGFP 24h
Ad.Zeb2 24h

Figure 27: Zeb2 overexpression inhibits the migration of P1 myofibroblasts. A) P1 myofibroblasts were transduced with Ad.EGFP (200 MOI) or Ad.HA.Zeb2 (200 MOI) and incubated for 96 hours. After 96 hours, culture inserts were removed and images were taken at indicated time points (4x objective). B) The number of cells in the wounded area was quantified using ImageJ software. Histographic representation shows the number of migrated cells in Ad.EGFP (200 MOI) and Ad.HA.Zeb2 (200 MOI) infected plates. n=3, *P ≤ 0.05 vs. Ad.EGFP at 18 hours; **P ≤ 0.01 vs. Ad.EGFP at 24 hours. Error bars represent SEM. Data were analyzed by ANOVA with Brown-Forsythe test for equal variance and Tukey post-hoc analysis.

A

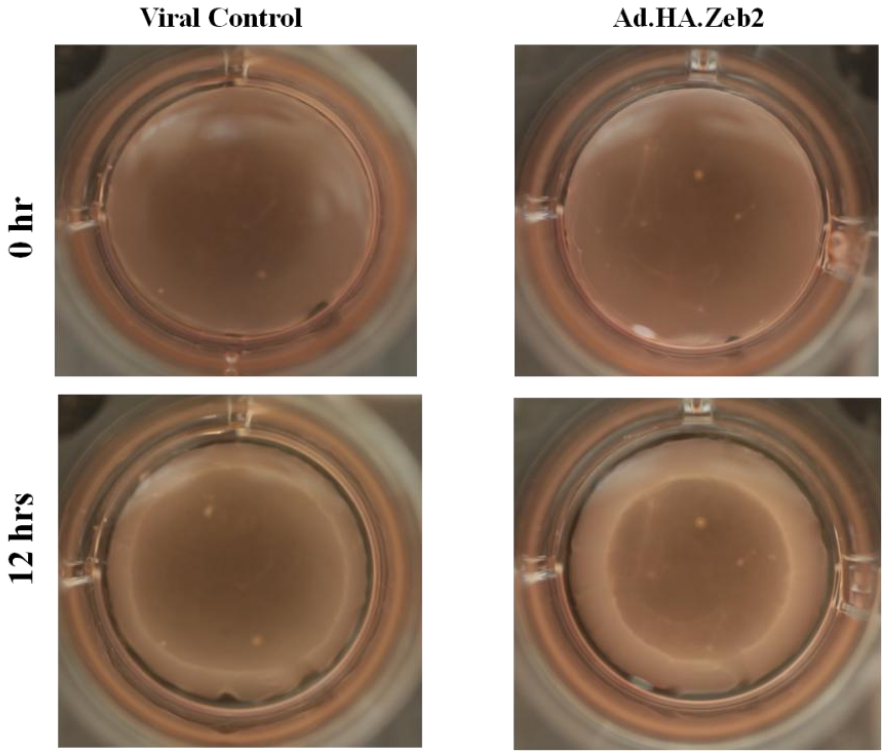
Viral Control
Ad.HA.Zeb2
0 hr
12 hrs

B

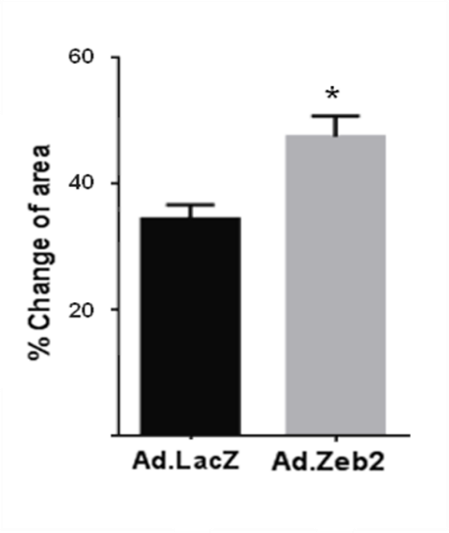
60
40
20
% Change of area
*
Ad.LacZ
Ad.Zeb2

Figure 28: Zeb2 overexpression increases contraction of P1 myofibroblasts- a characteristic of mature myofibroblast. A) P1 cells were plated on collagen gels and transduced with either Ad.LacZ (200 MOI) or Ad.HA.Zeb2 (200 MOI) and incubated for 72 hours. After 72 hours, collagen gels were cut and allowed to contract for 12 hours. Images were taken at 0 hour and 12 hours time points. B) The gel size was quantified using Measuregel software. Histographic representation shows the percentage of change of area in case of Zeb2 infected gels compared to Ad.LacZ control. n=3, *P $\leq$ 0.05 Vs Ad.LacZ. Error bars represent SEM. Data were analyzed by performing Student's t-test.

4.10: Effect of Zeb2 on stress fiber formation

The formation of complex and organized stress fibres is a characteristic feature of myofibroblasts. To determine the effect of Zeb2 on myofibroblast stress fiber formation, P1 myofibroblasts were plated on chamber slides and transduced with either Ad.LacZ (200 MOI) or Ad.HA.Zeb2 (200 MOI) and incubated for different time points: 16 hours, 24 hours, 48 hours, 72 hours and 96 hours. Cells were then fixed with 4% PFA and stained with rhodamine phalloidin stain. However, no significant difference in the organization of stress fibers could be detected between Ad.LacZ and Ad.HA.Zeb2 infected cells (Figure 29).

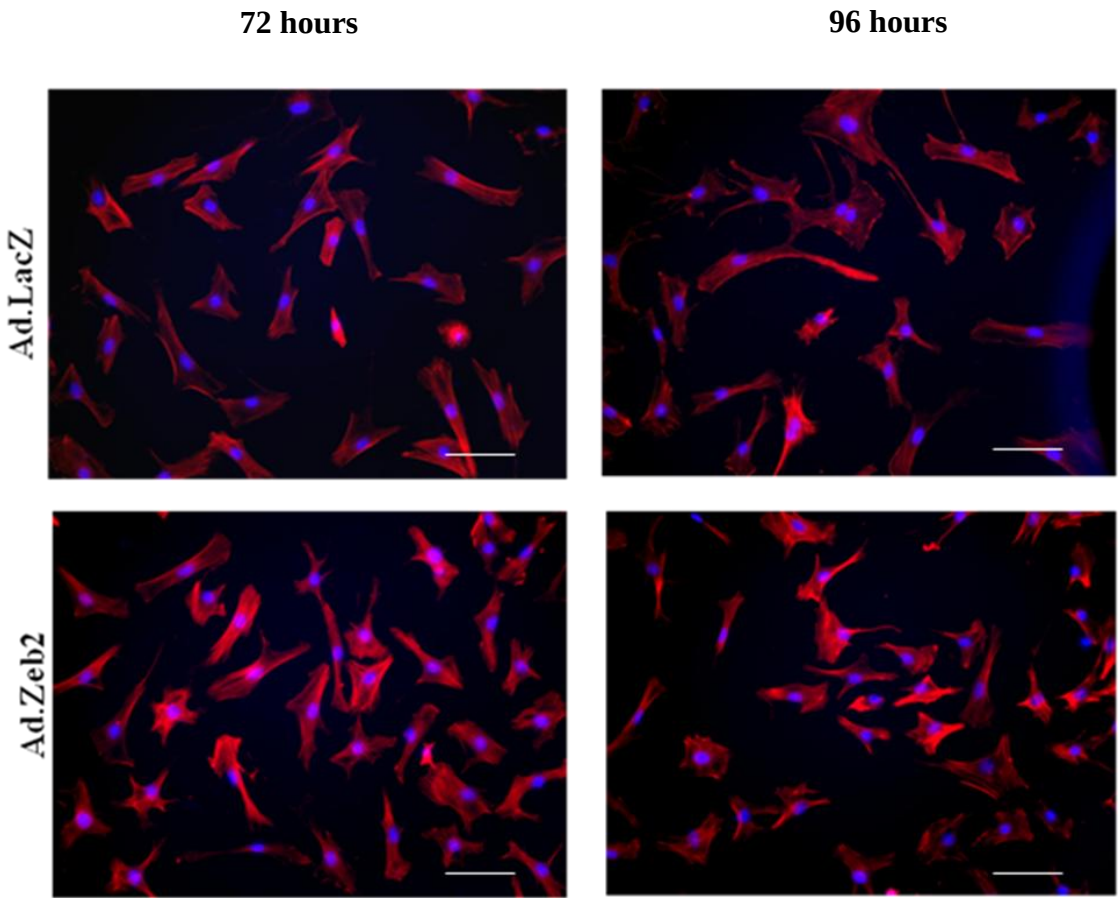

Figure 29: Effect of Zeb2 on stress fiber formation. P1 myofibroblasts were plated on chamber slides and transduced with either Ad.LacZ (200 MOI) or Ad.HA.Zeb2 (200 MOI) and incubated for different time points: 16 hours, 24 hours, 48 hours, 72 hours and 96 hours. Cells were then fixed with 4% PFA and stained with rhodamine phalloidin stain. However, no significant difference in the organization of stress fibers could be seen between Ad.LacZ and Ad.HA.Zeb2 infected cells. Images shown above represent 72 hours and 96 hours time points. Scale bar represents 100µM. Images are representative of 3 different experiments.

4.11: Effect of Zeb2 on Meox2 expression

Next we determined the effect of Zeb2 on Meox2 expression. We have shown that P1 myofibroblasts express very low levels of Meox2 protein thus it was not possible to use these cells to show the effect of Zeb2 on Meox2 expression. Using P0 fibroblasts would be technically challenging since it is not possible to count freshly isolated cardiac fibroblasts before infecting them. Moreover, if P0 cells are kept for more than 48 hours, Meox2 expression levels would decrease due to the gradual phenoconversion and this would cause experimental variability. For this reason, we used HUVECs to determine the effect of Zeb2 protein on Meox2 expression as HUVECs express Meox2. At first we determined Ad.HA.Zeb2 mediated overexpression condition in HUVECs. Cells were transduced with Ad.EGFP (50 MOI) or Ad.HA.Zeb2 (50, 100 or 200 MOI) and incubated for 72 hours. At 200 MOI of Ad.HA.Zeb2 infection, significant levels of Zeb2 overexpression was achieved (Figure 30) and there was a significant downregulation of Meox2 expression as compared to Ad.EGFP (200 MOI) viral control (n=3, *$P \leq 0.05$ vs. Ad.EGFP) (Figure 31). Thus, Zeb2 has the potential to induce myofibroblast phenotype indirectly by inhibiting anti-fibrotic Meox2 pathway in P1 myofibroblasts.

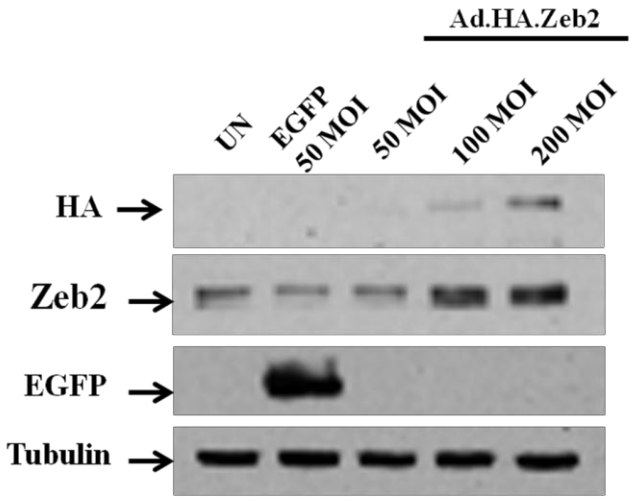

Figure 30: Ad.HA.Zeb2 overexpression in endothelial cells. HUVECs were transduced with either Ad.EGFP (50 MOI) or Ad.HA.Zeb2 (50,100 or 200 MOI) and incubated for 72 hours for Western blot analysis. Rabbit polyclonal anti-Zeb2 (Sigma) and rabbit polyclonal anti-HA (Rockland) antibodies were used to detect Zeb2 expression. α-tubulin was used as a loading control.

A

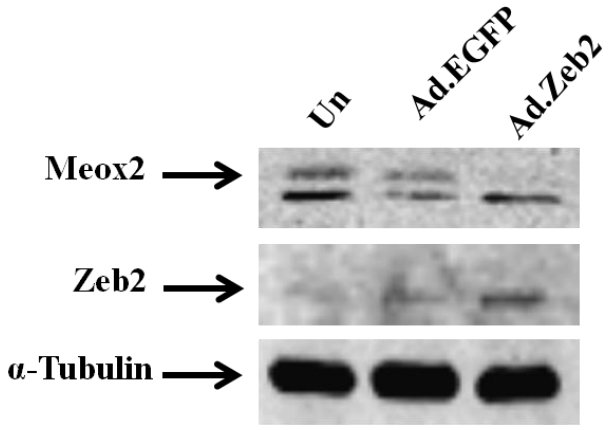

B

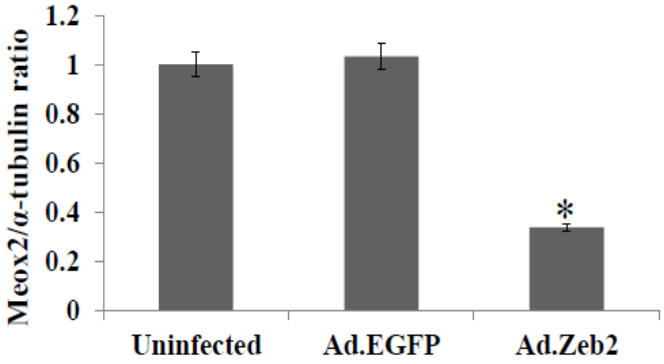

Figure 31: Effect of Ad.HA.Zeb2 overexpression on Meox2. A) HUVECs were infected with either Ad.EGFP or Ad.HA.Zeb2 at 200 MOI and incubated for 72 hours for Western blot analysis. α- tubulin was used as a loading control. Increased expression of Zeb2 results in decreased levels of Meox2 protein in endothelial cells. B) Histograph representing the relative levels of Meox2 expression. n=3, *P ≤ 0.05 vs. Ad.EGFP. Error bar represents SEM. Data were analyzed by performing Student's t-test.

5. CHAPTER V: DISCUSSION

In this study, we have shown for the first time that Zeb2 regulates cardiac fibroblast to myofibroblast phenoconversion. We have shown that the levels of Zeb2 expression increase as fibroblasts phenoconvert to myofibroblasts. Zeb2 overexpression increased the expression levels of three key myofibroblast markers: α-SMA, SMemb and ED-A fibronectin. Ectopic Zeb2 expression induced a less migratory and more contractile phenotype, which is a characteristic of mature myofibroblasts. On the other hand, the anti-fibrotic Meox2 protein showed an inverse pattern of expression as compared to Zeb2 expression in cardiac fibroblasts and myofibroblasts; and ectopic Zeb2 expression inhibited Meox2 expression in primary human endothelial cells.

Previously our group has shown that Ski, a negative regulator of TGF-β signaling, can prevent myofibroblast phenoconversion by downregulating Zeb2 expression which in turn causes an upregulation of its target Meox2. Ectopic Meox2 expression led to increased α-SMA and ED-A fibronectin expression levels [119]. Moreover, Zeb2 has been previously shown to regulate TGF-β mediated EMT process [132]. Thus, we sought to elucidate the role of Zeb2 in regulating myofibroblast phenotype and function.

5.1: Zeb2 expression increases in phenoconverted myofibroblasts

To determine Zeb2 expression in fibroblasts and myofibroblasts, we first tested two rabbit polyclonal Zeb2 antibodies. These antibodies detected exogenous HA tagged Zeb2 protein at specific size (171 kDa) (Figure 14). However, these antibodies also detected lower bands. This might be due to non-specific reactions of the antibodies since the molecular weight of the lower band varied for these antibodies. Other reasons might be

Zeb2 protein degradation or alternative splicing of the Zeb2 mRNA. Next, we determined the level of Zeb2 expression in rat primary cardiac fibroblasts and myofibroblasts. We found that Zeb2 expression significantly increases during fibroblast to myofibroblast transition suggesting that Zeb2 may play a role in this phenoconversion process (Figure 15). Subcellular studies by both Western blotting and immunocytochemistry confirmed increased nuclear localization of Zeb2 in P1 myofibroblasts (Figure 16-17). However, in the subcellular fractionation study we detected low levels of Zeb2 expression in P0 fibroblasts that was not seen in the studies of total protein. This might be due to several reasons: 1) in total cell lysates nuclear proteins may get diluted and become more difficult to detect; 2) for the fractionation study we have allowed P0 fibroblasts to grow for 72 hours (an additional 24 hours) to achieve sufficient cell pellet for Western blotting, which might have allowed them to adopt a more proto-myofibroblast like phenotype; 3) reagents and procedure used for extracting total protein and nuclear fraction were different. Moreover in the subcellular fractionation study, for P2 myofibroblasts we did not find similar results for Zeb2 expression as compared to data obtained from total protein study and subcellular study by immunocytochemistry. We found that Zeb2 expression levels in the nuclear fraction of P2 cells markedly decreased whereas in immunocytochemistry P2 myofibroblasts showed levels of nuclear Zeb2 comparable to P1 cells. This difference might be due to the different cell culture conditions for these two experiments. For the fractionation study, P0 cells were allowed to grow for an additional 24 hours and thus the passaging times for P1 and P2 myofibroblasts were also shifted. This indicates that Zeb2 expression is time dependent (*in vitro*) and its increased expression may play a critical role during the early phase of phenoconversion process.

However, increased Zeb2 expression may not be required by the cells at the later stages when they tend to become more senescent.

Conversely, Meox2 expression significantly decreases during fibroblast to myofibroblast transition (Figure 20). By both Western blotting and immunofluorescence, increased nuclear localization of Meox2 was observed in cardiac fibroblasts which suggested that Meox2 acts to prevent the myofibroblast phenoconversion process (Figure 21-22). In case of Meox2 a cytoplasmic band was also observed by Western blotting, however its level did not change with increasing passage numbers. To confirm this data we did immunofluorescence experiment and Meox2 was detected only in the nuclei of cardiac fibroblasts. Using a rat infarct model we previously showed that Zeb2 expression levels increase whereas Meox2 expression levels decrease during acute and healing Post-MI stages [119]. Together our data indicates that Zeb2 may be critical for fibroblast to myofibroblast transition based on its expression pattern and known role in TGF-β activated signaling. Zeb2 might also be exerting its pro-fibrotic effect by causing downregulation of Meox2 expression and thus promoting myofibroblast formation.

5.2: Zeb2 regulates cardiac myofibroblast phenotype

Cardiac myofibroblasts exhibit characteristic expression of α-SMA, SMemb and ED-A fibronectin [133-135]. Among these markers SMemb and α-SMA are the two major contractile proteins expressed by myofibroblasts that give a characteristic contractile property [133, 135]. ED-A fibronectin is considered as one of the major drivers of myofibroblast phenoconversion that plays role in the induction of α-SMA expression, collagen deposition and cell contractility [134].

As fibroblasts are difficult to transfect with expression vectors using liposomal based methods, we employed an adenoviral mediated overexpression approach. Infection with adenovirus encoding Zeb2 at 200 MOI for 96 hours significantly increases Zeb2 protein levels in cardiac myofibroblasts, which in turn induces increased expression of these myofibroblast markers (Figure 24-26). Thus, it is evident that Zeb2 is sufficient for the increased expression of the major myofibroblast markers and plays a crucial role in driving the phenoconversion of cardiac fibroblasts to myofibroblasts. Although we have used a high MOI, we have achieved a four-fold induction of Zeb2 expression which is physiologically relevant. We have shown that increased Zeb2 expression induces myofibroblast marker expression; however, the question arises if the effect is via a direct transcriptional activation or involves other transcriptional regulators or other pathways. We have previously shown that Ski overexpression leads to Zeb2 downregulation and subsequently increased Meox2 protein levels [119]. This suggests that an increase in Zeb2 protein levels in P1 myofibroblasts can lead to downregulation of Meox2 expression which in turn can increase α-SMA and ED-A fibronectin protein levels. However, in Meox2 overexpression studies we did not see an increase in SMemb expression levels which suggests that Zeb2 has the potential to regulate myofibroblast phenoconversion either directly or via some other Meox2-independent pathway. Interestingly Zeb2 is also known as a Smad interacting protein which again suggests that Zeb2 might be required for the activation of these myofibroblast markers via binding to Smad transcriptional complex.

5.3: Zeb2 regulates cardiac myofibroblast migration

Since myofibroblasts are hypersynthetic they are thought to be less motile. Results from the wound healing migration assay show that Zeb2 regulates the migratory property of cardiac myofibroblasts. Zeb2 overexpression reduced the migratory ability of myofibroblasts as indicated by the decreased number of cells migrating to the cell-free gap region in the wound-healing assay (Figure 27). This result is consistent with the findings of our marker analysis where Zeb2 overexpression was shown to induce a hypersynthetic mature myofibroblast phenotype. Data also suggests that Zeb2 might be involved in inducing increased adhesion to its substrate via focal adhesions and thus preventing myofibroblast migration.

5.4: Zeb2 regulates cardiac myofibroblast contraction

Myofibroblasts have a characteristic contractile property that helps in the process of wound closure. Myofibroblasts maintain the wound area under tension which helps in reducing wound size and ensures rapid healing [87]. Myofibroblasts synthesize large amounts of contractile proteins such as α-SMA and SMemb, which generates tension by actively contracting to generate force [136, 137]. There are also other pathways that can contribute in inducing contractile property of myofibroblasts for example Ca^{2+} signaling and Rho/ROCK signaling [138]. We have demonstrated that Zeb2 overexpression in myofibroblasts leads to increased contractility as compared to the Ad.LacZ control (Figure 28). Thus, the finding of increasing myofibroblast marker expression (α-SMA and SMemb) does reflect on inducing a more contractile mature cardiac myofibroblast phenotype.

5.5: Effect of Zeb2 on myofibroblast stress fiber formation

Myofibroblasts exhibit the characteristic presence of stress fibers that are connected to the plasma membrane-bound focal adhesion complexes [137]. To determine the effect of Zeb2 on myofibroblast stress fiber formation, myofibroblasts were transduced with either Ad.LacZ (200 MOI) or Ad.HA.Zeb2 (200 MOI) and a range of time points were assessed. However, we did not observe any obvious increases in stress fiber formation with Zeb2 overexpression (Figure 29). It might be because sufficient Zeb2 overexpression is only achieved at longer time points and by that time these myofibroblasts already possess an abundance of stress fibers, which may have been maximized at this matured myofibroblastic condition. Incorporation of α-SMA to stress fibers and formation of super mature focal adhesions connected to stress fibers are the hall marks of mature myofibroblasts [139]. Thus, further experiments should be done to detect co-localization of α-SMA to stress fibers and increase in focal adhesion molecules for example paxillin, vinculin, tensin etc.

5.6: Zeb2 regulates Meox2 expression

Due to the technical difficulty of using P0 fibroblasts, we have used HUVECs as a model to determine if Zeb2 overexpression can cause knockdown of Meox2 protein. Cells transduced with Ad.HA.Zeb2 (200 MOI) showed significant downregulation of Meox2 expression compared to Ad.EGFP control (n=3, $*P \leq 0.05$) (Figure 31). This suggested that Zeb2 may also induce myofibroblast phenotype indirectly by inhibiting anti-fibrotic Meox2 pathway.

Overall, the study suggests that Zeb2 promotes the phenoconversion of cardiac fibroblast to myofibroblast (Figure 32). We propose that Zeb2 promotes myofibroblast phenoconversion by increasing the myofibroblast marker expression, which in turn induces a less motile and more contractile mature myofibroblast phenotype. Zeb2 overexpression study in endothelial cells indicates that Zeb2 also has the potential to inhibit the anti-fibrotic Meox2 pathway. This is also supported by the results obtained from *in vitro* Zeb2/Meox2 expression experiments done in this study as well as the previous studies of Zeb2/Meox2 expression in the post-MI model and Ski mediated Zeb2 knockdown study done in P1 cardiac myofibroblasts where Meox2 showed an inverse expression pattern as compared to Zeb2 expression [119].

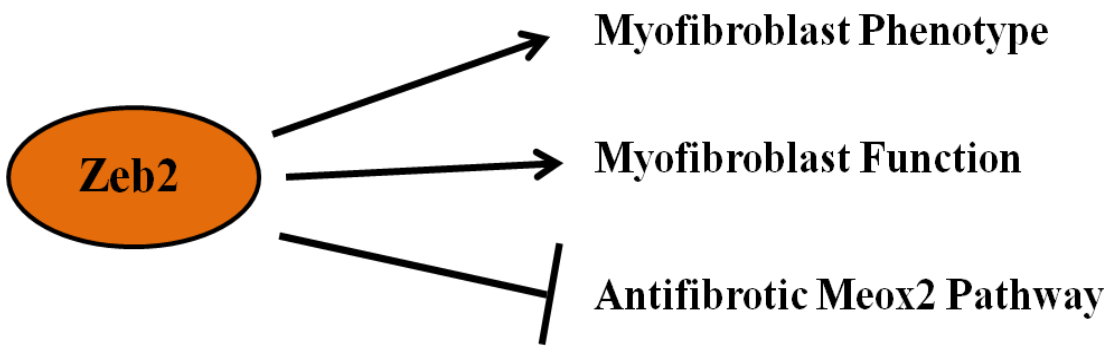

Figure 32: Role of Zeb2 in regulating cardiac myofibroblast phenotype: Zeb2 is a critical contributor to myofibroblast formation. Zeb2 plays a crucial role in fibroblast to myofibroblast phenoconversion by increasing expression of myofibroblast markers, by inducing a less migratory and more contractile myofibroblast and by inhibiting the anti-fibrotic Meox2 pathway.

6. CHAPTER VI: CONCLUSIONS

In summary, we have demonstrated the following:

1. We have shown for the first time that Zeb2 expression is higher in myofibroblasts and lower in fibroblasts *in vitro*.
2. By Western blot analysis, Zeb2 expression was found to be higher in the myofibroblast nuclear fraction as compared to that of fibroblasts.
3. By immunofluorescence, Zeb2 was observed in the myofibroblast nuclei and not in the fibroblast nuclei.
4. Zeb2 overexpression increased the expression levels of three key myofibroblast markers: α-SMA, SMemb and ED-A fibronectin.
5. Ectopic Zeb2 expression induced a less migratory and more contractile mature myofibroblast phenotype.
6. On the other hand, Meox2 expression is higher in fibroblasts and lower in myofibroblasts *in vitro*.
7. By Western blot analysis Meox2 expression was found to be higher in the fibroblast nuclear fraction as compared to that of myofibroblasts.
8. By immunofluorescence, Meox2 was observed in the fibroblast nuclei and a much lower level in myofibroblast nuclei.
9. Zeb2 overexpression repressed Meox2 expression levels in endothelial cells which suggested that Zeb2 can also induce myofibroblast phenoconversion by inhibiting anti-fibrotic Meox2 pathway.

7. CHAPTER VII: SIGNIFICANCE

Pathological fibrosis is associated with most cardiovascular diseases and progressive fibrosis worsens patient outcome which eventually leads to heart failure [7]. Although it is a major health problem worldwide, there is no effective therapy available that can specifically target fibrosis because the mechanism behind the pathological remodeling is poorly understood. Common drugs used in diseases associated with cardiac fibrosis are statins, the angiotensin-converting enzyme (ACE) inhibitors, beta blockers which help in reducing cholesterol levels, hypertension and high blood pressure, respectively [140-142]. However, none of the treatments can prevent the progression to chronic remodeling of the heart. Multiple therapeutic strategies have been developed to target pro-fibrotic pathways including TGF-β, IGF-1, interleukin (IL)-4, CTGF, basic FGF (bFGF), and angiotensin II to block fibrosis. However, the broad spectrum targeting of these pathways is not therapeutically feasible due to the side effects on other cellular and organ functions [85].

Thus, it is critical to identify novel regulators of fibrosis for developing selective anti-fibrotic strategies. In this regard, understanding the key factors that are involved in the cardiac fibroblast to myofibroblast phenoconversion process will enable us to identify specific regulators that could be therapeutically targeted to prevent myofibroblast phenoconversion at the later stages of wound healing in order to block progressive fibrosis. Findings from this study contribute to our understanding of the biological role of Zeb2 in modulating cardiac fibroblast phenotype during cardiac fibrosis. It will advance our current knowledge of the mechanism behind cardiac fibrosis and will provide a basis

for the development of Zeb2 based novel anti-fibrotic drug in the future. Hydrocarbon staple peptide or adenoviral mediated gene therapy approach could be employed to control Zeb2 expression in post-MI heart as a therapeutic strategy.

8. CHAPTER VIII: STUDY LIMITATIONS AND FUTURE DIRECTIONS

The present study provides a proof of concept that Zeb2 plays an important role in regulating cardiac fibroblast to myofibroblast phenoconversion. However, a number of questions need to be answered regarding the role of Zeb2 in myofibroblast phenoconversion and cardiac fibrosis. In wound healing migration assay, reduced serum medium (1% FBS containing DMEM-F12) was used and images were taken within 24 hours to eliminate the possibility of cell proliferation. However, the effect of Zeb2 on myofibroblast proliferation and apoptosis needs to be determined in order to test if Zeb2 overexpression has an anti-proliferative or apoptotic effect. Moreover, a number of cells were found to migrate to the wounded area in case of Zeb2 overexpression as well. Thus, the percentage of cells expressing exogenous Zeb2 needs to be determined by labeling the cells with anti-HA antibody. In addition to gain of function studies, a Zeb2 loss of function study and a rescue experiment need to be done to determine whether Zeb2 is required for the myofibroblast phenotype and function and not simply sufficient for the process. Additionally, promoter assays should be done to determine whether Zeb2 is required for direct transcriptional activation of α-SMA, SMemb and ED-A fibronectin. Due to the technical difficulty of using P0 cardiac fibroblasts, we have used HUVECs to see the effect of Zeb2 overexpression on Meox2. However to establish whether Zeb2 can drive transcriptional repression of Meox2 during cardiac myofibroblast phenoconversion, a chromatin immunoprecipitation (ChIP) assay needs to be done using rat cardiac fibroblasts/myofibroblasts. Moreover, overexpression studies can be employed using ‘heart-soft’ (12 kPa) dishes (made of silicon substrates) to culture cardiac fibroblasts that preserve fibroblastic phenotype and will enable to determine the effect of Zeb2 on

Meox2 expression. Similarly, the effect of Zeb2 on myofibroblast stress fiber formation can be determined using 'heart-soft' dishes. Although we did not see any obvious increase in stress fiber formation in Zeb2 overexpressed cells, a co-localization study to detect α-SMA and focal adhesion complexes connected to stress fibers will reveal the role of Zeb2 in complex stress fiber organization. To validate our findings, a fibroblast specific Zeb2 conditional knockout animal study will be useful to reveal its role in cardiac fibroblast and myofibroblast phenotype and function *in vivo*. Furthermore, the mechanism of Zeb2 regulation and the effect of its modulation in other cell types of the heart need to be addressed.

9. CHAPTER IX: REFERENCES

1. Martin, P., *Wound healing--aiming for perfect skin regeneration.* Science, 1997. **276**(5309): p. 75-81.
2. Eckes, B., et al., *Interactions of fibroblasts with the extracellular matrix: implications for the understanding of fibrosis.* Springer Semin Immunopathol, 1999. **21**(4): p. 415-29.
3. Weber, K.T., *Monitoring tissue repair and fibrosis from a distance.* Circulation, 1997. **96**(8): p. 2488-92.
4. Eghbali, M. and K.T. Weber, *Collagen and the myocardium: fibrillar structure, biosynthesis and degradation in relation to hypertrophy and its regression.* Mol Cell Biochem, 1990. **96**(1): p. 1-14.
5. Micallef, L., et al., *The myofibroblast, multiple origins for major roles in normal and pathological tissue repair.* Fibrogenesis Tissue Repair, 2012. **5**(Suppl 1): p. S5.
6. Jahan, F. and J.T. Wigle, *Diverse Cellular Origins of Cardiac Fibroblasts*, in *Cardiac Fibrosis and Heart Failure: Cause or Effect?*, I.M.C. Dixon and J.T. Wigle, Editors. 2015, Springer: Canada. p. 125-145.
7. Gabbiani, G., *The myofibroblast in wound healing and fibrocontractive diseases.* J Pathol, 2003. **200**(4): p. 500-3.
8. Krenning, G., E.M. Zeisberg, and R. Kalluri, *The origin of fibroblasts and mechanism of cardiac fibrosis.* J Cell Physiol, 2010. **225**(3): p. 631-7.
9. Souders, C.A., S.L. Bowers, and T.A. Baudino, *Cardiac fibroblast: the renaissance cell.* Circ Res, 2009. **105**(12): p. 1164-76.

10. Camelliti, P., T.K. Borg, and P. Kohl, *Structural and functional characterisation of cardiac fibroblasts.* Cardiovasc Res, 2005. **65**(1): p. 40-51.

11. Bostrom, H., et al., *PDGF-A signaling is a critical event in lung alveolar myofibroblast development and alveogenesis.* Cell, 1996. **85**(6): p. 863-73.

12. Tomasek, J.J., et al., *Myofibroblasts and mechano-regulation of connective tissue remodelling.* Nat Rev Mol Cell Biol, 2002. **3**(5): p. 349-63.

13. Turner, N.A. and K.E. Porter, *Function and fate of myofibroblasts after myocardial infarction.* Fibrogenesis Tissue Repair, 2013. **6**(1): p. 5.

14. Petrov, V.V., R.H. Fagard, and P.J. Lijnen, *Stimulation of collagen production by transforming growth factor-beta1 during differentiation of cardiac fibroblasts to myofibroblasts.* Hypertension, 2002. **39**(2): p. 258-63.

15. Leask, A. and D.J. Abraham, *TGF-beta signaling and the fibrotic response.* FASEB J, 2004. **18**(7): p. 816-27.

16. Kutz, S.M., et al., *TGF-beta1-induced PAI-1 gene expression requires MEK activity and cell-to-substrate adhesion.* J Cell Sci, 2001. **114**(Pt 21): p. 3905-14.

17. Thiery, J.P. and J.P. Sleeman, *Complex networks orchestrate epithelial-mesenchymal transitions.* Nat Rev Mol Cell Biol, 2006. **7**(2): p. 131-42.

18. Zhou, B., et al., *Genetic fate mapping demonstrates contribution of epicardium-derived cells to the annulus fibrosis of the mammalian heart.* Dev Biol, 2010. **338**(2): p. 251-61.

19. Lie-Venema, H., et al., *Origin, fate, and function of epicardium-derived cells (EPDCs) in normal and abnormal cardiac development.* ScientificWorldJournal, 2007. **7**: p. 1777-98.

20. von Gise, A. and W.T. Pu, *Endocardial and epicardial epithelial to mesenchymal transitions in heart development and disease.* Circ Res, 2012. **110**(12): p. 1628-45.

21. Gittenberger-de Groot, A.C., et al., *Epicardium-derived cells contribute a novel population to the myocardial wall and the atrioventricular cushions.* Circ Res, 1998. **82**(10): p. 1043-52.

22. Acharya, A., et al., *The bHLH transcription factor Tcf21 is required for lineage-specific EMT of cardiac fibroblast progenitors.* Development, 2012. **139**(12): p. 2139-49.

23. de Lange, F.J., et al., *Lineage and morphogenetic analysis of the cardiac valves.* Circ Res, 2004. **95**(6): p. 645-54.

24. Miquerol, L., et al., *Multiple developmental roles of VEGF suggested by a LacZ-tagged allele.* Dev Biol, 1999. **212**(2): p. 307-22.

25. Dor, Y., et al., *VEGF modulates early heart valve formation.* Anat Rec A Discov Mol Cell Evol Biol, 2003. **271**(1): p. 202-8.

26. Armstrong, E.J. and J. Bischoff, *Heart valve development: endothelial cell signaling and differentiation.* Circ Res, 2004. **95**(5): p. 459-70.

27. Enciso, J.M., et al., *Elevated glucose inhibits VEGF-A-mediated endocardial cushion formation: modulation by PECAM-1 and MMP-2.* J Cell Biol, 2003. **160**(4): p. 605-15.

28. de la Pompa, J.L., et al., *Role of the NF-ATc transcription factor in morphogenesis of cardiac valves and septum.* Nature, 1998. **392**(6672): p. 182-6.

29. Timmerman, L.A., et al., *Notch promotes epithelial-mesenchymal transition during cardiac development and oncogenic transformation.* Genes Dev, 2004. **18**(1): p. 99-115.

30. Hurlstone, A.F., et al., *The Wnt/beta-catenin pathway regulates cardiac valve formation.* Nature, 2003. **425**(6958): p. 633-7.

31. Zeisberg, E.M. and R. Kalluri, *Origins of cardiac fibroblasts.* Circ Res, 2010. **107**(11): p. 1304-12.

32. Lucas, J.A., et al., *Inhibition of transforming growth factor-beta signaling induces left ventricular dilation and dysfunction in the pressure-overloaded heart.* Am J Physiol Heart Circ Physiol, 2010. **298**(2): p. H424-32.

33. Fredj, S., et al., *Interactions between cardiac cells enhance cardiomyocyte hypertrophy and increase fibroblast proliferation.* J Cell Physiol, 2005. **202**(3): p. 891-9.

34. Ljungqvist, A. and G. Unge, *The proliferative activity of the myocardial tissue in various forms of experimental cardiac hypertrophy.* Acta Pathol Microbiol Scand A, 1973. **81**(3): p. 233-40.

35. Mandache, E., et al., *The proliferative activity of the heart tissues in various forms of experimental cardiac hypertrophy studied by electron microscope autoradiography.* Virchows Arch B Cell Pathol, 1973. **12**(2): p. 112-22.

36. van Wijk, B., et al., *Cardiac regeneration from activated epicardium.* PLoS One, 2012. **7**(9): p. e44692.

37. Zhou, B. and W.T. Pu, *Epicardial epithelial-to-mesenchymal transition in injured heart.* J Cell Mol Med, 2011. **15**(12): p. 2781-3.

38. Lepilina, A., et al., *A dynamic epicardial injury response supports progenitor cell activity during zebrafish heart regeneration.* Cell, 2006. **127**(3): p. 607-19.

39. Zhou, B., et al., *Adult mouse epicardium modulates myocardial injury by secreting paracrine factors.* J Clin Invest, 2011. **121**(5): p. 1894-904.

40. Kim, J., et al., *PDGF signaling is required for epicardial function and blood vessel formation in regenerating zebrafish hearts.* Proc Natl Acad Sci U S A, 2010. **107**(40): p. 17206-10.

41. Kovacic, J.C., et al., *Epithelial-to-mesenchymal and endothelial-to-mesenchymal transition: from cardiovascular development to disease.* Circulation, 2012. **125**(14): p. 1795-808.

42. Krenning, G., et al., *Vascular smooth muscle cells for use in vascular tissue engineering obtained by endothelial-to-mesenchymal transdifferentiation (EnMT) on collagen matrices.* Biomaterials, 2008. **29**(27): p. 3703-11.

43. Moonen, J.R., et al., *Endothelial progenitor cells give rise to pro-angiogenic smooth muscle-like progeny.* Cardiovasc Res, 2010. **86**(3): p. 506-15.

44. Zeisberg, E.M., et al., *Endothelial-to-mesenchymal transition contributes to cardiac fibrosis.* Nat Med, 2007. **13**(8): p. 952-61.

45. Widyantoro, B., et al., *Endothelial cell-derived endothelin-1 promotes cardiac fibrosis in diabetic hearts through stimulation of endothelial-to-mesenchymal transition.* Circulation, 2010. **121**(22): p. 2407-18.

46. Ghosh, A.K., et al., *Genetic deficiency of plasminogen activator inhibitor-1 promotes cardiac fibrosis in aged mice: involvement of constitutive transforming*

growth factor-beta signaling and endothelial-to-mesenchymal transition. Circulation, 2010. **122**(12): p. 1200-9.

47. Yoshimatsu, Y. and T. Watabe, *Roles of TGF-beta signals in endothelial-mesenchymal transition during cardiac fibrosis.* Int J Inflam, 2011. **2011**: p. 724080.

48. Aisagbonhi, O., et al., *Experimental myocardial infarction triggers canonical Wnt signaling and endothelial-to-mesenchymal transition.* Dis Model Mech, 2011. **4**(4): p. 469-83.

49. Yano, T., et al., *Intracardiac fibroblasts, but not bone marrow derived cells, are the origin of myofibroblasts in myocardial infarct repair.* Cardiovasc Pathol, 2005. **14**(5): p. 241-6.

50. Kania, G., et al., *Heart-infiltrating prominin-1+/CD133+ progenitor cells represent the cellular source of transforming growth factor beta-mediated cardiac fibrosis in experimental autoimmune myocarditis.* Circ Res, 2009. **105**(5): p. 462-70.

51. Mollmann, H., et al., *Bone marrow-derived cells contribute to infarct remodelling.* Cardiovasc Res, 2006. **71**(4): p. 661-71.

52. van Amerongen, M.J., et al., *Bone marrow-derived myofibroblasts contribute functionally to scar formation after myocardial infarction.* J Pathol, 2008. **214**(3): p. 377-86.

53. Chu, P.Y., et al., *Bone marrow-derived cells contribute to fibrosis in the chronically failing heart.* Am J Pathol, 2010. **176**(4): p. 1735-42.

54. Haudek, S.B., et al., *Bone marrow-derived fibroblast precursors mediate ischemic cardiomyopathy in mice.* Proc Natl Acad Sci U S A, 2006. **103**(48): p. 18284-9.

55. van Amerongen, M.J., et al., *Macrophage depletion impairs wound healing and increases left ventricular remodeling after myocardial injury in mice.* Am J Pathol, 2007. **170**(3): p. 818-29.

56. Wang, H., et al., *Key role of macrophages in the pathogenesis of CD18 hypomorphic murine model of psoriasis.* J Invest Dermatol, 2009. **129**(5): p. 1100-14.

57. Abe, R., et al., *Peripheral blood fibrocytes: differentiation pathway and migration to wound sites.* J Immunol, 2001. **166**(12): p. 7556-62.

58. Bucala, R., *Circulating fibrocytes: cellular basis for NSF.* J Am Coll Radiol, 2008. **5**(1): p. 36-9.

59. Strieter, R.M., et al., *The role of circulating mesenchymal progenitor cells, fibrocytes, in promoting pulmonary fibrosis.* Trans Am Clin Climatol Assoc, 2009. **120**: p. 49-59.

60. Ogawa, M., A.C. LaRue, and C.J. Drake, *Hematopoietic origin of fibroblasts/myofibroblasts: Its pathophysiologic implications.* Blood, 2006. **108**(9): p. 2893-6.

61. Zulli, A., et al., *CD34 Class III positive cells are present in atherosclerotic plaques of the rabbit model of atherosclerosis.* Histochem Cell Biol, 2005. **124**(6): p. 517-22.

62. Sundberg, C., et al., *Pericytes as collagen-producing cells in excessive dermal scarring.* Lab Invest, 1996. **74**(2): p. 452-66.

63. Covas, D.T., et al., *Multipotent mesenchymal stromal cells obtained from diverse human tissues share functional properties and gene-expression profile with CD146+ perivascular cells and fibroblasts.* Exp Hematol, 2008. **36**(5): p. 642-54.

64. Humphreys, B.D., et al., *Fate tracing reveals the pericyte and not epithelial origin of myofibroblasts in kidney fibrosis.* Am J Pathol, 2010. **176**(1): p. 85-97.

65. Hung, C., et al., *Role of lung pericytes and resident fibroblasts in the pathogenesis of pulmonary fibrosis.* Am J Respir Crit Care Med, 2013. **188**(7): p. 820-30.

66. Corda, S., J.L. Samuel, and L. Rappaport, *Extracellular matrix and growth factors during heart growth.* Heart Fail Rev, 2000. **5**(2): p. 119-30.

67. Bowers, S.L., I. Banerjee, and T.A. Baudino, *The extracellular matrix: at the center of it all.* J Mol Cell Cardiol, 2010. **48**(3): p. 474-82.

68. Bosman, F.T. and I. Stamenkovic, *Functional structure and composition of the extracellular matrix.* J Pathol, 2003. **200**(4): p. 423-8.

69. Tsuruda, T., L.C. Costello-Boerrigter, and J.C. Burnett, Jr., *Matrix metalloproteinases: pathways of induction by bioactive molecules.* Heart Fail Rev, 2004. **9**(1): p. 53-61.

70. Gaudesius, G., et al., *Coupling of cardiac electrical activity over extended distances by fibroblasts of cardiac origin.* Circ Res, 2003. **93**(5): p. 421-8.

71. Miragoli, M., G. Gaudesius, and S. Rohr, *Electrotonic modulation of cardiac impulse conduction by myofibroblasts.* Circ Res, 2006. **98**(6): p. 801-10.

72. Hu, H. and F. Sachs, *Stretch-activated ion channels in the heart.* J Mol Cell Cardiol, 1997. **29**(6): p. 1511-23.

73. Isenberg, G., et al., *Differential effects of stretch and compression on membrane currents and [Na+]c in ventricular myocytes.* Prog Biophys Mol Biol, 2003. **82**(1-3): p. 43-56.

74. Kamkin, A., et al., *Cardiac fibroblasts and the mechano-electric feedback mechanism in healthy and diseased hearts.* Prog Biophys Mol Biol, 2003. **82**(1-3): p. 111-20.

75. Risau, W., *Mechanisms of angiogenesis.* Nature, 1997. **386**(6626): p. 671-4.

76. Bergmann, O., et al., *Evidence for cardiomyocyte renewal in humans.* Science, 2009. **324**(5923): p. 98-102.

77. Engel, F.B., et al., *p38 MAP kinase inhibition enables proliferation of adult mammalian cardiomyocytes.* Genes Dev, 2005. **19**(10): p. 1175-87.

78. Kuhn, B., et al., *Periostin induces proliferation of differentiated cardiomyocytes and promotes cardiac repair.* Nat Med, 2007. **13**(8): p. 962-9.

79. Freed, D.H., et al., *Emerging evidence for the role of cardiotrophin-1 in cardiac repair in the infarcted heart.* Cardiovasc Res, 2005. **65**(4): p. 782-92.

80. Willems, I.E., et al., *The alpha-smooth muscle actin-positive cells in healing human myocardial scars.* Am J Pathol, 1994. **145**(4): p. 868-75.

81. Kalluri, R. and M. Zeisberg, *Fibroblasts in cancer.* Nat Rev Cancer, 2006. **6**(5): p. 392-401.

82. McAnulty, R.J., *Fibroblasts and myofibroblasts: their source, function and role in disease.* Int J Biochem Cell Biol, 2007. **39**(4): p. 666-71.

83. Khan, R. and R. Sheppard, *Fibrosis in heart disease: understanding the role of transforming growth factor-beta in cardiomyopathy, valvular disease and arrhythmia.* Immunology, 2006. **118**(1): p. 10-24.

84. Undas, A. and R.A. Ariens, *Fibrin clot structure and function: a role in the pathophysiology of arterial and venous thromboembolic diseases.* Arterioscler Thromb Vasc Biol, 2011. **31**(12): p. e88-99.

85. Czubryt, M.P., *Common threads in cardiac fibrosis, infarct scar formation, and wound healing.* Fibrogenesis Tissue Repair, 2012. **5**(1): p. 19.

86. Hewitson, T.D., H.L. Wu, and G.J. Becker, *Interstitial myofibroblasts in experimental renal infection and scarring.* Am J Nephrol, 1995. **15**(5): p. 411-7.

87. Gabbiani, G., G.B. Ryan, and G. Majne, *Presence of modified fibroblasts in granulation tissue and their possible role in wound contraction.* Experientia, 1971. **27**(5): p. 549-50.

88. Li, J., Y.P. Zhang, and R.S. Kirsner, *Angiogenesis in wound repair: angiogenic growth factors and the extracellular matrix.* Microsc Res Tech, 2003. **60**(1): p. 107-14.

89. Yaguchi, T., et al., *Immunohistochemical and gelatin zymography studies for matrix metalloproteinases in bleomycin-induced pulmonary fibrosis.* Pathol Int, 1998. **48**(12): p. 954-63.

90. Desmouliere, A., et al., *Apoptosis mediates the decrease in cellularity during the transition between granulation tissue and scar.* Am J Pathol, 1995. **146**(1): p. 56-66.

91. Snider, P., et al., *Origin of cardiac fibroblasts and the role of periostin.* Circ Res, 2009. **105**(10): p. 934-47.

92. Sharma, U.C., et al., *Galectin-3 marks activated macrophages in failure-prone hypertrophied hearts and contributes to cardiac dysfunction.* Circulation, 2004. **110**(19): p. 3121-8.

93. Funahashi, J., et al., *Delta-crystallin enhancer binding protein delta EF1 is a zinc finger-homeodomain protein implicated in postgastrulation embryogenesis.* Development, 1993. **119**(2): p. 433-46.

94. Vandewalle, C., F. Van Roy, and G. Berx, *The role of the ZEB family of transcription factors in development and disease.* Cell Mol Life Sci, 2009. **66**(5): p. 773-87.

95. Van de Putte, T., et al., *Mice lacking ZFHX1B, the gene that codes for Smad-interacting protein-1, reveal a role for multiple neural crest cell defects in the etiology of Hirschsprung disease-mental retardation syndrome.* Am J Hum Genet, 2003. **72**(2): p. 465-70.

96. Takagi, T., et al., *DeltaEF1, a zinc finger and homeodomain transcription factor, is required for skeleton patterning in multiple lineages.* Development, 1998. **125**(1): p. 21-31.

97. Seuntjens, E., et al., *Sip1 regulates sequential fate decisions by feedback signaling from postmitotic neurons to progenitors.* Nat Neurosci, 2009. **12**(11): p. 1373-80.

98. Wakamatsu, N., et al., *Mutations in SIP1, encoding Smad interacting protein-1, cause a form of Hirschsprung disease.* Nat Genet, 2001. **27**(4): p. 369-70.

99. Amiel, J., et al., *Large-scale deletions and SMADIP1 truncating mutations in syndromic Hirschsprung disease with involvement of midline structures.* Am J Hum Genet, 2001. **69**(6): p. 1370-7.

100. van Grunsven, L.A., et al., *XSIP1, a Xenopus zinc finger/homeodomain encoding gene highly expressed during early neural development.* Mech Dev, 2000. **94**(1-2): p. 189-93.

101. Van de Putte, T., et al., *Neural crest-specific removal of Zfhx1b in mouse leads to a wide range of neurocristopathies reminiscent of Mowat-Wilson syndrome.* Hum Mol Genet, 2007. **16**(12): p. 1423-36.

102. Kong, D., et al., *Cancer Stem Cells and Epithelial-to-Mesenchymal Transition (EMT)-Phenotypic Cells: Are They Cousins or Twins?* Cancers (Basel), 2011. **3**(1): p. 716-29.

103. Lim, J. and J.P. Thiery, *Epithelial-mesenchymal transitions: insights from development.* Development, 2012. **139**(19): p. 3471-86.

104. Park, S.M., et al., *The miR-200 family determines the epithelial phenotype of cancer cells by targeting the E-cadherin repressors ZEB1 and ZEB2.* Genes Dev, 2008. **22**(7): p. 894-907.

105. Prislei, S., et al., *Role and prognostic significance of the epithelial-mesenchymal transition factor ZEB2 in ovarian cancer.* Oncotarget, 2015.

106. Gauchat, D., et al., *Evolution of Antp-class genes and differential expression of Hydra Hox/paraHox genes in anterior patterning.* Proc Natl Acad Sci U S A, 2000. **97**(9): p. 4493-8.

107. Candia, A.F. and C.V. Wright, *Differential localization of Mox-1 and Mox-2 proteins indicates distinct roles during development.* Int J Dev Biol, 1996. **40**(6): p. 1179-84.

108. Douville, J.M., et al., *Mechanisms of MEOX1 and MEOX2 regulation of the cyclin dependent kinase inhibitors p21 and p16 in vascular endothelial cells.* PLoS One, 2011. **6**(12): p. e29099.

109. Gorski, D.H., et al., *Molecular cloning of a diverged homeobox gene that is rapidly down-regulated during the G0/G1 transition in vascular smooth muscle cells.* Mol Cell Biol, 1993. **13**(6): p. 3722-33.

110. Gorski, D.H. and A.J. Leal, *Inhibition of endothelial cell activation by the homeobox gene Gax.* J Surg Res, 2003. **111**(1): p. 91-9.

111. Liu, P., et al., *Cross talk among Smad, MAPK, and integrin signaling pathways enhances adventitial fibroblast functions activated by transforming growth factor-beta1 and inhibited by Gax.* Arterioscler Thromb Vasc Biol, 2008. **28**(4): p. 725-31.

112. Pantalacci, S., et al., *Patterning of palatal rugae through sequential addition reveals an anterior/posterior boundary in palatal development.* BMC Dev Biol, 2008. **8**: p. 116.

113. Jin, J.Z. and J. Ding, *Analysis of Meox-2 mutant mice reveals a novel postfusion-based cleft palate.* Dev Dyn, 2006. **235**(2): p. 539-46.

114. Weiss, K.M., F.H. Ruddle, and J. Bollekens, *Dlx and other homeobox genes in the morphological development of the dentition.* Connect Tissue Res, 1995. **32**(1-4): p. 35-40.

115. Schwab, K., et al., *Comprehensive microarray analysis of Hoxa11/Hoxd11 mutant kidney development.* Dev Biol, 2006. **293**(2): p. 540-54.

116. Quinn, L.M., S.E. Latham, and B. Kalionis, *The homeobox genes MSX2 and MOX2 are candidates for regulating epithelial-mesenchymal cell interactions in the human placenta.* Placenta, 2000. **21 Suppl A**: p. S50-4.

117. Valcourt, U., et al., *Functional role of Meox2 during the epithelial cytostatic response to TGF-beta.* Mol Oncol, 2007. **1**(1): p. 55-71.

118. Pfaff, N., et al., *miRNA screening reveals a new miRNA family stimulating iPS cell generation via regulation of Meox2.* EMBO Rep, 2011. **12**(11): p. 1153-9.

119. Cunnington, R.H., et al., *The Ski-Zeb2-Meox2 pathway provides a novel mechanism for regulation of the cardiac myofibroblast phenotype.* J Cell Sci, 2014. **127**(Pt 1): p. 40-9.

120. Chen, Y., et al., *Regulation of the expression and activity of the antiangiogenic homeobox gene GAX/MEOX2 by ZEB2 and microRNA-221.* Mol Cell Biol, 2010. **30**(15): p. 3902-13.

121. Leask, A., *Potential therapeutic targets for cardiac fibrosis: TGFbeta, angiotensin, endothelin, CCN2, and PDGF, partners in fibroblast activation.* Circ Res, 2010. **106**(11): p. 1675-80.

122. Leask, A., *TGFbeta, cardiac fibroblasts, and the fibrotic response.* Cardiovasc Res, 2007. **74**(2): p. 207-12.

123. Wolf, G., *New insights into the pathophysiology of diabetic nephropathy: from haemodynamics to molecular pathology.* Eur J Clin Invest, 2004. **34**(12): p. 785-96.

124. Vallance, B.A., et al., *TGF-beta1 gene transfer to the mouse colon leads to intestinal fibrosis.* Am J Physiol Gastrointest Liver Physiol, 2005. **289**(1): p. G116-28.

125. Tomita, H., et al., *Early induction of transforming growth factor-beta via angiotensin II type 1 receptors contributes to cardiac fibrosis induced by long-term blockade of nitric oxide synthesis in rats.* Hypertension, 1998. **32**(2): p. 273-9.

126. Massague, J., S.W. Blain, and R.S. Lo, *TGFbeta signaling in growth control, cancer, and heritable disorders.* Cell, 2000. **103**(2): p. 295-309.

127. Chen, W. and S.M. Wahl, *TGF-beta: receptors, signaling pathways and autoimmunity.* Curr Dir Autoimmun, 2002. **5**: p. 62-91.

128. Dobaczewski, M., et al., *Smad3 signaling critically regulates fibroblast phenotype and function in healing myocardial infarction.* Circ Res, 2010. **107**(3): p. 418-28.

129. Kim, S.J., et al., *Molecular mechanisms of inactivation of TGF-beta receptors during carcinogenesis.* Cytokine Growth Factor Rev, 2000. **11**(1-2): p. 159-68.

130. Tang, B., et al., *Transforming growth factor-beta1 is a new form of tumor suppressor with true haploid insufficiency.* Nat Med, 1998. **4**(7): p. 802-7.

131. Smith, P.K., et al., *Measurement of protein using bicinchoninic acid.* Anal Biochem, 1985. **150**(1): p. 76-85.

132. Vandewalle, C., et al., *SIP1/ZEB2 induces EMT by repressing genes of different epithelial cell-cell junctions.* Nucleic Acids Res, 2005. **33**(20): p. 6566-78.

133. Darby, I., O. Skalli, and G. Gabbiani, *Alpha-smooth muscle actin is transiently expressed by myofibroblasts during experimental wound healing.* Lab Invest, 1990. **63**(1): p. 21-9.

134. Serini, G., et al., *The fibronectin domain ED-A is crucial for myofibroblastic phenotype induction by transforming growth factor-beta1.* J Cell Biol, 1998. **142**(3): p. 873-81.

135. Frangogiannis, N.G., L.H. Michael, and M.L. Entman, *Myofibroblasts in reperfused myocardial infarcts express the embryonic form of smooth muscle myosin heavy chain (SMemb).* Cardiovasc Res, 2000. **48**(1): p. 89-100.

136. Hinz, B., et al., *Alpha-smooth muscle actin expression upregulates fibroblast contractile activity.* Mol Biol Cell, 2001. **12**(9): p. 2730-41.

137. Santiago, J.J., et al., *Cardiac fibroblast to myofibroblast differentiation in vivo and in vitro: expression of focal adhesion components in neonatal and adult rat ventricular myofibroblasts.* Dev Dyn, 2010. **239**(6): p. 1573-84.

138. Follonier Castella, L., et al., *Regulation of myofibroblast activities: calcium pulls some strings behind the scene.* Exp Cell Res, 2010. **316**(15): p. 2390-401.

139. Pichard, A.L. and W.Y. Cheung, *Cyclic 3':5'-nucleotide phosphodiesterase. Stimulation of bovine brain cytoplasmic enzyme by lysophosphatidylcholine.* J Biol Chem, 1977. **252**(14): p. 4872-5.

140. Brilla, C.G., R.C. Funck, and H. Rupp, *Lisinopril-mediated regression of myocardial fibrosis in patients with hypertensive heart disease.* Circulation, 2000. **102**(12): p. 1388-93.

141. Alehagen, U., et al., *Association Between Use of Statins and Mortality in Patients With Heart Failure and Ejection Fraction of Greater Than or Equal to 50.* Circ Heart Fail, 2015.

142. Shi, Y., et al., *Enalapril effects on atrial remodeling and atrial fibrillation in experimental congestive heart failure.* Cardiovasc Res, 2002. **54**(2): p. 456-61.